2015-03-30

A New Production Casing Design to Withstand Combined Installation Compression Loading and High Multi-Stage Hydraulic Fracturing Pressures in Montney Shale Horizontal Wells

Suarez Jerez, Nino Alexander

UNIVERSITY OF CALGARY

A New Production Casing Design to Withstand Combined Installation Compression Loading and High Multi-Stage Hydraulic Fracturing Pressures in Montney Shale Horizontal Wells

by

Nino Alexander Suarez Jerez

A THESIS

SUBMITTED TO THE FACULTY OF GRADUATE STUDIES

IN PARTIAL FULFILMENT OF THE REQUIREMENTS FOR THE

DEGREE OF MASTER OF ENGINEERING

CHEMICAL AND PETROLEUM ENGINEERING

CALGARY, ALBERTA

MARCH, 2015

Abstract

In order to make a low permeability shale reservoir economically attractive, it is critical to maximize the well contact with the reservoir by drilling long horizontal wells into the producing formation, and then to stimulate the well by means of massive multi-stage hydraulic fracturing.

To this end, the well is equipped with a casing tubular system that initially serves as the pipe by which hydraulic fracturing is done, and subsequently acts as the conduit that transports hydrocarbons from the reservoir to the surface.

In recent years, there has been production casing failures characterized by pipe leaking during hydraulic fracturing jobs in the Montney shale of British Columbia. Costs of these failures have ranged between $2MM and $15MM in NPV loss.

These technical and economic failures have inspired the research presented in this thesis. Key contribution of this work: Development of a new tapered string made out of 22.4 x 17.3 kg/m casing, which takes into account all acting loads during casing installation and withstands high pressures during multi-stage hydraulic fracturing jobs in horizontal wells. The cost of the improved tapered string is similar to the cost of previous casing designs.

Casing design has been traditionally done to withstand the most critical loads during the production phase of the well life. Fracturing loading has been incorporated into the casing design process merely as a casing burst load defined by the hydrostatic pressure of the fracturing fluid plus the surface pressure applied to that column of fluid. However, there has been minimum work done to incorporate the combined casing installation and hydraulic fracturing loads into the design process. The research presented in this thesis meets that need.

Acknowledgements

I would like to thank my supervisor, Professor Roberto Aguilera for his support and guidance during the preparation of this project.

Also, I want to thank Shell Upstream Americas wells engineers for guiding and providing me with the tools to develop this project.

To Clari, Vale and Santi…my treasures,

I took their own time to do this thesis…

Table of Contents

List of Tables

List of Figures and Illustrations

List of Symbols, Abbreviations and Nomenclature

°C	Degrees Celsius
Ai	Internal area of pipe
Ao	External area of pipe
API	American Petroleum Institute
BHA	Bottom Hole Assembly
BOP	Blowout Preventers
cm	centimeter
E	Young's modulus
FEA	Finite Element Analysis
F_e	Effective force
Fn	Normal force
F_s	Critical buckling force
Ft	True tension
F_{true}	True axial force
H2S	Hydrogen Sulfide
I	Second Moment of Inertia
ID	Inside Diameters
kg	kilogram
kg/m	kilogram per meter
kN	kilo newton (1000 newton)
ksi	Kilo pounds per square inch (1000 psi)
L80	Steel grade material with 80 ksi yield strength
LTC	Long Thread Casing coupling
m	meters
MD	Measure Depth
MM	Millions
mm	millimeters
MMscf	Millions of standard cubic feet
MPa	Mega Pascals
MWD	Measurement While Drilling
N/m^2	Newton per square meter
NPV	Net Present Value
OD	Outside Diameter
P110	Steel grade material with 110 ksi yield strength
Pa	Pascals
PDC	Poly Diamond Crystalline bit
Pi	Internal pressure
Po	External pressure
PSV	Pressure Safety Valves
r_c	radial clearance

SG	Specific Gravity
TD	Total Depth
T	metric ton
TVD	True Vertical Depth
Ys	Yield Strength
Δf	Change in tension
ΔL	Elongation or change in length
ΔM	Change in bending moment
$\Delta \alpha$	Change in wellbore inclination
$\Delta \phi$	Change in azimuth
μ	Coefficient of friction
π	Pi Number
ν	Poisson's ratio
σa	Axial stress
σb	Bending stress
σe	Effective stress or triaxial stress
σr	Radial stress
σt	Tangential stress
Θ	Well inclination

Chapter One: **Well Design in the Groundbirch Montney play: Production Casing Integrity Challenges**

1.1 Background and Study Purpose

In recent years development of tight plays (shales, sands and coals) has gained popularity and considerable attention. To obtain good production and insure that these tight plays are economically feasible it is critical to maximize the well contact with the reservoir by drilling horizontal wells into the producing formation.

Horizontal wells have been designed in many ways, with two and three casing string designs being the most prevalent. Usually, a surface hole is drilled to a few meters below the last strata capable of carrying water; afterwards a casing string is run to protect that aquifer. After the "surface section" is drilled and cased, there are two well design options for the remainder of the well:

Two string design; a monobore well is drilled from the surface casing shoe to the final total depth. Casing is then run into the hole to serve as a production string.

Three string design; the well is first drilled to an intermediate depth and intermediate casing will be set prior to drilling and casing the final production hole. The purpose of the intermediate string is to case off troubled areas, such as formations containing high pore pressures or lost circulation zones.

The two string well design, Figure 1.1, has become a cost effective option when formations with high pressures in the well, before entering the target reservoir, are not expected. The field data that will be used to support this thesis has been acquired from an operator that drills primarily two-string wells.

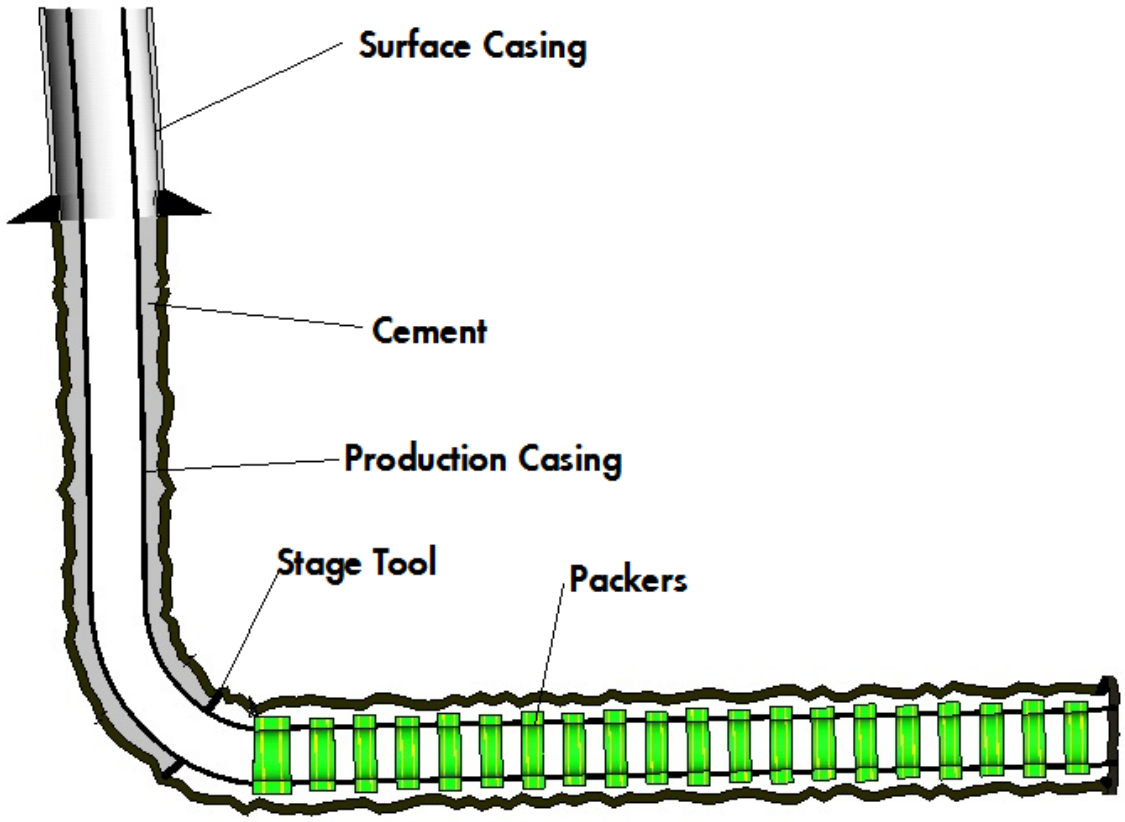

Figure 1.1. Typical two-string well design.

When running production casing in two-string wells, the casing is dragging through the open hole until it is landed at the toe. Thus, the casing is constantly in direct contact with the formations. The contact forces experienced along the casing string could, at some point, prevent the casing system from getting to the planned final position. The extremely high forces that the casing experiences during the running process create important bending and compressive stresses along the entire casing string.

One of the important events that happen while running casing is called buckling. Buckling is a state of instability that a beam or tubular can suffer when it is exposed to a high compressive force along its longitudinal axis.

Buckling in the Oil and Gas industry has been exhaustively investigated over the last 50 years. Buckling is a function of a pipe (casing) geometry, mechanical properties, pipe lateral constraints, buoyancy (when the pipe is immersed in fluids), well inclination and compressive force. Buckling can cause plastic or elastic deformation of the tubular depending on the loads (compression) seen during the running process.

The Operator developing the Groundbirch field is pushing the technical limits every day by drilling longer horizontal wells and running more complex completions systems. Consequently, buckling has become a critical issue since excessive loads are applied to the casing to break friction and run the casing to its final depth. Additionally, the casing is landed at the wellhead in a Mandrel type hanger (Figure 1.2) which does not allow for the casing to be pulled in tension to alleviate the compressive forces created by buckling.

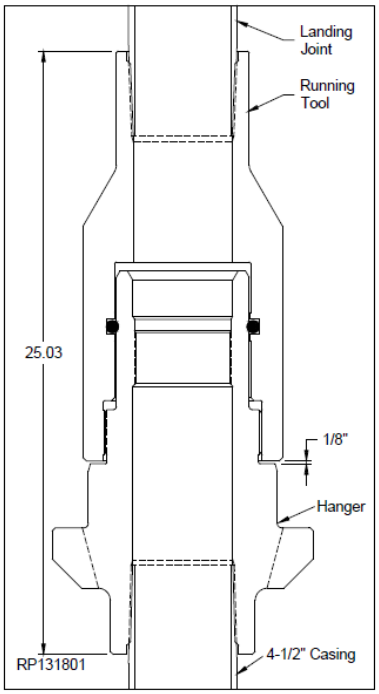

Figure 1.2. Mandrel hanger that supports production casing string into the surface wellhead.

On the other hand, casing design has been traditionally done to withstand the most critical loads during the production phase of the well life. These are ***full evacuation[1], hot and cold tubing leak[2] and hot and cold shut in[3].*** Once all the key inputs (temperatures, pressures and forces) have been determined, load cases are defined and then forces, stresses and strains for each load are calculated. Next, calculated stresses are compared with mechanical properties of the casing/tubing materials (yield stress) to ensure that the selected tubular meets the design factors previously defined by the Oil and Gas company (operator) and/or regulatory body.

Design safety factors are dimensionless parameters that indicate how close a given load case is to exceed the specified minimum yield strength of the casing. Following this process, casing and tubing is selected for the different application in the well design process.

However, there is an additional load that needs to be properly incorporated into the casing design process for wells that are to be hydraulically fractured. To develop a tight play an intense hydraulic fracturing process, commonly referred to as fracking in the public domain, is required. Hydraulic fracturing uses large quantities of water that are pumped down the well (along with some chemical agents and proppants) at high rates and high pressures to fracture the reservoir with a view to produce the desired hydrocarbon. The entire casing string is subjected to pressure during fracturing (i.e. in the case of the two casing string design there is no production zone isolation by means of a packer). Until now, fracturing has been incorporated into the casing

[1] Full Evacuation to Gas: This load case models a well completely displacing the well gas to surface. This load case results in full reservoir pressure minus the gas gradient exerted on the casing string.
[2] Tubing Leak: This load case models the situation of a production casing leak which would result in the surface casing being subjected to the full shut in pressure of the well
[3] Shut In: This load case models a shut in for an extended period of time to ensure the well can be safely shut in without either the production casing leaking, or venting gas to surface.

design process merely as a burst load defined by the hydrostatic pressure of the fracturing fluid plus the surface pressure applied to that column of fluid.

A few years ago, the operator experienced some failures characterized by casing leaking during the hydraulic fracturing process. After some engineering analysis and modeling, it was determined that the casing was fit to support the extremely high pressures seen during fracturing. However, it was determined that extreme bending (wrinkling) of the casing, attributed to buckling during the casing run (Figure 1.3, Figure 1.4, Figure 1.5), compounded with the hydraulic fracturing loads caused the casing to fail. The buckled or wrinkled pipe was plastically deformed during the casing string installation leaving residual stresses trapped in the buckled pipe. These residual stresses compounded with additional axial stresses and a large differential pressure due to hydraulic fracturing that ultimately caused the casing to fail, loss of the well and loss of important production value.

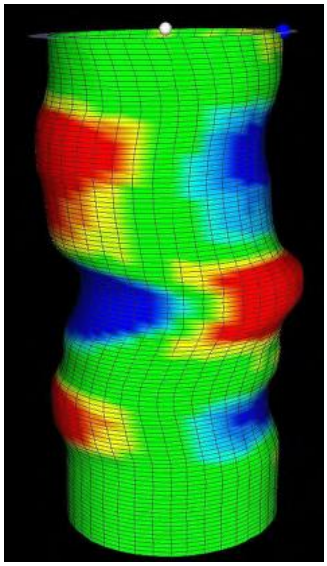

Figure 1.3. Depiction of severely buckled casing, USIT log run in one of the Groundbirch Wells, 2013.

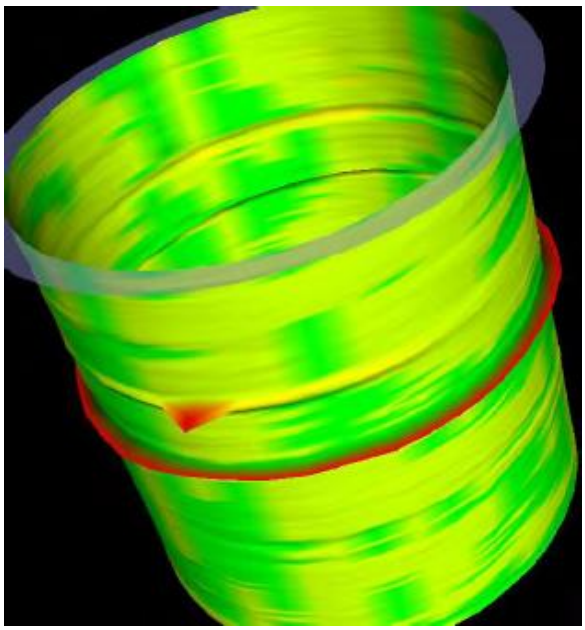

Figure 1.4. Caliper log showing casing wrinkling due to excessive compression during the running-in hole operation, Groundbirch 2014.

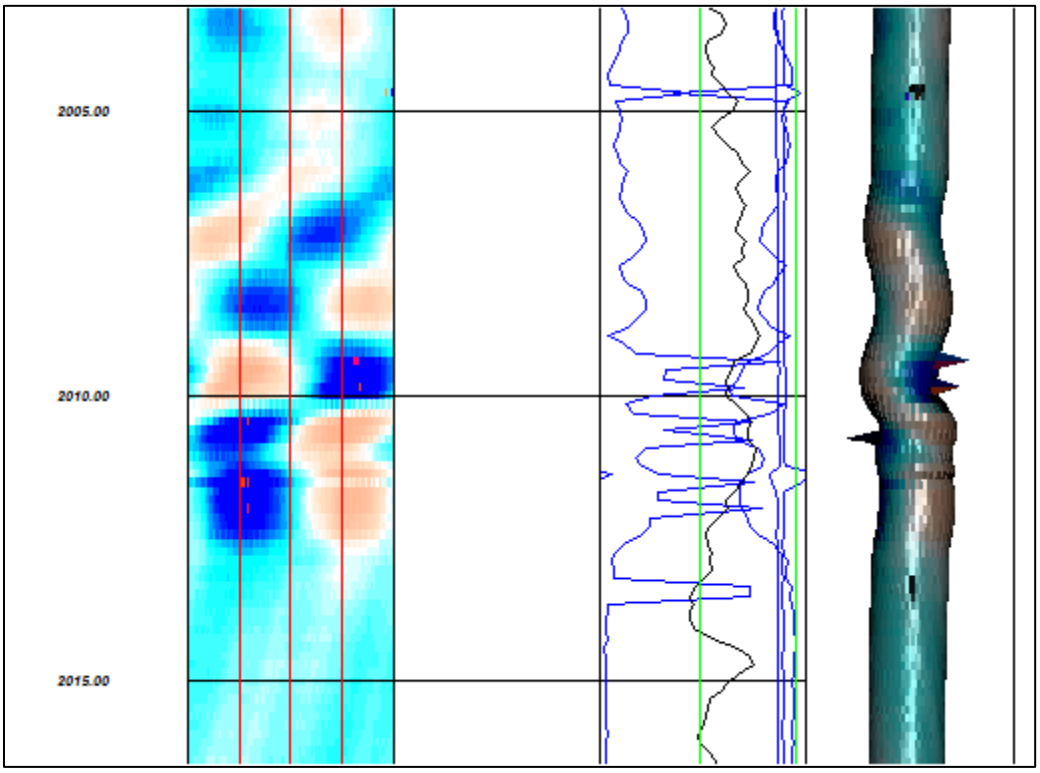

Figure 1.5. Caliper log showing buckling in a 114.3 mm casing section, Groundbirch 2013.

It was therefore concluded that the mechanism of failure was a combination of two loads, excessive buckling and high fracturing loads.

There is currently no commercial software available to model these two loads simultaneously. Current applications assume the casing is locked in place after it is run, or in other words the casing is modelled as-cemented[4]. This means that any residual stresses in the casing due to the casing run (buckling) are not considered when the fracturing load is applied.

The key question is, if the casing failure mechanism is a combination of buckling and fracturing loads, then how can we prevent the failure from occurring? In practice, hydraulic fracturing pressures cannot be changed as they are dictated by the reservoir stress regime. One possible solution is to control the casing running load and the resulting compressive forces that the casing experiences. A second option would be to change the well design and select a stronger and possibly more expensive casing type.

Casing run loads can be controlled only in the field by the rig crew. It is therefore critical to define a parameter that the rig crew can use to measure how much the casing can be pushed during the running process to ensure they are not exceeding the compressive force that would result in a casing failure during hydraulic fracturing.

Up to now there has been little to no work completed to incorporate both loads into the casing design process. Considering the number of horizontal wells currently being drilled and the extremely high cost of repairing casing or even worst losing a well, it is imperative to develop a model that analyses the combined stress of both loads and its effect on casing integrity. A typical

[4] As cemented: An as-cemented model is a static model that assumes the casing has no residual stresses when it is cemented in place. The as-cemented model only takes into account the load cases that are modelled and any axial stresses modelled.

casing failure intervention costs approximately 1 million dollars in upfront costs and potentially millions in lost production. Repairing casing involves patching the interior of the casing, which causes a reduction in internal diameter. This reduction in internal diameter can cause the loss of stages of the completion and ultimately results in the loss of production.

The primary objective of this thesis is to develop a practical model to match and understand the failure mechanism under combined stresses of the two loads in question. The key parameters required to develop the model are: thermal gradients, pore pressures, cement properties, casing properties, drilling fluids, dogleg severity, hook load data during casing run, caliper data to establish actual hole geometry, fracturing parameters such as flow volumes, flow rates, brine densities and fracturing pressures.

The secondary objective of the project is to apply the model at the field level to use the hookload measurements to limit the compression load applied on the casing to a value that will not compromise casing integrity during the hydraulic fracturing process.

1.2 Case Study Operation

The data used in this thesis comes from a tight gas play targeting the Montney formation in Northern BC for hydrocarbon production. The base well design is a two-string design with 177.8 mm surface casing set at approximately 600 m TVD and 114.3 mm production casing set at 2100-2300 m TVD with lateral lengths ranging from 1400 m to 2800 m resulting in wells with total measured depths of 4300 m to 6500 m. All information surrounding the drilling and completion of a typical well drilled by the operator is outlined in this section. This data will be used for the remainder of the thesis.

Each well has two main sections: Surface hole and main or production hole. The surface hole is drilled using a 222 mm PDC[5] drill bit using fresh water as drilling fluid. The surface hole is drilled to a depth of approximately 600 m TVD[6] to allow for casing to be set across all water bearing formations to protect against ground water contamination. The entire surface section is drilled using fresh water with a density of 1,000 kg/m^3. Viscous pills (small injections of viscous fluid) are regularly pumped into the hole to aid with hole cleaning by removing cuttings. The pills are required due to the waters lack of rheology. Once the surface hole is drilled to the total planned depth, cleanup cycles are performed and the BHA[7] is pulled out of the hole. Next, 177.8 mm surface casing is run into the hole and cemented in place. The purpose of this surface casing is to protect groundwater and to serve as a "drilling string" to allow for a BOP[8] to be mounted on the wellhead. The BOP is critical for well control for the ability to shut in the well and circulate out any gas influxes. The surface casing will also serve as secondary containment in the event of a production casing failure during the life of the well. The surface casing is typically cemented in place with 1,750 kg/m^3 cement. Typically, all surface holes are drilled and cased as a batch prior to drilling production holes. For example, the surface holes will be drilled from wells A through G then once all surface sections are completed, production holes will be drilled in the opposite direction (Figure 1.6).

[5] PDC: Polycrystalline Diamond Compact, refers to a type of drill bit that utilizes PDC cutters as the part of the drill bit that physically makes contact with the formation.
[6] TVD: True Vertical Depth, notates vertical depth, as compared to MD (measured depth) which indicates the length of a well.
[7] BHA: Bottom hole assembly refers to the entire assembly that allows drilling to occur. Accounts for all downhole tools, primarily the drill bit, the motor, and MWD tool.
[8] BOP: Blow out preventer, a large valve use to seal and control a well.

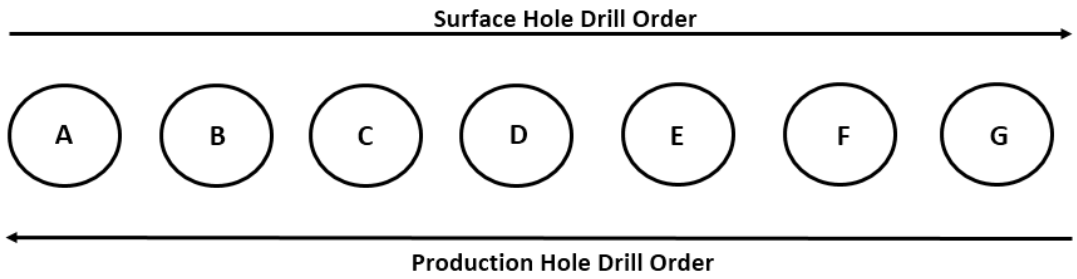

Figure 1.6. Well drilling sequence.

The surface casing is designed to withstand gas influx loads, full evacuation loads, and shut in tubing leak loads. Typically, the surface casing design is driven by the shut in tubing leak load. This load ensures that the surface casing is capable of withstanding the pressure caused in the event that the production casing was to leak gas into the production casing annulus when the well is shut in. This ensures the surface casing will maintain integrity, ground water is protected and prevention against venting gas to the atmosphere.

Previously, the operator drilled 311 mm hole and cased with 244.5 mm casing to allow for the option to run a 177.8 mm contingency casing string. However, after getting sufficient experience in the area the contingency string was deemed unnecessary for this specific area in the field. This reduced annular space helps reduce buckling tendency of the production casing within the surface casing.

The production hole is drilled through using a 159 mm PDC bit with fresh water as drilling fluid. As the production hole nears the North Pine Salt formation, the drilling crew begins to saturate the water with Sodium Chloride to become fully saturated prior to reaching salt bearing

formations. Salt bearing formations can have massive wellbore enlargement[9] if drilled with fresh water as the drilling fluid will dissolve the salt in the formation. Furthermore, saturated salt water helps to maintain borehole stability and reduce borehole enlargements in shales and other rock formations as can be seen in caliper logs (Figure 1.7). To generate the log a caliper with multiple arms is run into the wellbore and takes multiple readings of the diameter of the well. As can be seen in the caliper log, Well B that was drilled with salt saturated water has a borehole that is less enlarged than in Well A. Overall Well B has a smoother borehole.

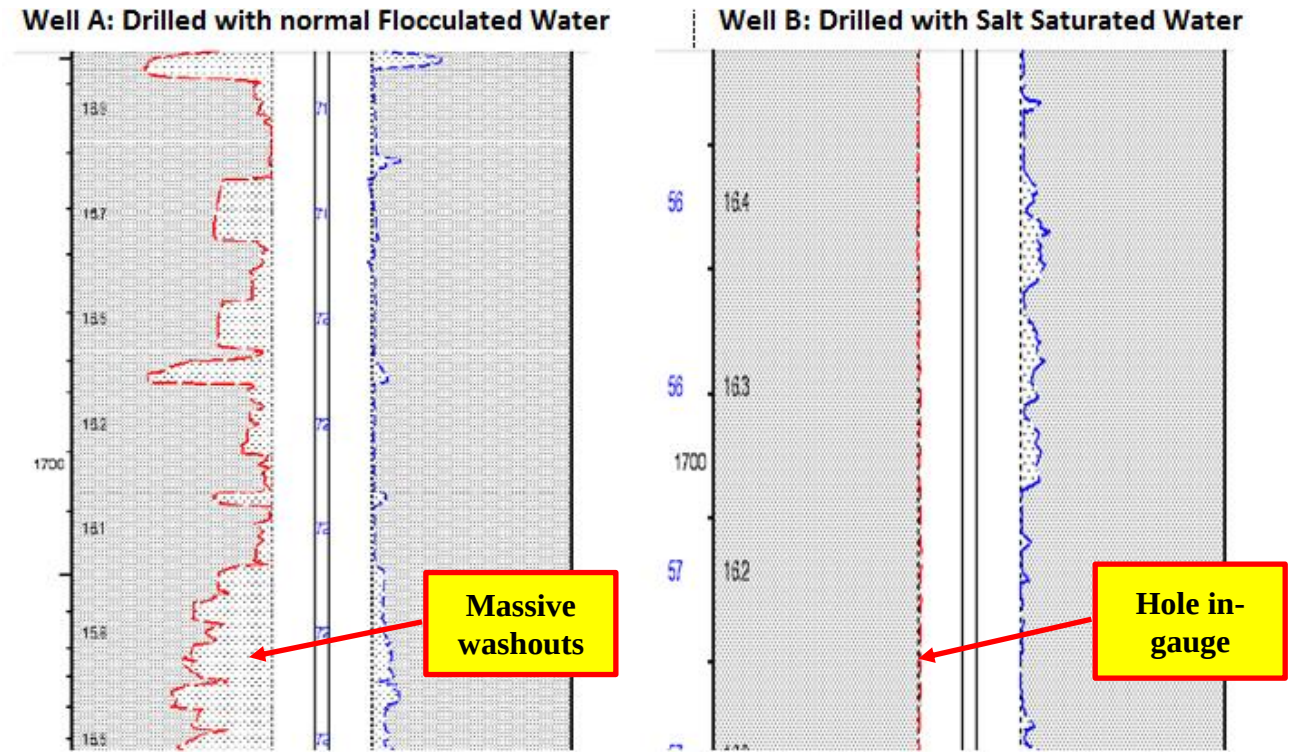

Figure 1.7. Caliper log of two wells comparing normal flocculated water drilling, to salt saturated flocculate water, multi caliper log.

[9] Wellbore enlargement: Also known as washouts are the result of drilling fluid eroding the wellbore and can result in large increases in wellbore diameter.

Once the drilling fluid is fully salt saturated, it has a density of 1200 kg/m^3. The water remains fully saturated for the remainder of the drilling section before transitioning the mud system to an invert mud[10]. Avoiding borehole enlargements in salt formations is important both for borehole stability and to maintain a smooth gauge hole to avoid increasing the clearance between the production casing and borehole to reduce buckling tendency. An opening, such as a borehole enlargement, can provide space in the borehole for the production casing to buckle. Drilling with salt flocculated water through salt sections helps to mitigate this problem.

In the vertical section, the well reaches a point where a tangent needs to be put into the well trajectory to follow the planned well path. This tangent serves to "step out" the lateral leg of the well to maximize production from a pad (Figure 1.8), while having the surface holes close enough to each other to be able to move the rig easily across the pad. The tangent is kicked off with planned doglegs of 4.0 degrees/30 m at 1,750 m TVD. The tangent is drilled with a conventional directional motor and bit. The directional motor drills vertically in rotary mode, while rotating the entire drill string, with the entire drill string and motor rotating the bit. However, when altering either the azimuth or inclination of the well, a well section is drilled without rotating the drill string but rotating only the end of the motor using drilling mud flow, this is commonly known as sliding drilling. By maintaining a certain direction of the bent motor (also referred to as toolface) the well trajectory can be guided in a certain direction. Figure 1.9 shows an illustration of the difference between sliding and rotary drilling. Once the tangent is achieved, a second point is reach where further inclination is put into the well trajectory to complete the transition from vertical to horizontal. This section of the well is called the build

[10] Invert: mineral oil based drilling fluid

section, where inclination is “built” to 90 degrees to achieve a horizontal wellbore at the heel of the well. Generally, the wells have an inclination slightly higher than 90 degrees to maintain a “toe up” trajectory to allow for drainage of any reservoir fluids. The build section is also drilled with a bent motor and bit. The reason for drilling with a conventional motor and bit is because this allows the operator to achieve an optimum technical and economic rate of penetration. The build is kicked off with planned doglegs of 5.6 degrees/30 m at 2100 m TVD. Figure 1.10 and Figure 1.11 illustrate actual doglegs in the build and lateral sections of a typical well.

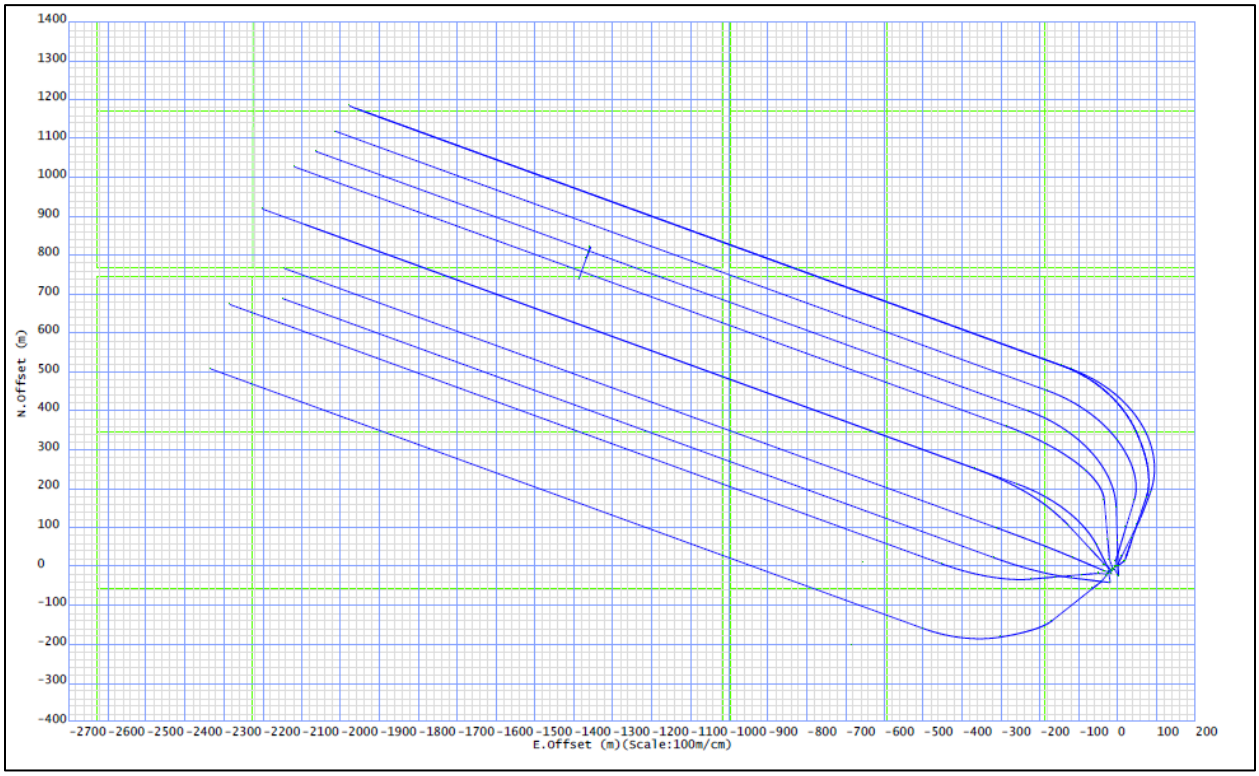

Figure 1.8. Top down view of the operator’s typical well pad layout.

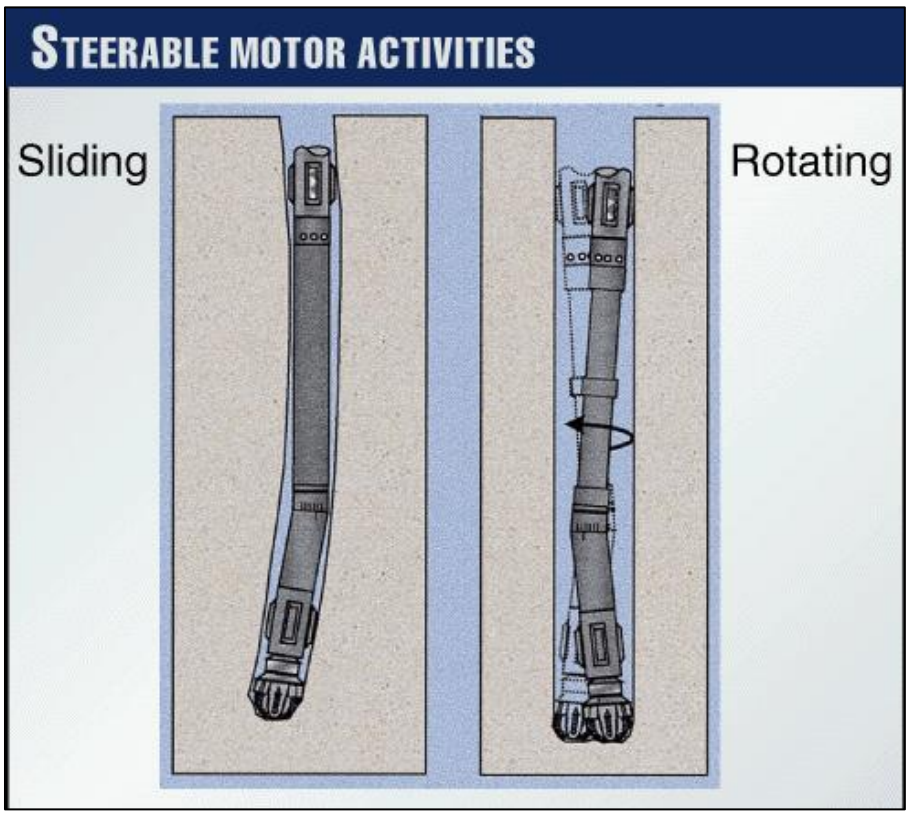

Figure 1.9. Steerable bent motor activities (sliding vs rotating), Oil and Gas Journal (1998).

The lateral leg is then also drilled with a bent motor and bit, generally sliding occurs minimally in the lateral section of the well. Sliding is used to adjust the well path when the positioning of the lateral leg varies too far from the target landing window. The operator gives drilling a general target window with 5 m above and 5 m below the planned well path and 20 m to the left and 20 m to the right.

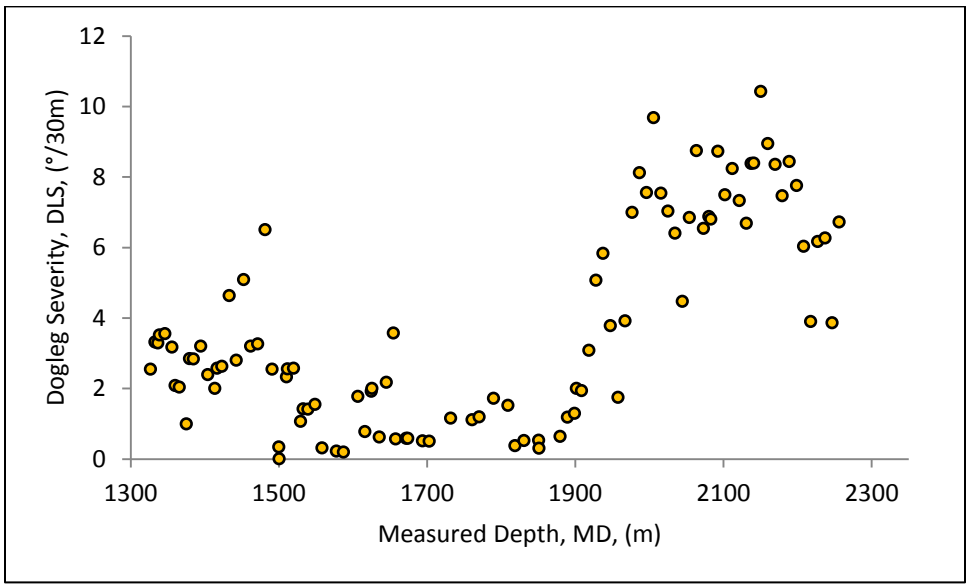

Figure 1.10. Build section typical dogleg severity.

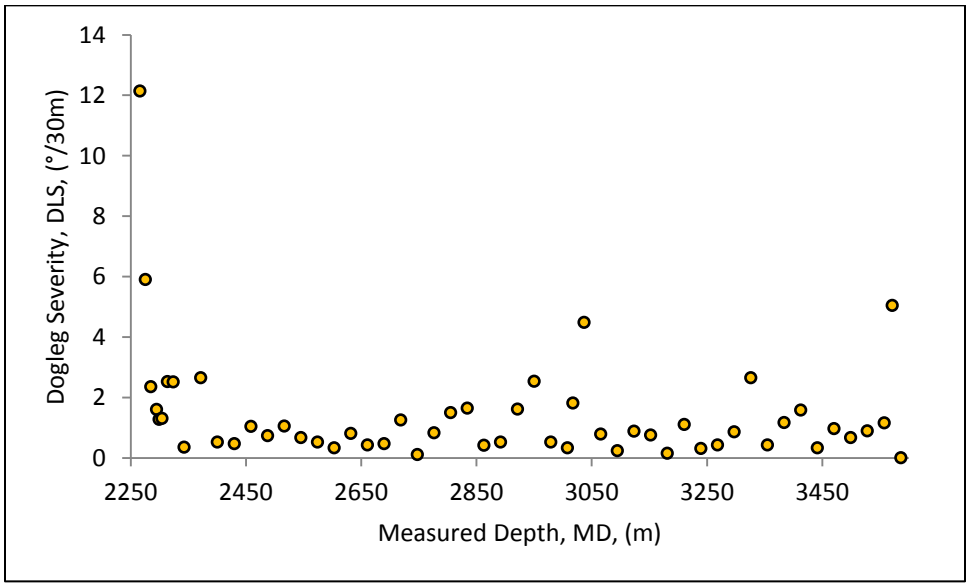

Figure 1.11. Lateral section typical dogleg severity.

Typically, as discussed above, the top vertical section is drilled with fresh water. The fresh water is salted up prior to entering the North Pine Salt with a density of approximately 1200 kg/m^3. The saturated salt water is used until the MWD[11] system loses communication, or until issues with borehole stability or cleaning are encountered. This requires transitioning the mud system from salt saturated water to oil based mud. Oil based muds, unlike water systems, have rheology allowing them to carry cuttings and clean the wellbore better. Furthermore, MWD signals travel better in oil based mud systems. One of the major downsides of oil based mud systems is that bit cooling is a problem due to poorer heat capacity. Furthermore, the rate of penetration is significantly reduced compared to drilling with water. and water aids in breaking up shale and transporting drill cuttings due to dynamic viscosity phenomena. Refer to SPE/IADC 2936B which discusses the relationship between dynamic viscosity and rate of penetration while drilling.

The reduced rate of penetration when drilling with oil based muds is the main driver for delaying the flip to oil based muds for as long as possible. However, when required the mud system is transitioned. An important disadvantage of a water based system is that in the case of a well control scenario (for example a potential blowout) the water systems weight cannot be increased past the 1200 kg/m^3. Oil based mud can be weighted up with barite to much higher weights in the event of a gas influx and the need to kill the well. The operator's rigs typically have 1400-1450 kg/m^3 weight mud on hand at all times to transition to, in the event of a well control scenario.

[11] MWD: measurement while drilling tools are used to take surveys of the well as it is being drilled to accurately map the trajectory of the well. Many formation evaluation well logs can be taken during MWD.

Once the well is landed, 6-7 clean up cycles are done at the end of the well prior to pulling the drill string out of hole. Additional two-clean up cycles may be done in the mid lateral depending on hole conditions, and further clean up cycles are done at the heel to move any remaining drill cuttings up the wellbore. Once the well is cleaned the casing string is run into the hole. Hole cleaning is important due to the fact that it has a large impact on drag and hence on the ability to deploy casing.

The casing string is typically run with an open-hole completion system that utilizes packers and fracturing sleeves (Figure 1.12) to isolate segments of the lateral leg of the well for hydraulic fracturing. The packers and fracturing sleeves are spaced at 100 m intervals. The presence of the packers in the string adds more contact forces, hence more friction which contributes to buckling in the vertical section of the casing string. A stage tool is then set at the heel of the well to allow for the vertical section to be cemented to isolate all formations (but the target reservoir) as well as to act as a secondary barrier to the casing, and to act as a barrier between gas-bearing formations and surface.

Figure 1.12. Completions packer system used in current wells.

The production casing design is primarily driven by the fracturing and fracturing screen-out case. The fracturing is a 63.5 MPa surface load and screen-out is a 69 MPa load. The screen-out case represents an overpressure of the system with 69 MPa. This is the maximum pressure before Pressure Safety Valves (PSV) open to avoid over-pressuring and protect surface equipment. The overpressure seen during a hydraulic fracturing screen out is due to a blockage of the formation that rapidly causes the pressure to build-up due to a lack of flow. This rapid build in pressure and subsequent cut-off at 69 MPa due to the safety valve is illustrated in Figure 1.13.

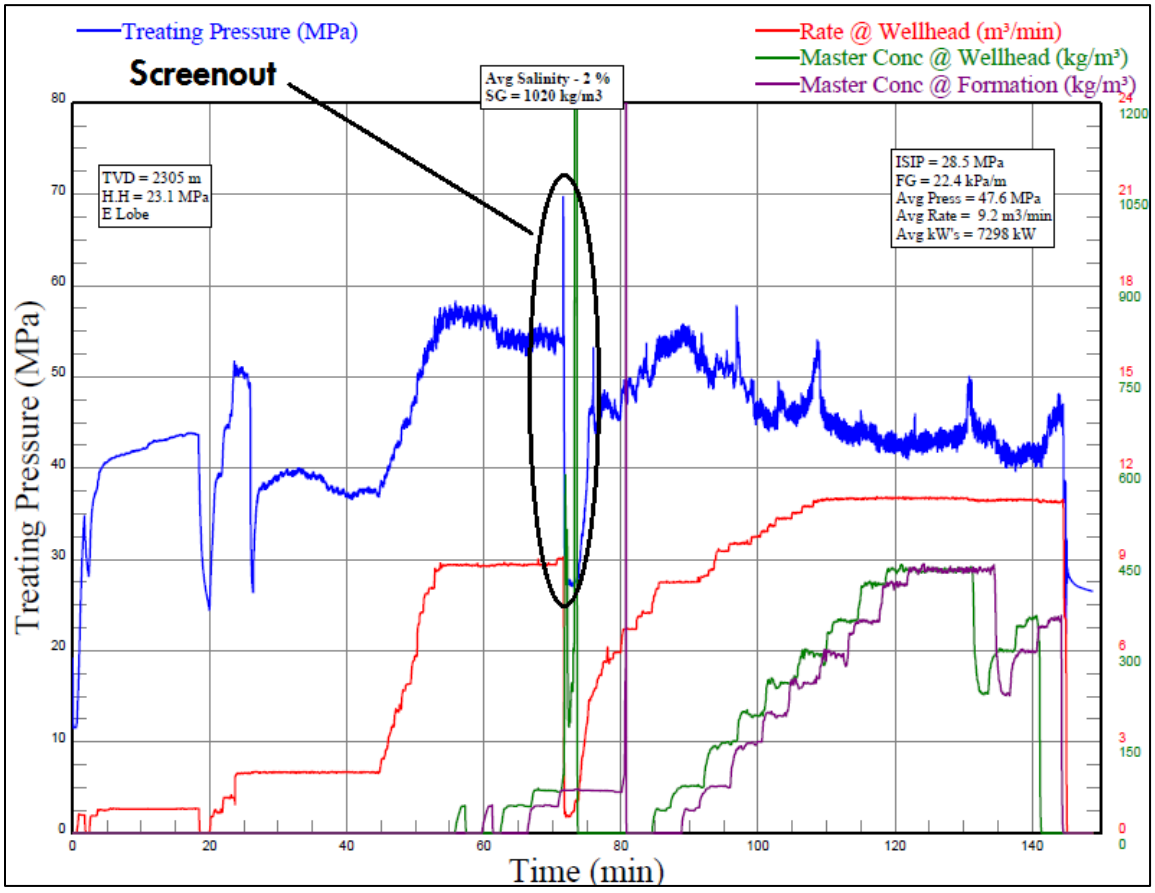

Figure 1.13. Screen-out pressure during hydraulic fracturing operations.

The operator does the hydraulic fracturing stimulation through their production casing to reduce friction losses and maximize pump rates. A typical fracturing job uses 1300 kg/m^3 water based fluid with brine and sands. The operator uses 61 metric ton (T) stimulation per 100m stage. Each fracturing stage includes: 1 T of 50/140 mesh sand, 50 T of 40/70 sand, and 10 T of 20/40 resin sand.

During the fracturing process a special equipment rated to 69 MPa is installed on top of the wellhead, this equipment is the fracturing tree (Figure 1.14).

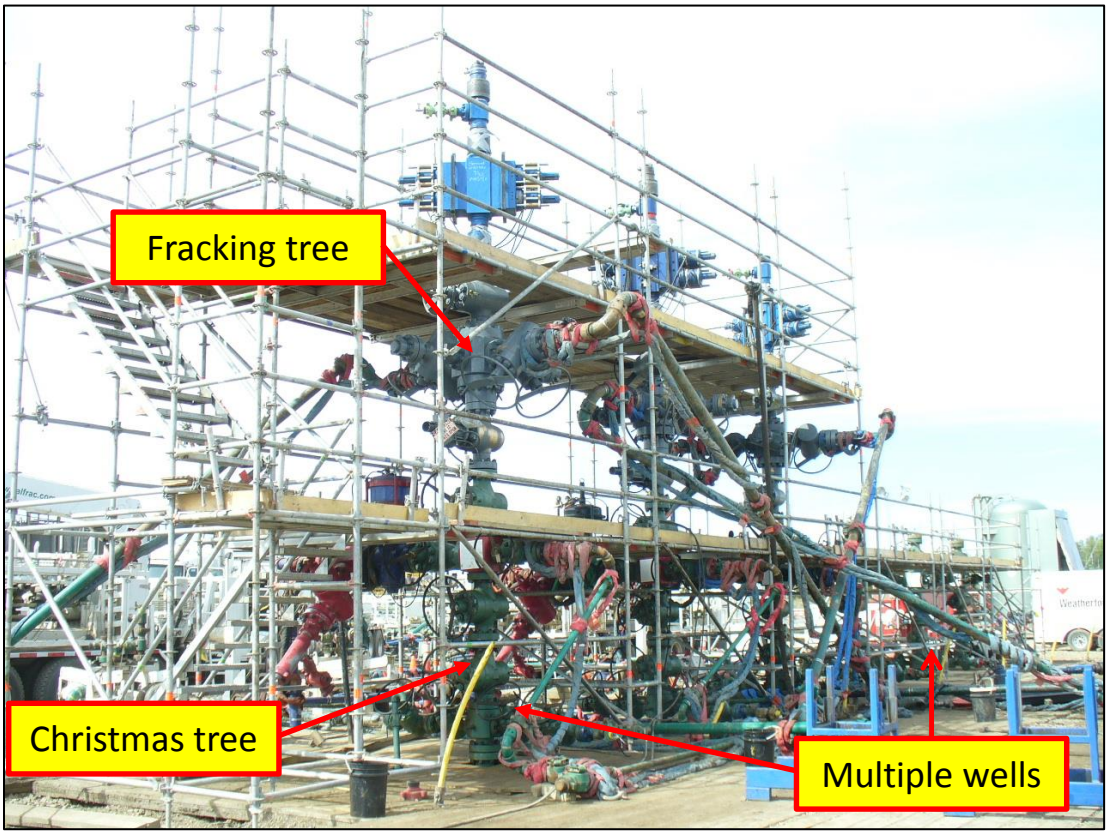

Figure 1.14. Hydraulic fracturing well surface equipment setup.

The typical wellbore temperature profile during a fracturing job is assumed to be 4 °C at surface to 20 °C bottom-hole temperature. This is much colder than the typical temperatures of 10-15 °C at surface and 65-70 °C bottom-hole as can be seen in Figure 1.15.

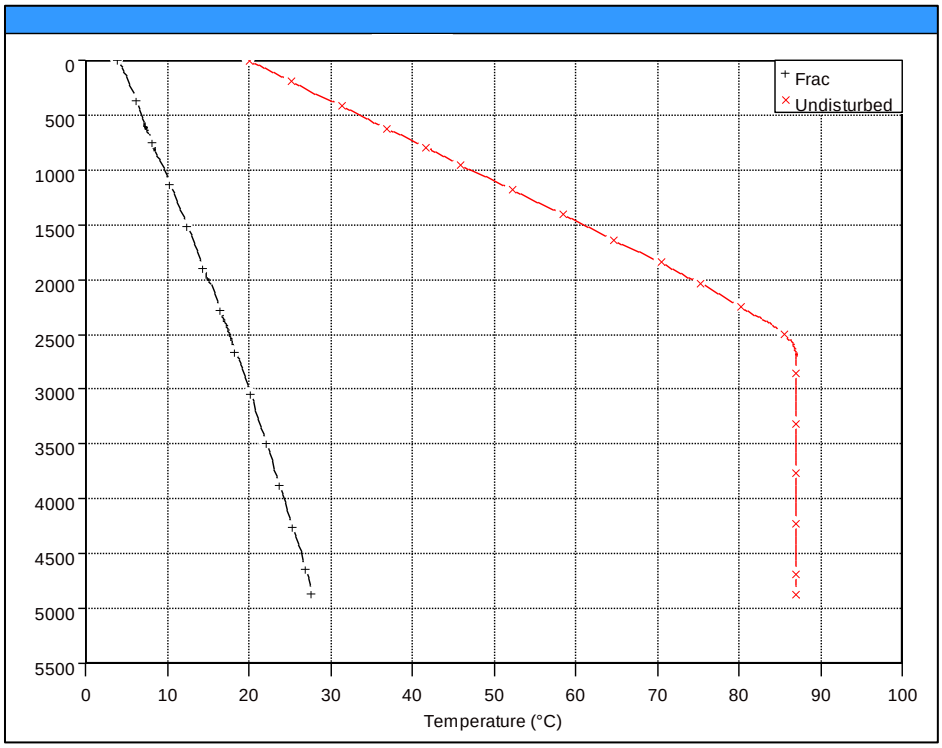

Figure 1.15. Well temperature profile during the hydraulic fracturing operation.

The lower temperatures during the fracturing job are due to the fluid temperatures of the fracturing slurry storage on tanks on location which can vary with weather. Bottom-hole temperatures are as low as 20 °C due to circulation of a cold fluid in the wellbore. This cooling effect happens very rapidly as can be seen in Figure 1.16, in less than an hour the casing is cooled down from undisturbed downhole temperatures to fracturing temperatures. The cooling effect has an impact on the mechanical loads acting on the casing pipe. It is known that lower temperatures will cause contraction of the casing, this would create compression stresses,

however since the pipe is restricted from movement in the wellbore, the effective stress is not compression but tension

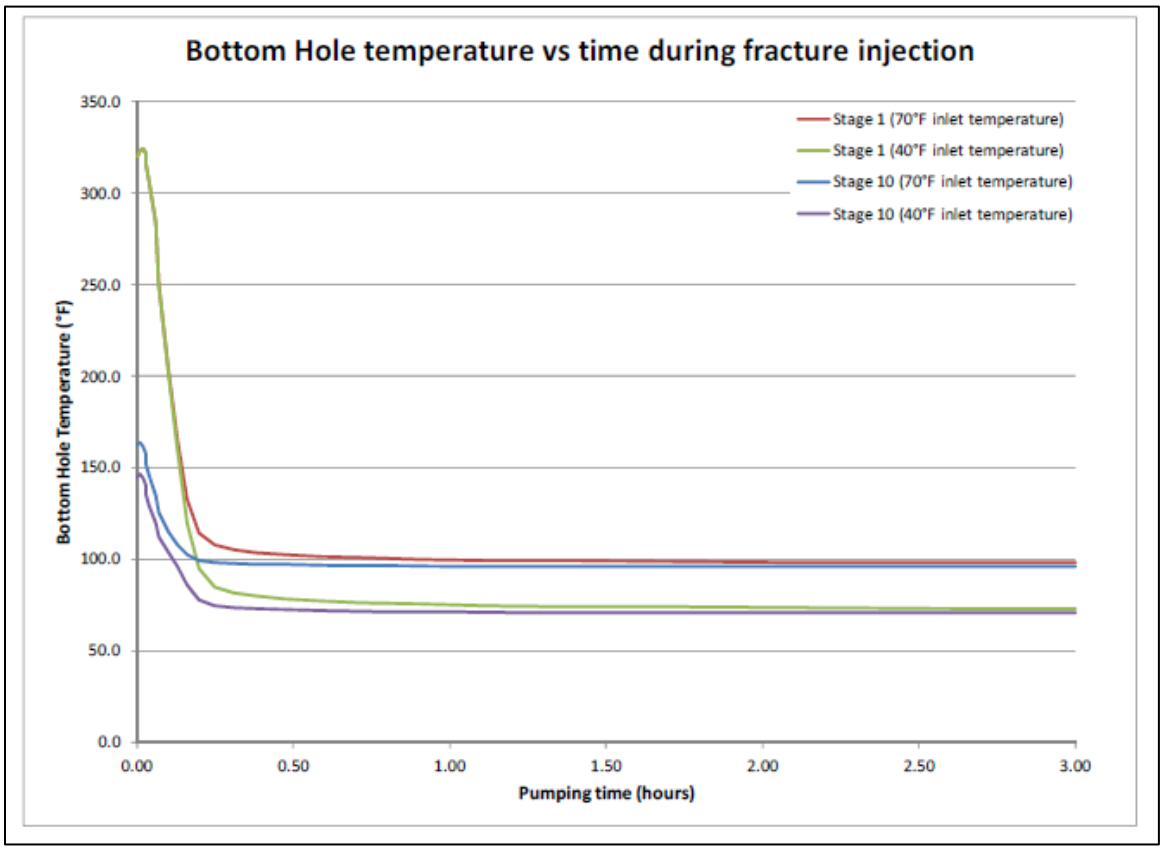

Figure 1.16 Bottom hole temperature vs time during hydraulic fracturing, SPE 151470.

The casing is designed to withstand the loads seen during fracturing of the well as seen in Figure 1.17, Figure 1.18, Figure 1.19. These figures depict the pressure profile seen over the production casing, as well as the Von Mises triaxial envelope and triaxial safety factor (these concepts will be explained in Chapter 2). The compression locked into the string when the casing is landed is included in the triaxial model; however, it does not account for any deformation that may occur while running casing. The operator's current modelling process will be explored further in subsequent sections of this thesis.

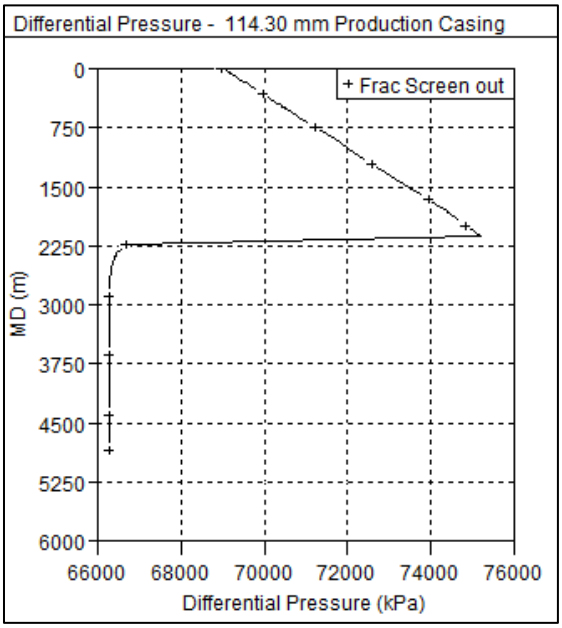

Figure 1.17. Hydraulic fracturing screen-out load differential pressure across production casing string.

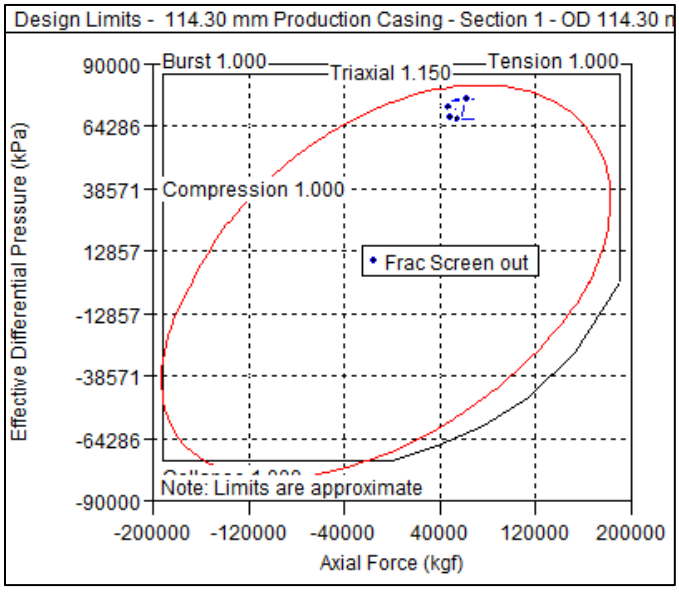

Figure 1.18. Fracturing screen-out design limits plot on 114.3 mm 20.09 kg/m P110 casing.

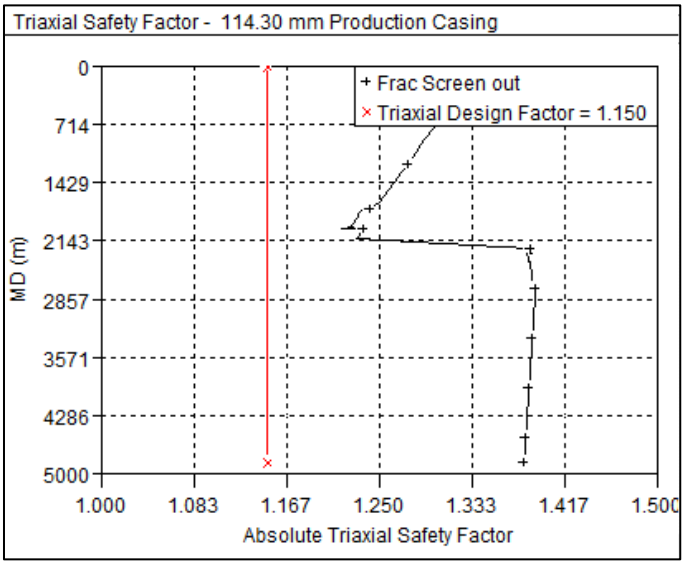

Figure 1.19. Fracturing screen-out triaxial safety factor on 114.3 mm 20.09 kg/m P110.

The operators primarily ran a 'plug and perforate' completions design in the past. This involves running plain casing into the hole and cementing the entire string from total depth to surface. The casing would then be perforated in stages and hydraulic fracturing was done through these perforations. The operator has now moved to primarily open hole completions systems, where the casing string in the horizontal section is not cemented. As mentioned, these systems involve a series of packers and sleeves as seen in Figure 1.20. These downhole tools add complexity due to larger outside diameters equipment, stiffness, and more weight in the lateral section of the well making it difficult to effectively model torque and drag, and buckling of the casing string. The greater diameter results in more friction, which ultimately leads to more buckling in the vertical section of the well.

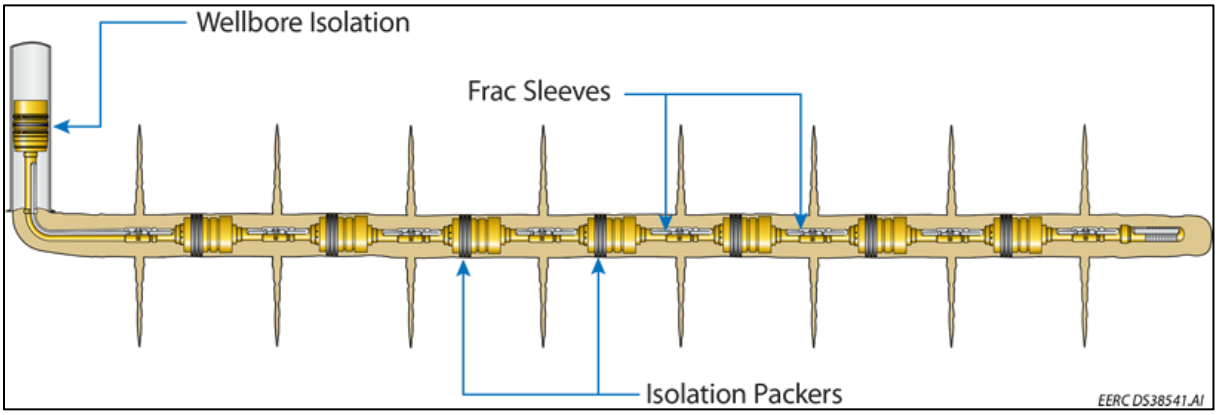

Figure 1.20. Packer and fracturing sleeve spacing and orientation, Energy and Environmental Research Center.

In the past, the operator used to case the wellbore with 139.7 mm casing in 200 mm hole, but it has recently switched to 114.3 mm casing and 159 mm hole. This was done as a cost savings effort. It is worth mentioning that no production decrease has been seen as of yet. An important point to note is that 114.3 mm casing is much less stiff than 139.7 mm casing and is much more prone to buckling. This can be seen in equation (1) which depicts flexural stiffness as a function of the moment of inertia. This relation shows stiffness (*I, m^4*) is proportional to the radius (*R, meter*) to the 4^{th} power; the greater the OD the greater the stiffness.

$$I = \pi * 0.25R^4 \quad (1)$$

Furthermore, the operator used to drill with water based muds only. This resulted in holes that were much more enlarged. A larger than gauge hole results in higher buckling tendency. The switch to drilling with invert based mud in the lateral has greatly reduced the hole enlargement in the wells.

When the casing string is landed at total depth, the full string is landed inside the hanger. As previously mentioned, the operator uses a mandrel hanger design, which does not allow for

relieving tension in the casing string. This results in the casing string always being landed in compression. A mandrel hanger is used due to its ease of use and the fact that the string can be landed and cemented immediately. In addition, the casing is run into the hole very quickly as the operator is performance driven. This can also result in more buckling.

Finally, the operator has had problems with uniform cement on the backside of the vertical section of the production casing. These results in the casing having no back support which results in a potential weak spot that may fail during hydraulic fracturing.

The operator has seen failures in the past due to excessive compression locked in the string prior to fracturing. The reports issued for these failures concluded that the failures were due to compressive and fracturing loads acting together. These two loads in conjunction ultimately caused the failures. Hence, a model needs to be developed to identify a maximum compressive load to avoid casing failure during hydraulic fracturing.

1.3 Production Casing Failures

The operator concerns on casing integrity during hydraulic fracturing started when it experienced six casing failures of which three resulted in a complete loss of well integrity and further well abandonment.

Failures occurred in the vertical or low inclination section of the casing at zones where there is a significant likelihood for buckling due to high axial loading accumulated during the casing installation against the high reaction forces acquired during the installation of the long horizontal sections of the casing.

All casing strings were landed with mandrel hangers instead of slips, which resulted in residual compressive stresses being cemented-in thus increasing the likelihood for buckling.

The formations known for their sour gas contamination are located at depths that coincide with the location where the loads on the casing are highest. In addition, all casings were 114.3 mm, 20.1 kg/m API 5CT grade P-110, a high strength quench and tempered material with very low resistance to sulphide stress cracking.

The casing failures were detected either as sour gas contaminated leaks or sand plugs after about 7-8 fracturing cycles (maximum injection pressure about 62 MPa).

The analysis of the three wells showed that the casing failure in two of them, C9 and C16, consisted in the development of short longitudinal cracks. The caliper logs from the wells provided a more accurate image of the ruptures, C9 log showed a longitudinal casing rupture 12.5 cm long at 1593 m depth in the vertical section of the well as shown in Figure 1.21. The rupture was 1.7 m higher than the closest connection and the caliper data showed that some global buckling was present.

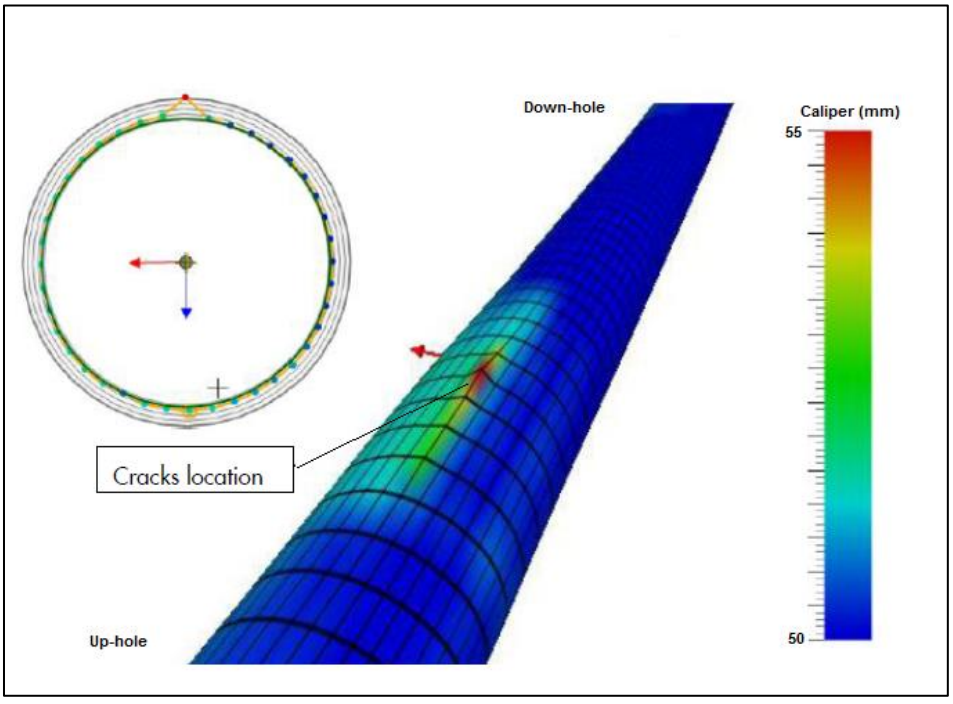

Figure 1.21. Caliper data showing 12.5 mm long through wall crack at 1593 m depth.

C16 caliper log analysis revealed three main features, one at 1591 m, consisting of the start of a 6mm lateral deviation from the casing axial direction that extended for about 2.5 m, a second event was recorded at 1593 m consisting of two through wall cracks in close proximity, 0.3m apart axially and 27 degrees radial spacing as shown in Figure 1.22. The upper rupture was approximately 7 cm in length and the lower rupture was 5cm in length. The H_2S concentration at this location (outside the casing) was reported to be 0.04%.

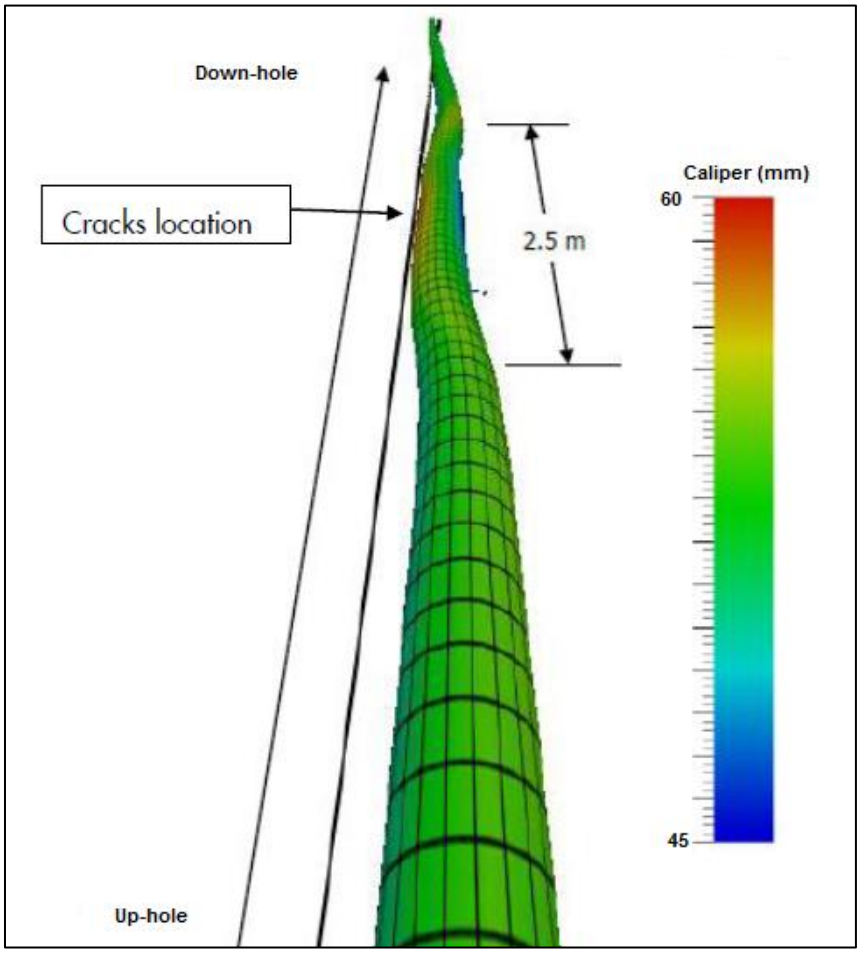

Figure 1.22. Caliper data showing the casing lateral deviation and the location of the cracks.

The C16 well was selected for further analysis due to the unusual crack configuration and at the time of failure, a sour gas leak was not recorded in spite that the casing was crossing a sour gas-contaminated formation.

In order to characterize the events observed, a more detailed analysis of the caliper data was used to define the location, orientation and size of the features observed. A snapshot of the casing cracking is represented in Figure 1.23.

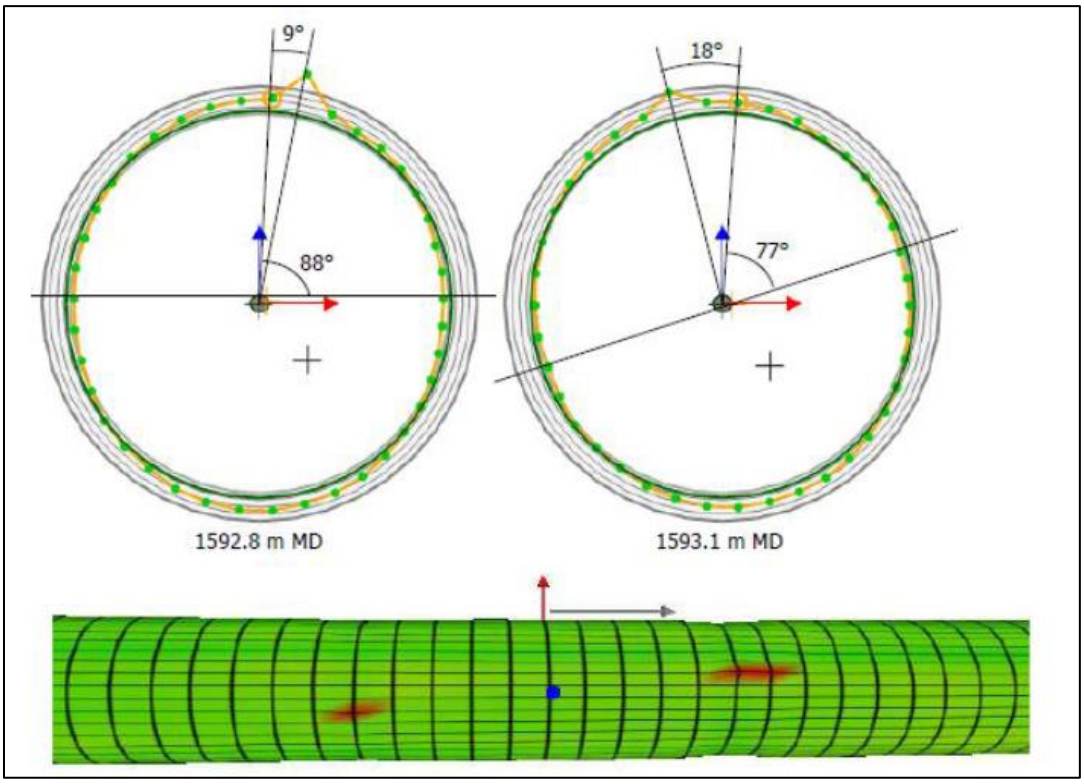

Figure 1.23. Cracks' relative orientation on the casing, 27 degrees radial direction and 0.3 m apart in axial direction.

The cracks' location were on a section of casing that showed a rather sharp but small radial displacement of about 6mm from the pipe axis, extending for 2.5 m. This radial displacement is associated to localized deformation due to pipe buckling.

The correlation between the axial deformation of the casing and the location of the cracks was studied by finite element analysis (FEA). The FEA modelling was used to determine the likelihood for crack initiation under loading conditions that combined the running loads during casing installation and several fracturing pressure cycles. The FEA results were also used to determine the approximate stress and strain values that affected the casing during the two main loading events, the casing installation and hydraulic fracturing pressure cycles.

The conclusions on the casing failure root cause were:

- Borehole enlargement with significant drag meaning that the pipe underwent localized buckling that created alternating bending loads while running in the hole
- The casing was landed with a fluted mandrel hanger which means that the last movement was down adding more compression to the casing string
- The casing was cemented in place without relieving the bending/buckling loads which act as residual stresses
- Hydraulic fracturing operations with highly abrasive fluids pumped downhole which results in additional internal wall loss
- Hydraulic fracturing pressures and temperatures that are cyclic prompting crack growth and propagation
- Longitudinal shape of the cracks that indicated "burst" type of pipe failure

In summary the report issued for these failures concluded that the failures were due to excessive compressive loads and fracturing loads together. These two loads in conjunction ultimately caused the failures. Hence, as indicated previously, a model needs to be developed to identify a maximum compressive load before potential casing failure during hydraulic fracturing.

As discussed previously, the plan for this thesis is to develop a model to identify a minimum hookload (maximum slack-off) value acceptable when running casing into the hole that will prevent a potential failure during the fracturing operations.

1.4 Casing Failures Cost Consequences

Having a casing integrity problem, like the one described previously in Section 1.3, has technical implications that could affect partially hydrocarbon production or even the total loss of a well. The cost associated with production loss or total well loss has an impact on the economics of the field development plan and ultimately on the operators balance sheet.

There are two main issues generated by having cracks or holes in the production casing that will communicate the inside of the production casing with the annular of the well, exposing cement or formations to hydrocarbons being produced, and also exposing the casing to unwanted fluids that are present in top sections of the well (i.e sour gas H_2S).

The first obvious issue is that by having a casing crack it is not possible to transfer pressure to the reservoir during a hydraulic fracturing operation since all the fluid will leak through the casing cracks or pinholes. Consequently, without the hydraulic fracturing reservoir stimulation, the well will not produce any hydrocarbons. The immediate solution for this issue is applying a patch onto the section where the leak is present (Figure 1.24). The cost of the patching operation is around $1 MM per well. It is important to highlight that if the casing leak is located in a

formation with high content of sour gas, the well is not a candidate for patching. In these cases and when the patch operation is not successful, the well is totally lost and has to be abandoned with the additional cost of abandonment estimated in $1.5 MM.

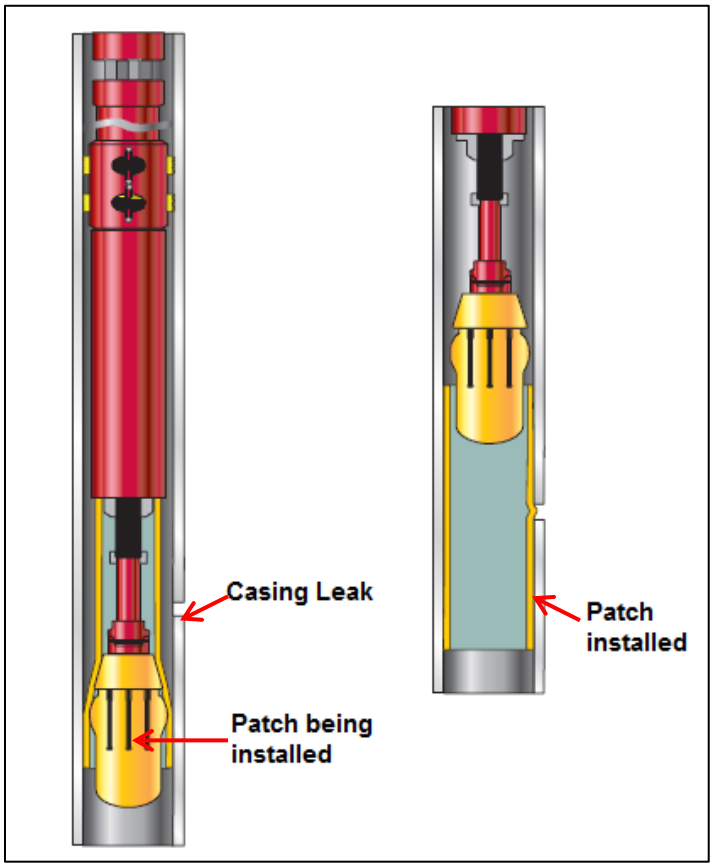

Figure 1.24. Casing Patch system (Weatherford HOMCO Internal Casing Patch).

However, in those wells where the patch has been installed and pressure tested successfully, there is an additional issue. As mentioned before, the operator has started running primarily open hole systems that have fracturing sleeves. The mechanism to activate the fracturing sleeves is balls of different diameters that are pumped downhole. The stages that are close to the toe of the well have smaller seats and use smaller balls to be activated. Conversely, the stages close to the

heel of the well use bigger balls. Placing a patch inside the casing does not allow the larger balls to pass through the pipe. Consequently the reservoir cannot be stimulated in some of the upper stages creating a loss in hydrocarbon production and its associated reduction in revenue.

To estimate the potential loss in production caused by casing integrity problems, it is necessary to examine the production type curves of the field for establishing the total production of the well in its life cycle.

Figure 1.25 shows an example of the type curves for different well production performance. Tier 1 Wells are the best producers.

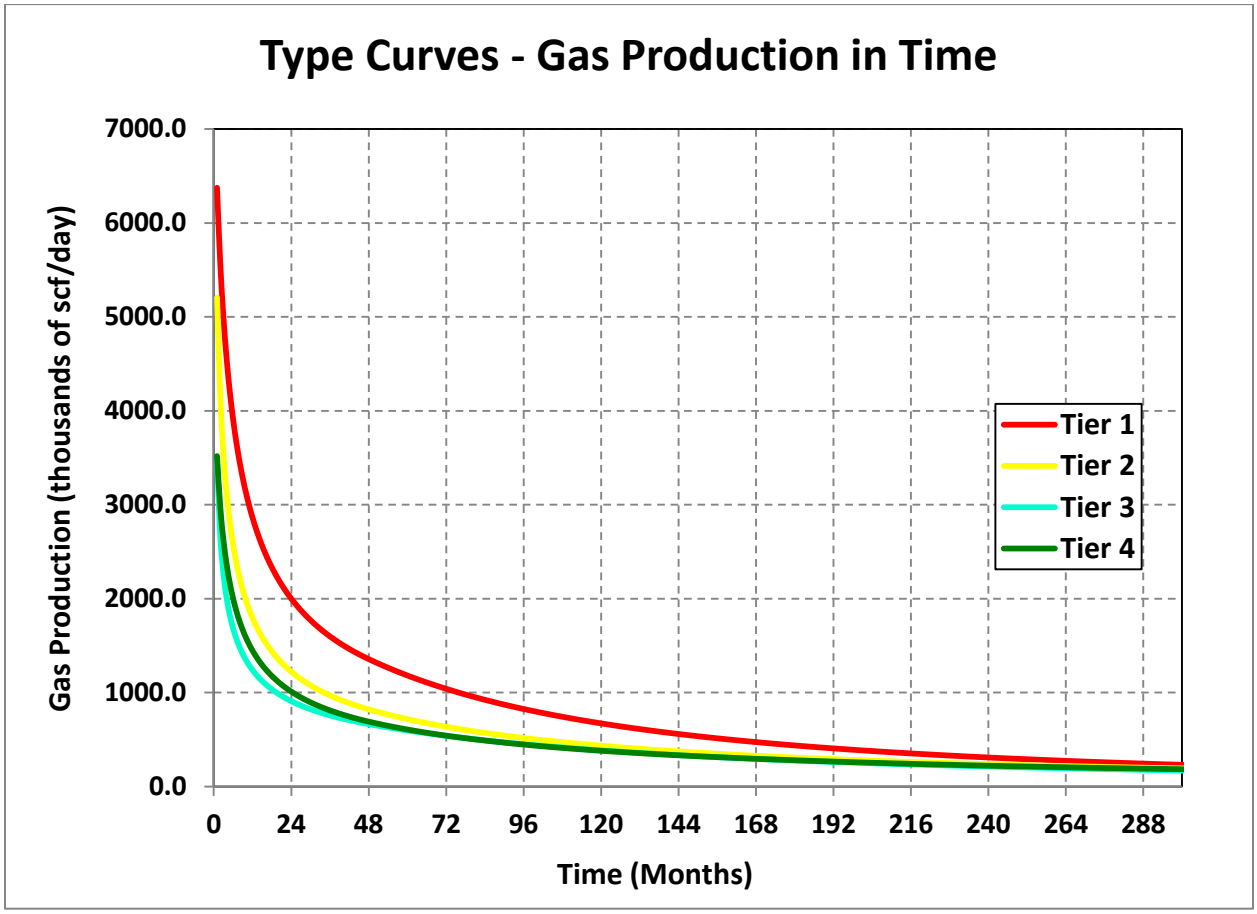

Figure 1.25. Gas production forecast during the total well life of 25 years.

Assuming a lateral length of 1800 m and fracturing stages of 100 m spacing, it is possible to estimate the total production loss due to fracturing stages not carried out because of casing integrity problems as shown in Figure 1.26.

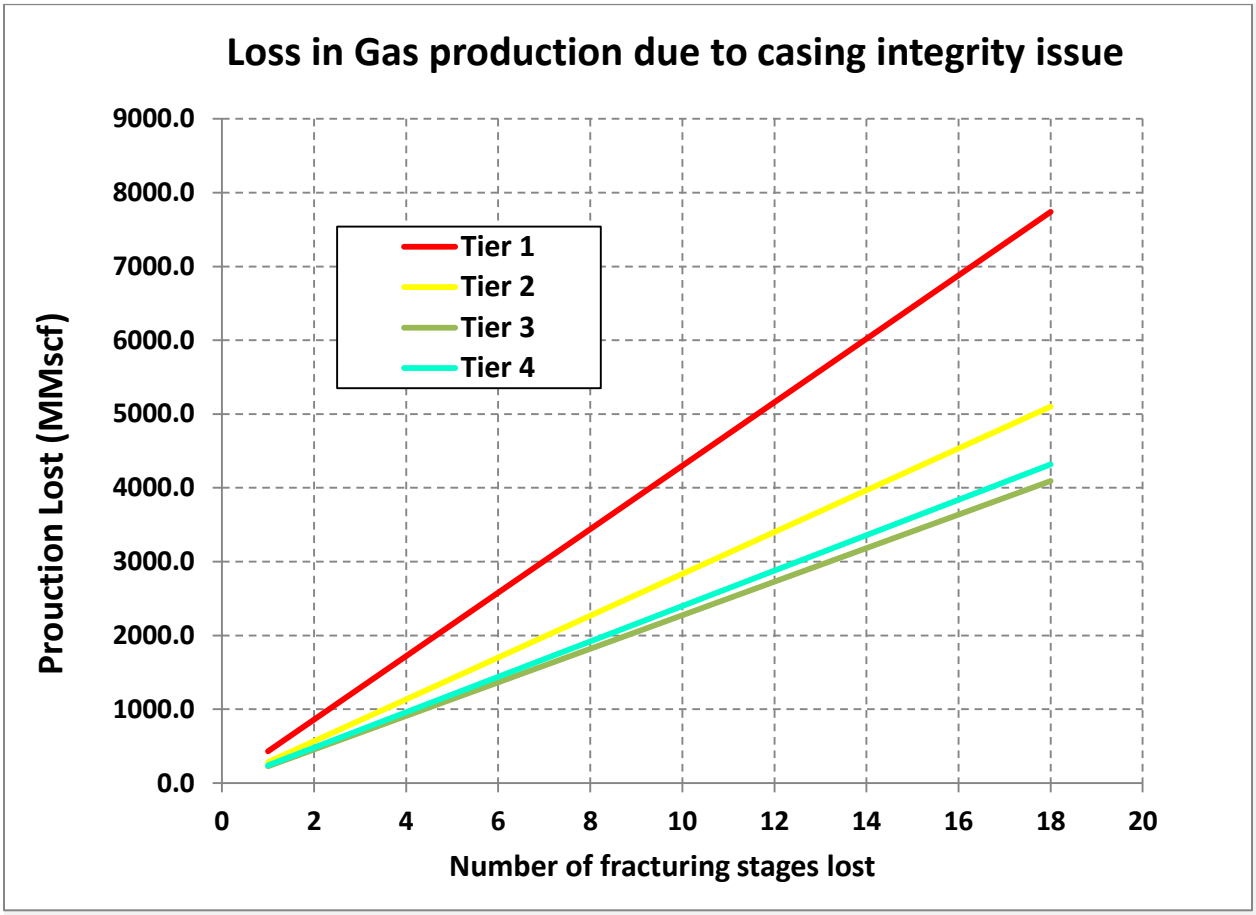

Figure 1.26. Reduction in ultimate gas recovery as a consequence of inability to stimulate a number of stages in the well due to casing failure (millions of standard cubic feet, MMscf).

The total loss in revenue attributed to a casing failure that was patched can also be calculated. The production lost is known from Figure 1.26, and the operator provided the key parameters to do a high level economics analysis (natural gas screen price value and discount rate for project analysis). The results can be seen in Figure 1.27.

From experience, it has been seen that a minimum of four (4) fracturing stages are lost after a patch has been installed. This means that the minimum revenue lost for a casing integrity problem in a Tier 1 (high producer) well issue is $1.6 MM.

Additional to the loss in gas production, there are the well remedial costs. This includes patching the casing (~$1 MM) and the abandonment cost when the well is totally lost (~$1.5 MM).

This cost analysis clearly shows the importance of making the effort to mitigate casing damage emanating from the combination of casing installation practices and hydraulic fracturing loading.

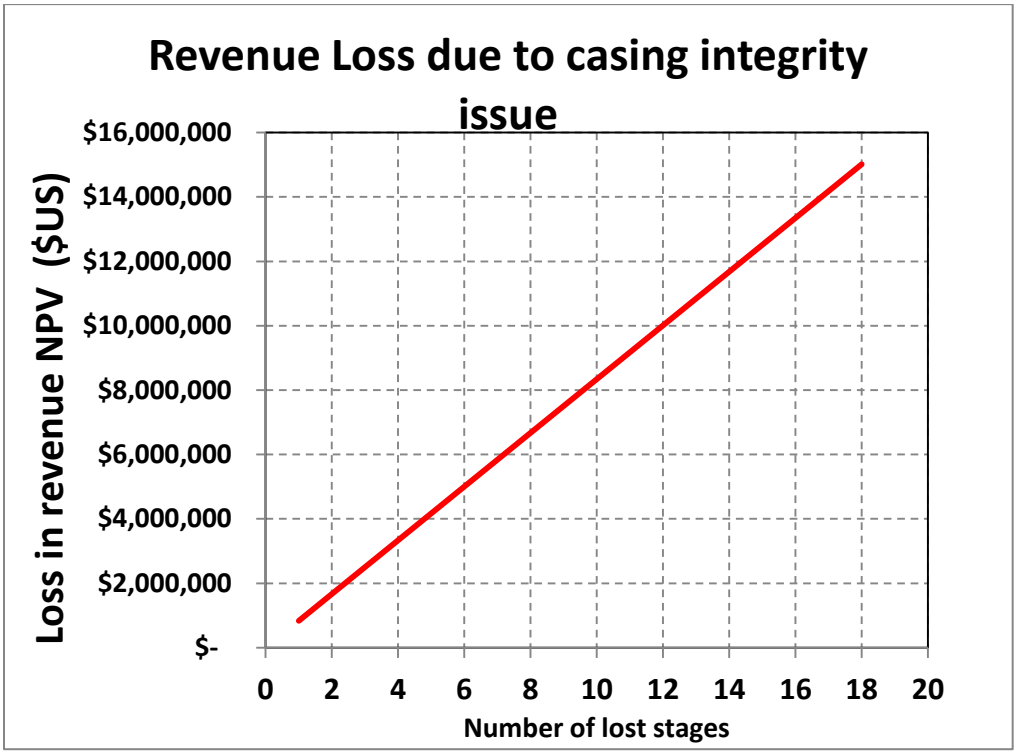

Figure 1.27. Total revenue erosion caused by loss of fracking stages.

Chapter Two: **Casing under Installation and Multi-Stage Hydraulic Fracturing Loading: A Review on Mechanical Design and Failure theory**

2.1 Background

Casing design for wells is an integral part of the engineering discipline whose main objective is to design, build and operate wells, while maximizing monetary value over their entire well life cycle, and guaranteeing safety and environmental standards.

The main objective of the casing design process is to ensure that the well's performance envelope is not exceeded by the predicted and subsequent actual, operating envelope. This is done by predicting the possible loads and conditions within the wellbore and then designing the different well sections with predicted load-bearing capacities (resistances) that exceed those loads.

The predicted loads include a variety of external and internal pressures, thermal loads and forces related to the weight of the casing and contact forces between casing and wellbore walls. The resistances should account for time related aspects such as wear, corrosion and fatigue, which influence the load resistance capacity of the casing string.

The loads that the system (well and installed casing) is going to experience need to be determined. This requires an understanding of the dynamics of the system, the ability to develop a mathematical model of the system, and the skill to be able to use the model to calculate the actual loads. How the system will behave under a number of different loads needs to be modelled and understood.

The mechanical properties of the casing to be used must be clearly understood, including how it deforms under load and also what is its yield and ultimate strength.

In casing design, it is necessary to compare the resistance of the pipe with the loads (from force or pressure) that act on the pipe during multiple operations in the well. It is necessary to differentiate three elements of casing design process:

- Capacity (resistance) of the pipe
- Loads caused by weight, fluid pressures, and temperatures and, sometimes, additional loads caused by reservoir (pore pressures), compaction or salt movement.
- Operations of the well that cause certain combinations of loads to occur

The resistance of the pipe is determined by three basic factors: Geometry (internal and external diameters), weight of the pipe and material grade.

Material grade refers to the type of steel of which the pipe is made. Simply explained, grading corresponds to the strength of the steel so that the higher grades have the greater strength (P110 casing is stronger than L80 casing).

During the design process, one can choose between using a heavier wall pipe (smaller internal diameter leaving a thicker pipe wall) in a lower grade of steel or a higher grade of steel in a lighter weight pipe to meet a particular set of design criteria.

Casing goes under different type of loads during its life cycle from the installation operation to the late production phase and abandonment. Those different stages generate several loading scenarios in the casing. Figure 2.1 shows all the mechanical forces that can act on the casing pipe during its life service.

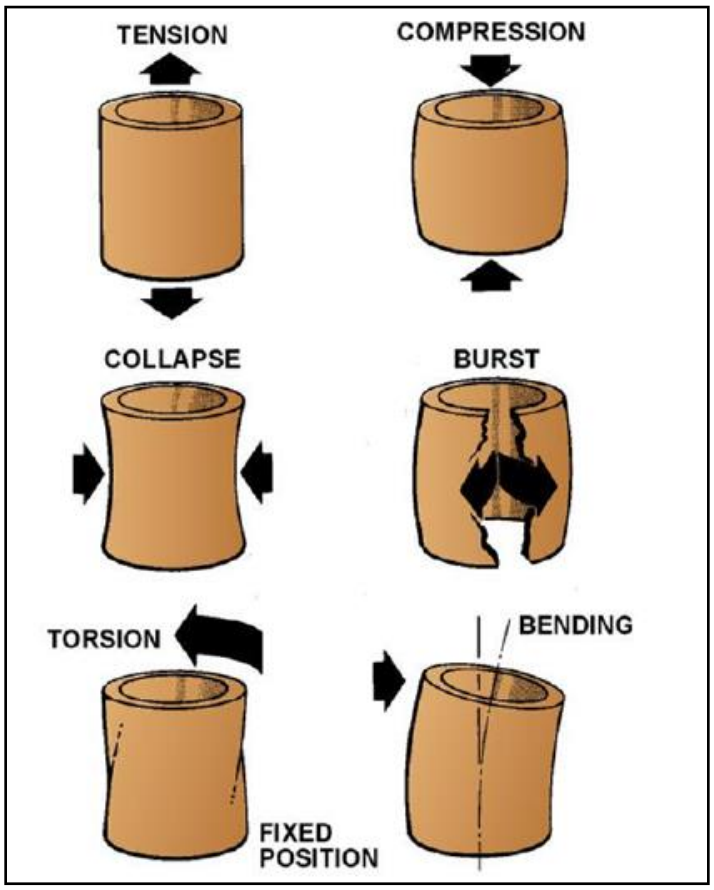

Figure 2.1. Forces acting on casing string during its life cycle (Shell Well Equipment learning handbook).

There are three main types of loads that the casing is subject to: Burst, Collapse and Tensile loading. This project will focus on Burst and Tension in later chapters. Bending is also studied in this thesis; however, bending ultimately has its effect on tension.

2.1.1 Burst Load

Burst loading is defined as the loading that occurs when the casing is in place in the well and is exposed to internal pressure greater than or equal to the external pressure. Burst loading can

result in failure due to yielding, by physical rupture (splitting open) of the pipe or by physical tensile parting of the pipe. Figure 2.2 shows an example of a pipe burst type of failure.

Figure 2.2. Casing pipe rupture due to burst failure.

2.1.2 Collapse Load

Collapse loading is defined as the loading that occurs when the casing or tubing is in place in the well and is exposed to external pressure greater than the internal pressure. Collapse loading can result in failure due to either yielding of the pipe or structural collapse (closure) of the casing cross section. Structural collapse can occur either due to yielding or due to instability of the cross section without yielding.

Figure 2.3. Casing pipe failure due to structural collapse.

2.1.3 Tensile Load

Tensile running loading is defined as the loading that occurs during the process of running the pipe into the well and setting it in place (installation process). This essentially is a loading during which internal and external pressures are balanced and do not play a role. Once the pipe is in place, residual stresses due to bending deformation can be trapped in the casing, once the casing string is installed the structural integrity of the pipe is defined by the burst and collapse loadings described previously. Depending on the strength of the pipe body and the connection, a pipe can fail during tensile installation loading in different forms:

- Exceeding yield stress of pipe body
- Exceeding yield stress of connection
- Parting of the connection
- Damage to the connection causing loss of containment

2.1.4 Casing material mechanical properties

The way in which a material behaves is described as its mechanical properties. When forces tend to stretch a material it is said to be in tension. When the forces squash the material it is said to be under compression. When forces tend to twist the material or to make one part of it move relative to another part it is described as being in shear.

The main mechanical properties that can be measured are:

- Stress / Strain
- Yield and tensile strength
- Stiffness - Young's Modulus
- Hardness.
- Toughness (Impact resistance)

2.1.4.1 Stress and Strain

Stress and strain are the quantities used to compare the effects of a force on a material. Instead of considering applied force, stress is used; and instead of extension (or compression), strain is used.

Stress is the force per unit area, which has the same units as pressure. The metric unit for stress is Newton per square metre, N/m^2, or Pascal, Pa. Stress allows comparison of the effects of a force on different cross sectional areas of steel and also on different types of steel.

While the tensile strength of steel relates to the ultimate stress that leads to failure of steel, the behavior of steel when subjected to stress is more complex. Strain is the change in dimensions of steel when subjected to stress. Strain is a relative measurement rather than an absolute value and

as such does not have a unit. Consequently, if a 1 meter steel bar stretches by 0.1 meter under load, the strain would be expressed as: $\Delta L/L = 0.1/1$, this is 0.1 or 10% strain.

2.1.4.2 Yield and Tensile Strength

A tensile test is used to find out the relationship between the load applied and the resultant elongation of a material as it is stretched. A sample is placed in a machine which pulls one end away from the other fixed end. A tensile force will stretch and, possibly, break the sample (Figure 2.4).

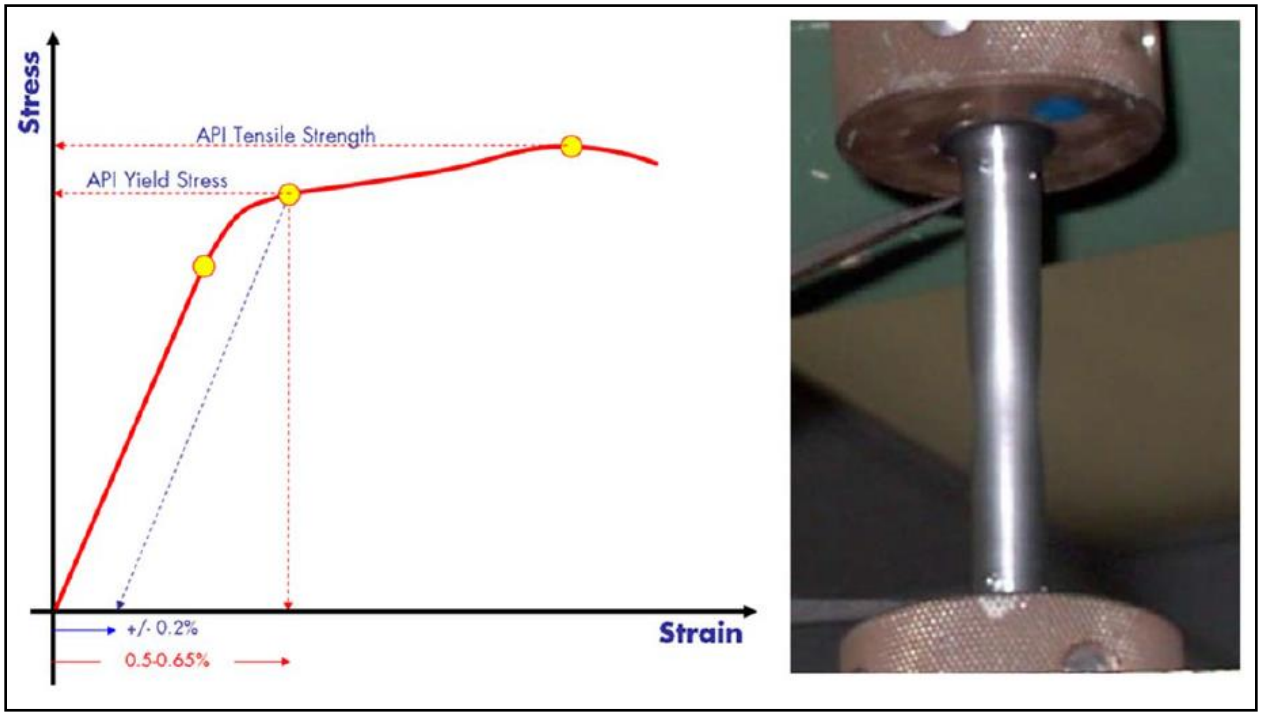

Figure 2.4. Behavior of a specimen when subject to increasing stress (tensile) (Casing Materials – Shell WLP).

The load needed to produce a given elongation or to break a sample will vary depending on the cross sectional area of the sample. For this reason the load is usually converted to stress before results are reported. Stress is a more useful measurement than load because it is constant for a given material. Test final results make possible to compare the strengths of different materials and different test pieces. When steel is placed under load the crystalline structure of the steel is placed under load. The crystal lattice structure defines how steel responds when stressed by combination of burst/collapse, tensile and torsional loads. The structure of the steel can withstand the load initially. If the load is released the steel will return to its original condition. If, however, the load exceeds a specific value, the crystals in the steel will move relative to each other along a slip plane (Figure 2.5).

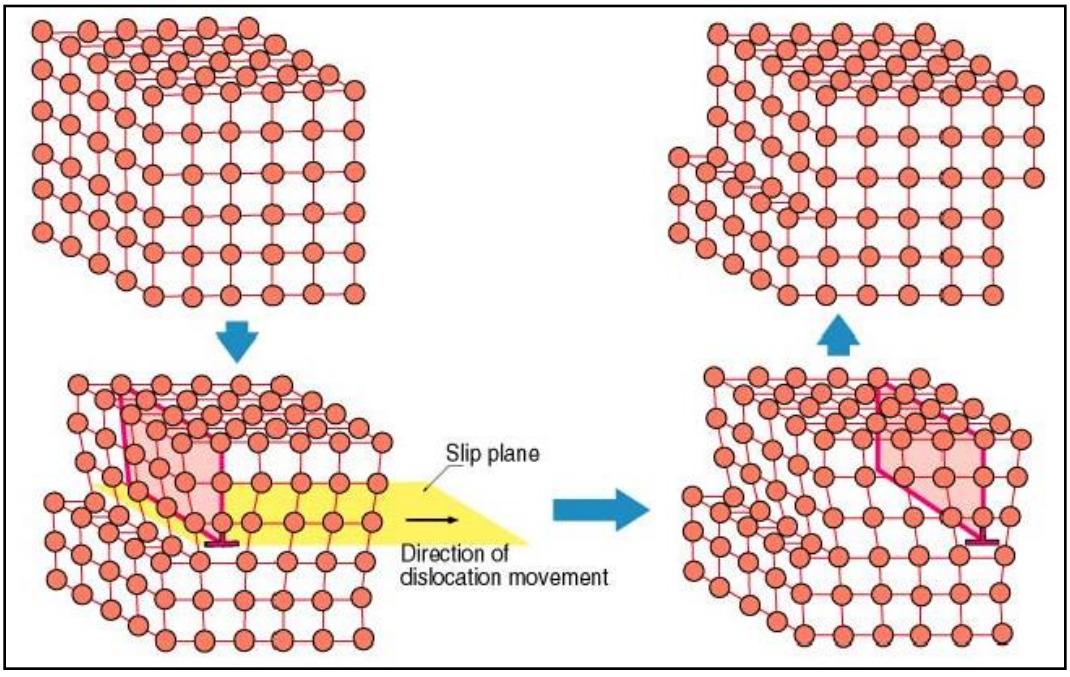

Figure 2.5. Effect of yielding on the steel crystalline structure (Casing Materials – Shell WLP).

Once this slippage has occurred the steel will not return to its original shape and permanent or plastic deformation has occurred. The crystalline structure of the steel has been altered. Because the steel is a three dimensional structure this effect can happen in any direction, depending on the combinations of loads that are being applied to a piece of casing. It is of the outmost importance to not consider each load independently but to combine them to determine the load being applied at the crystalline level of the steel. The result of combining these loads is called the Effective or triaxial (3 axis) stress. The process for doing this was defined by Richard Von Mises in 1913. The ultimate objective in casing design is to ensure that the equivalent stress must always be less than the level of stress that will cause yield in the pipe.

From the tension test, two values can be obtained: The Ultimate Tensile strength and the Yield strength. The ultimate tensile strength is the maximum stretching stress that the bar can withstand before breaking and is often reported, however it is not very useful engineering data. Instead the most useful measure of strength is the Yield strength (YS) which relates to a point in the stress/strain curve when yield begins.

The ultimate objective in casing design is to ensure that the equivalent stress (Von Mises triaxial) must always be less than the level of stress that will cause yield in the pipe (yield stress).

2.1.5 Pipe Burst Design

Pipe burst design is governed by the degree to which the Von Mises equivalent stress is below yield during loading where the internal pressure is greater than or equal to the external pressure.

If the von Mises equivalent stress ever equals or exceeds the yield stress, then the pipe permanently has yielded regardless of whether the load has been decreased so that the equivalent stress is reduced below yield. The calculation of the von Mises equivalent stress is a proven

means of combining the influence of individual stresses in order to account for the way that stresses combine to approach yielding. This calculation depends on stresses generated by pressures (the radial stress and the hoop stress) and by stresses generated by axial load (the axial stress). Therefore, the axial load is as important as the internal and external pressure for calculation of how close the loading brings the pipe to yield during burst design.

2.1.6 Tensile Running Design

Pipe tensile running design occurs while the pipe is being run into the well or pulled out of the well. Internal and external pressures are normally balanced and the temperature is not significantly changing during the operation, so that only the weight along the pipe and the bending and running-drag forces and possible dynamic (shock) loading influence loading.

The tensile (compressive) load during operations of the well with the pipe installed in place is also considered as part of the burst and collapse design processes, not as part of the running design process.

Because running loading is one-dimensional (pressures are balanced and do not come into play), the tensile running design of the pipe is determined only by comparing the pipe specified minimum yield strength with the axial stress, where the axial stress is determined by the running axial force divided by the pipe cross-sectional area. It is noted that in this particular operation, the Von Mises equivalent stress also reduces to the axial stress, so that this operation is still only checking equivalent stress compared with yield stress just as in burst design.

However, when the casing is being run into the well, buckling may occur. Buckling will cause permanent deformation of the casing into sinusoidal or helical shape (these concepts will be explained later). With the plastic deformation, residual stress will be trapped in the casing once

the installation operation is finished. Those residual stresses will have to be added to the triaxial analysis for subsequent loading such as multistage hydraulic fracturing.

2.2 Triaxial Stress Analysis

Pipe strength is most accurately described by triaxial yield. Historically it has been described in uniaxial terms such as in API 5C2 but in reality pipes are subjected to multiple pressure and axial loads at the same time. The loads a pipe can be subjected to can be summarized as three principal stresses (Figure 2.6):

- Tangential or Hoop stress: stress that results from the pipe trying to resist ballooning of the pipe due to internal pressures
- Axial stress: results from tension and bending
- Radial stress: results from pressures acting on the outside and inside of the pipe

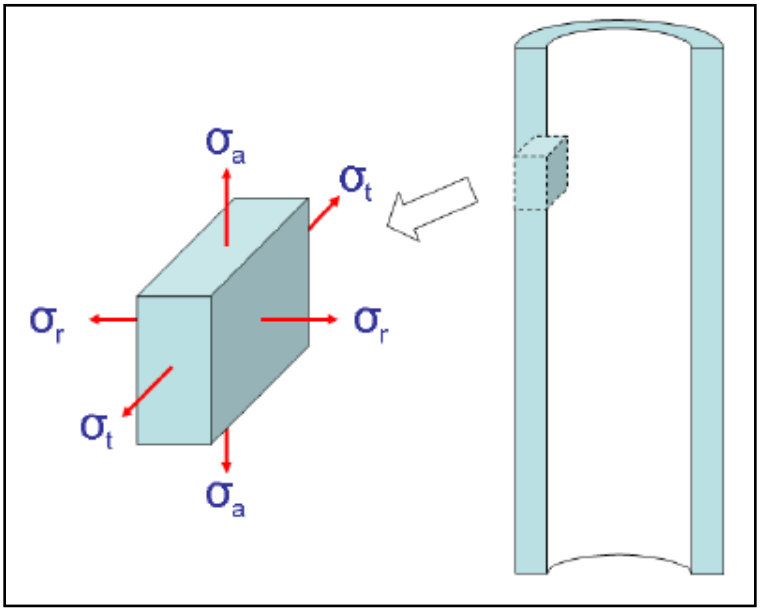

Figure 2.6 Von Mises principal stresses or triaxial stresses (Strength of tubulars, Shell WLP).

These stresses are not cumulative, and interact with each other, so in effect a different internal pressure is required to yield the pipe at differing axial loads.

Failure of the pipe is identified when the von Mises equivalent stress is found to be greater than the yield stress of the pipe. The Von Mises equivalent stress is calculated from the three stresses mentioned above using the following formula:

$$\sigma_{VME} = \sqrt{\frac{1}{2}[(\sigma_t - \sigma_r)^2 + (\sigma_t - \sigma_a)^2 + (\sigma_a - \sigma_r)^2 + 6\tau^2]} \quad (2.1)$$

Where the subscript ***t*** corresponds to tangential stress, ***r*** to radial stress, ***a*** to axial stress and ***τ*** to torsional stress. Torsional stress can be added into the equation in the event that the pipe is being rotated. Axial stress is a combination of tension/compression and bending effects on the pipe. Axial tensile stresses are calculated from the following equation:

$$\sigma_a = \frac{F_b}{\frac{\pi}{4}*(OD^2 - ID^2)} \quad (2.2)$$

Where σ_a equivalent to axial stress (MPa), *Fb* is equivalent to the buoyed weight of the pipe (newton), *OD* is equivalent to nominal outer diameter and *ID* is equivalent to nominal internal diameter (meter).

Axial bending stresses are calculated from the following equation:

$$\sigma_b = \frac{E * r * DLS}{191} \quad (2.3)$$

Where σ_b is equivalent to the bending stress (MPa), r is is the radial coordinate to the point of interest, OD in this thesis (meter), DLS is the dogleg severity (degrees/30 meter), E is Young's modulus (MPa), and the constant "191" is to obtain stress units in pascal. The total axial stress can be found as the sum of the average axial stress and bending stress. The radial stress on the outside of the pipe can be found using the following equation

$$\sigma_{ro} = -1 * P_o \quad (2.4)$$

Where σ_{ro} is equal to the radial stress on the outside of the pipe (Mpa), and Po is equal to the pressure on the outside of the pipe (MPa).

Similarly the radial stress on the inside of the pipe can be found using the following equation

$$\sigma_{ri} = -1 * P_i \quad (2.5)$$

Where σ_{ri} is equal to the radial stress on the inside of the pipe (MPa), and Pi is equal to the pressure on the inside of the pipe (MPa).

The tangential stress on the outside of the pipe can be found with the following equation

$$\sigma_{to} = \frac{2P_iA_i - P_o*(A_o+A_i)}{(A_o-A_i)} \quad (2.6)$$

Where σ_{to} is equivalent to the tangential stress on the outside of the pipe (MPa), *Po* to the pressure on the outside of the casing (MPa), *Pi* to the pressure on the inside of the casing (MPa) and *Ai* to the area inside and *Ao* to the area outside of the casing (square meter, m^2).

Similarly the tangential stress on the inside of the pipe can be found with the following equation

$$\sigma_{to} = \frac{P_i*(A_o+A_i) - 2P_oA_o}{(A_o-A_i)} \quad (2.7)$$

From the above formulas a triaxial stress envelope (Figure 2.7) can be generated that calculates the maximum pressure that the can be applied to the pipe at given axial loads for the equivalent stress to equal the yield stress.

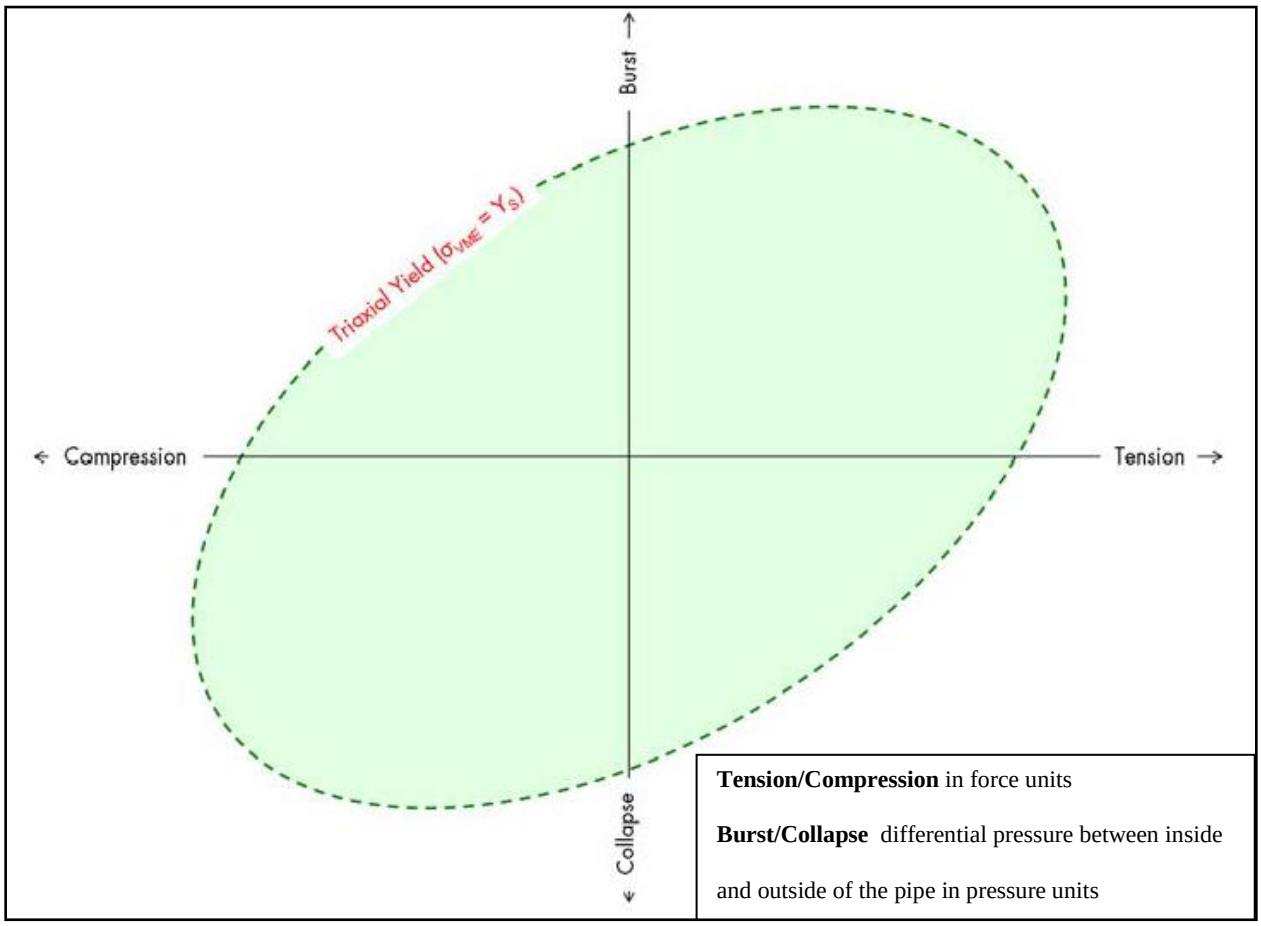

Figure 2.7 Representation of triaxial yield envelope, (Strength of tubulars, Shell WLP).

This calculation results in a triaxial yield ellipse that indicates the failure bounds of the pipe for given axial and pressure loads. It is important to note that the ellipse generated with this method assumes a constant external pressure so a new ellipse should be created when external pressure changes (Figure 2.8).

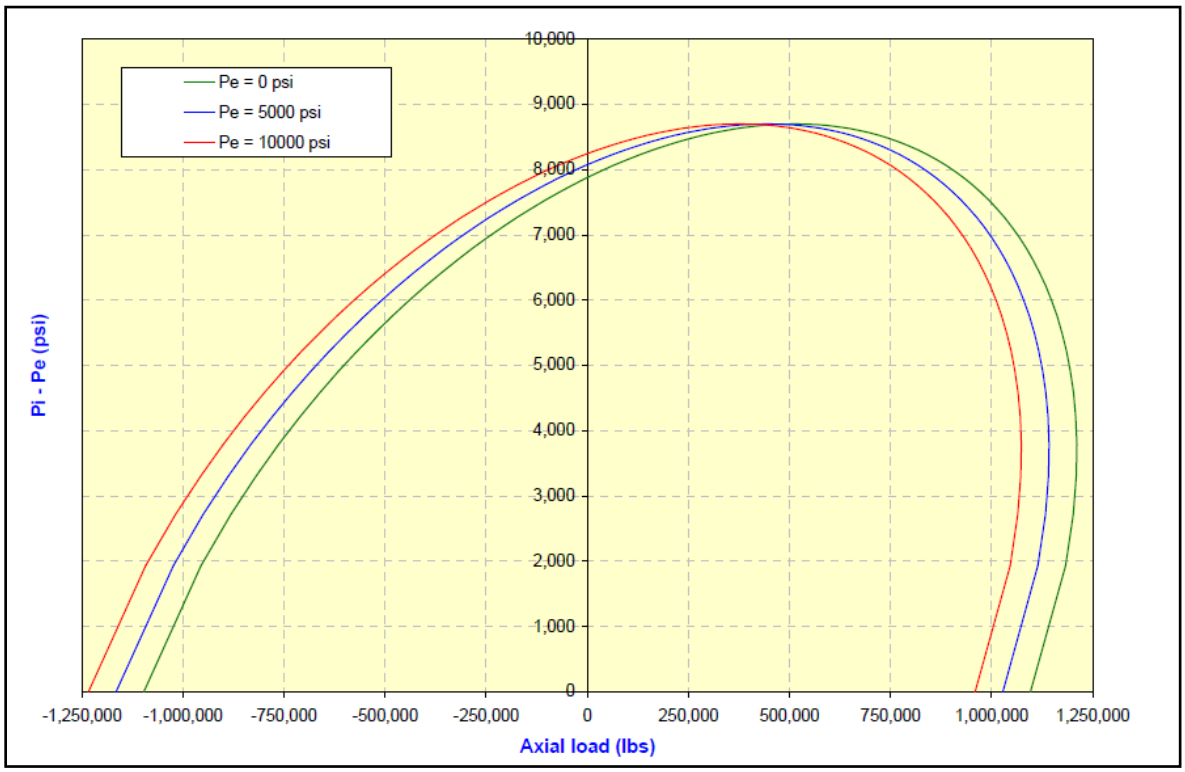

Figure 2.8. Triaxial envelope shift with external pressure change (Strength of tubulars, Shell WLP).

From the triaxial analysis the key point is that all the possible combination of loads acting on the casing must be inside the triaxial envelope to ensure casing integrity.

2.3 Torque and Drag Modeling

As it is evident, installation loads (tension/compression and bending) are a key input for the triaxial analysis. Torque and drag modeling is an important tool the well engineers use to estimate the loads acting on the casing during the installation process.

Torque and drag modelling is an extremely valuable tool used for well planning to ensure the "drilling a well" plan can be executed effectively. Torque and drag models have existed in industry for decades in various forms. Recently, there has been some advancements in

modelling, specifically the development of stiff string algorithms. This section will explore the two main torque and drag model types, stiff string, and soft string.

Torque and drag modelling is an advanced mathematical simulation of the forces acting on the casing when it is being run into the well or pulling out of it. Torque and drag modelling is used for multiple reasons when planning a well. Firstly, it is a method to ascertain if the well can be drilled with the available equipment, in this case, drill string. Furthermore, it can be used to determine the limit of drilling with the current equipment. For example, torque and drag software was used recently by the operator to determine the maximum lateral length the rig could drill. Torque and drag is used for both drilling modelling and running casing modelling. This paper will focus primarily on running casing. In addition to aiding in well planning, torque and drag modelling can be used in real time to watch for any deviations from the plan to allow for a fast response to any issues that may arise.

Historically, Torque and drag has been done with two different types of mathematical algorithms: Soft and stiff string models.

The soft string torque and drag model developed by Johancsik in 1973[12] is called soft string because it assumes the pipe string is a weighted cable without stiffness and ignores pipe bending stiffness effects. The pipe is effectively treated as a heavy rope that lays across in constant contact to the wellbore. The shape of the drill string is exactly the same shape as the wellbore with the same exact coordinates at each point. The soft string model only accounts for gravitational and frictional drag forces on the string. The resistance to movement of the drill string is calculated as a force equal to the normal force multiplied by a coefficient of friction,

[12] Torque and Drag in Directional Wells, Johancsik, Dawson, and Friesen, 1973.

where the normal force is equal to the contact force between the pipe strings and wellbore that is caused by gravitational force. The normal force can be calculated from the following equation:

$$F_N = \sqrt{(F_T \Delta\propto sin\bar{\theta}\,)^2 + (F_T \Delta\theta + W sin\bar{\theta}\,)^2} \quad (2.8)$$

Where F_N is the normal force acting on the element (newton), F_T is the increase in tension over the string element (newton), $\Delta\propto$ is the change in azimuth over the string section (radians), $\Delta\theta$ is the increase in inclination angle over the string element (radians), W is the buoyed weight of the string section (newton), and $\bar{\theta}$ is average inclination angle of the section (radians). The normal force is used to determine changes in moment and tension as illustrated in Equations 2.9 and 2.10.

$$\Delta M = \mu F_N r \quad (2.9)$$

$$\Delta F_T = W cos\bar{\theta} \pm \mu F_N \quad (2.10)$$

Where ΔM is the change in moment in the string section (newton-meter), r is the radius of curvature of the string section (meter), and the other parameters were explained previously. The model splits the string into multiple small sections that transmit compression, tension, and torsion. Figure 2.9 shows a pipe section diagram with the forces acting on it.

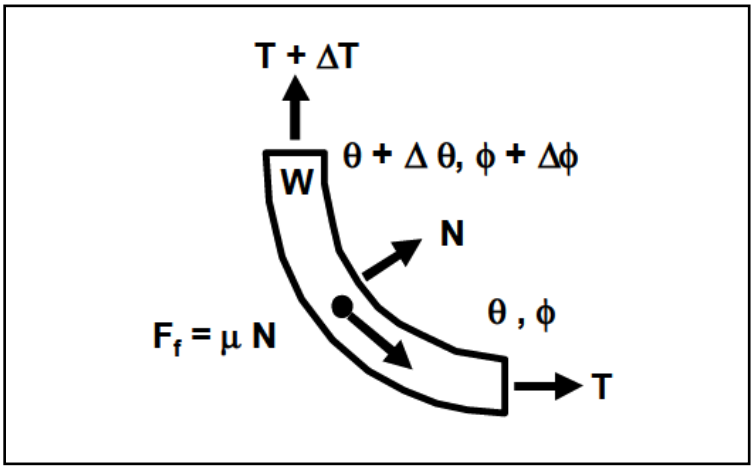

Figure 2.9. Forces involved in the soft string torque and drag model.

The soft string model completely ignores radial clearance and hence packers systems, fracturing sleeves, drill collars, heavy weight drill pipe, stabilizers, or any other sections of the pipe with a high diameter that may cause a restriction and hence more drag do not affect the model in any way other than by the weight of these respective components. When soft string models were initially created, horizontal wells were extremely rare and drill pipe was never intentionally compressed, hence buckling was rarely a concern. However, the advent of horizontal wells in the 1980's required the drill pipe to be run in compression. It is extremely important to be able to predict the onset of buckling to avoid drill string lock up. Current models utilize coiled tubing simulation in conjunction with soft string models to predict the minimum compression in the string required to cause helical buckling. These results are compared with the torque and drag data to determine if buckling will occur in certain sections of the well. Figure 2.10 illustrates how a soft string model visualizes a string within the wellbore.

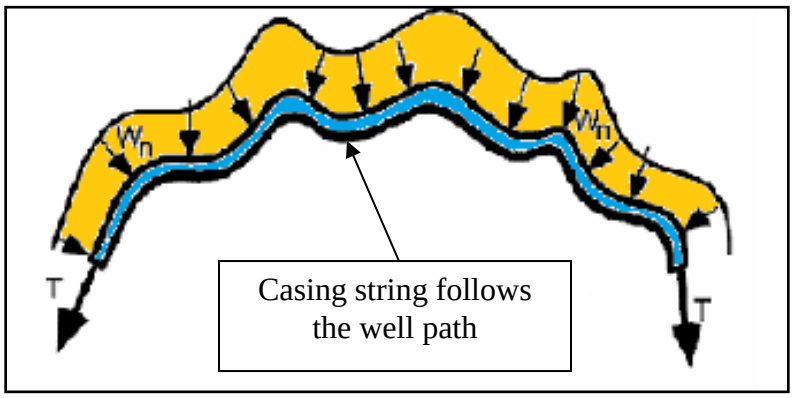

Figure 2.10. Soft string model representation (Wellscan®, training documentation).

The stiff string model is relatively new compared to the soft string model and is not used as prevalently. The stiff string model accounts for string bending stiffness forces and radial clearance. The stiff string model also accounts for both high side and low side forces. Some high side forces are being induced by bending due to buckling or doglegs across a tortuous wellbore.

Furthermore, the stiff string model should also account for bending moments at sections of the pipe with larger outer diameters. Stiff string models can be a valuable tool for wells running extremely stiff assemblies, wells with high tortuosity and/or high dogleg severity, and wells with tight radial clearances. Stiff string models are also more computer intensive due to their complexity. Another important note about the stiff string model is that the accuracy is dependent on the well surveys (changes in inclination and azimuth that generate doglegs and microdoglegs) input in the analysis. Furthermore, the actual path in between well surveys are unknown, which results in the model assuming a smooth path between surveys, which in reality is not true, for this reason it is a good practice to induce additional tortuosity between the reported surveys.

Soft string and stiff string models are both depending on a key modelling parameter: the coefficient of friction, or friction factor. The friction factor is dimensionless and represents the friction between casing string and wellbore. Mechanical friction can be separated into two types, static and dynamic. Static friction being the friction factor between two unmoving objects, and the dynamic friction is the friction factor between two steadily moving objects. In the torque and drag application, the friction factor does not only account for dynamic mechanical friction, it also takes into account many other downhole effects that are extremely hard to predict. Some of these effects may include but are not limited to pipe stiffness, viscous drag, wellbore obstructions, formation variances, pore pressure, wellbore instability, micro tortuosity and micro doglegs. Typically the friction factors associated with a stiff string model would be expected to be lower than those associated with a soft string model because the stiff string model should theoretically have less uncertainty and should account for some of the unknowns, which were previously built into the friction factor, in the model.

Current torque and drag models are extremely useful; however, one must be aware of their limitations. Torque and drag models are not affected by hole size, and, to a certain extent are very minimally effected by the presence of doglegs. Figure 2.11 illustrates how a stiff string model visualizes a string within the wellbore.

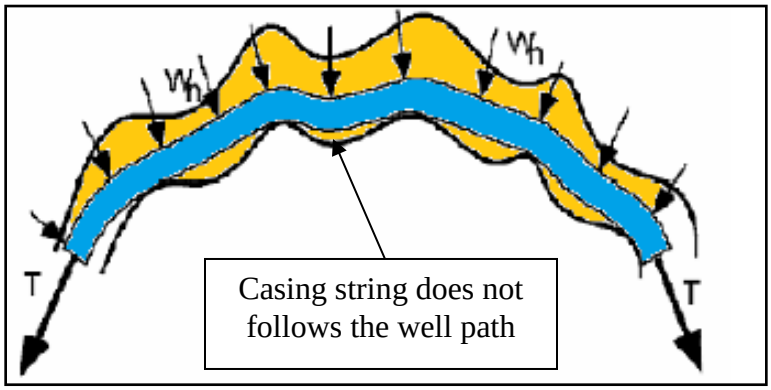

Figure 2.11. Stiff string model representation (Wellscan®, training documentation).

The Torque and drag computational modeling provides a realistic prediction of pipe deflections, internal stresses, wall contact forces due to friction (drag) and bending moments. The frictional.loads will have an effect on the weight being measured by the Weight Rig Indicator (Hookload sensor also known as Martin Decker gauge, Figure 2.12). The Martin Decker indicator will show a reduction in total string weight as the pipe is being run into the hole, friction increases and pipe starts going through the curve of the well. The string weight senses the weight at the drilling line therefore the measurement includes the weight of the traveling equipment and the top drive. Figure 2.13 shows a diagram of the hookload sensor location on the rig. The hookload numbers are predicted by the torque and drag model (Figure 2.14).

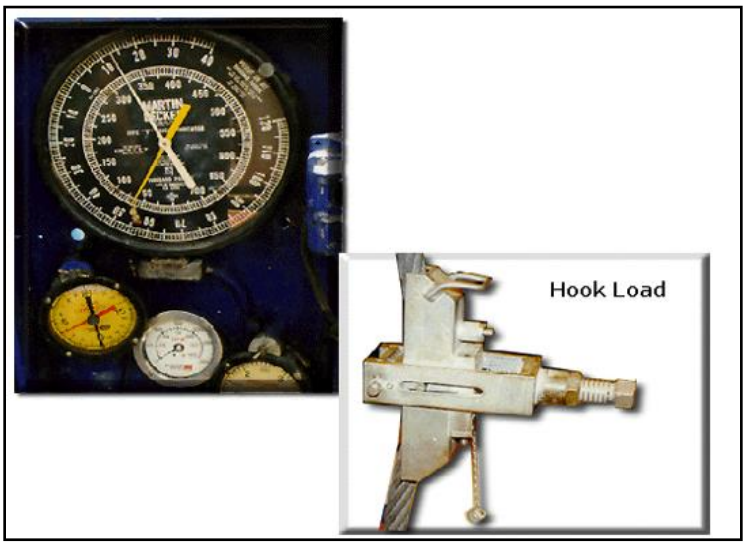

Figure 2.12. Driller's gauge and hookload Sensor (Schlumberger, Surface Equipment, Learning Material).

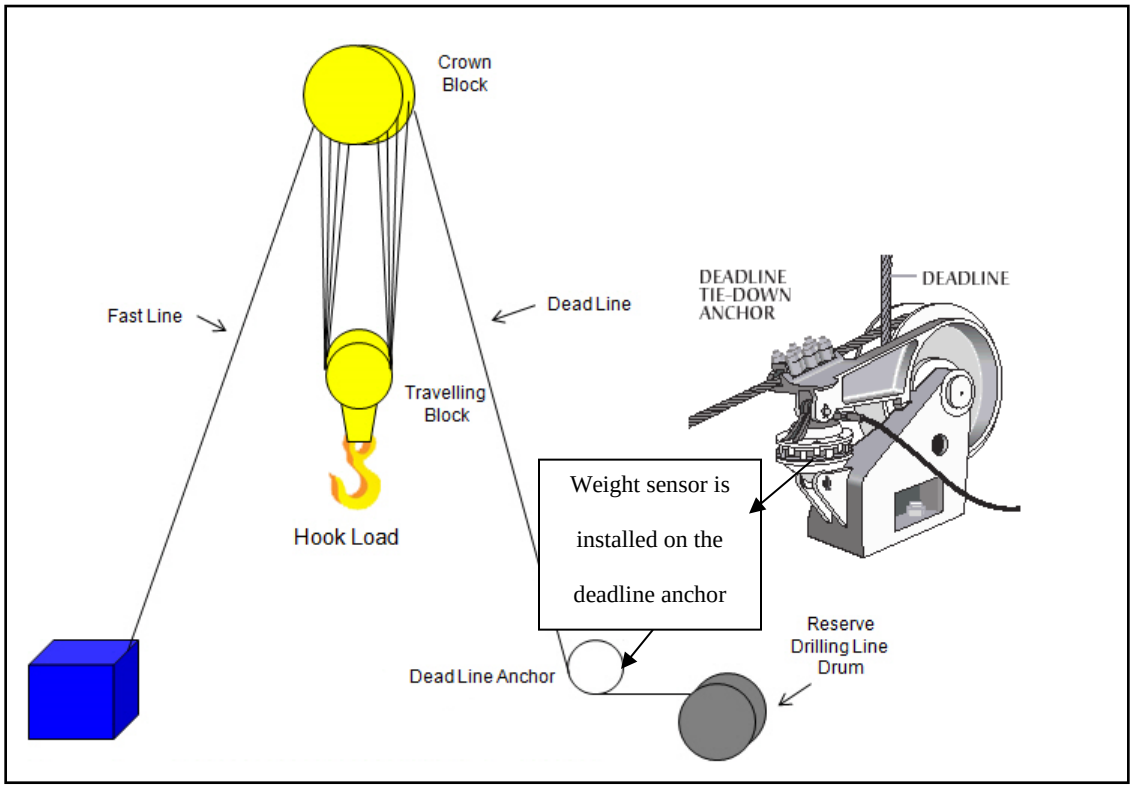

Figure 2.13. Drilling rig line (Drillingformulas.com).

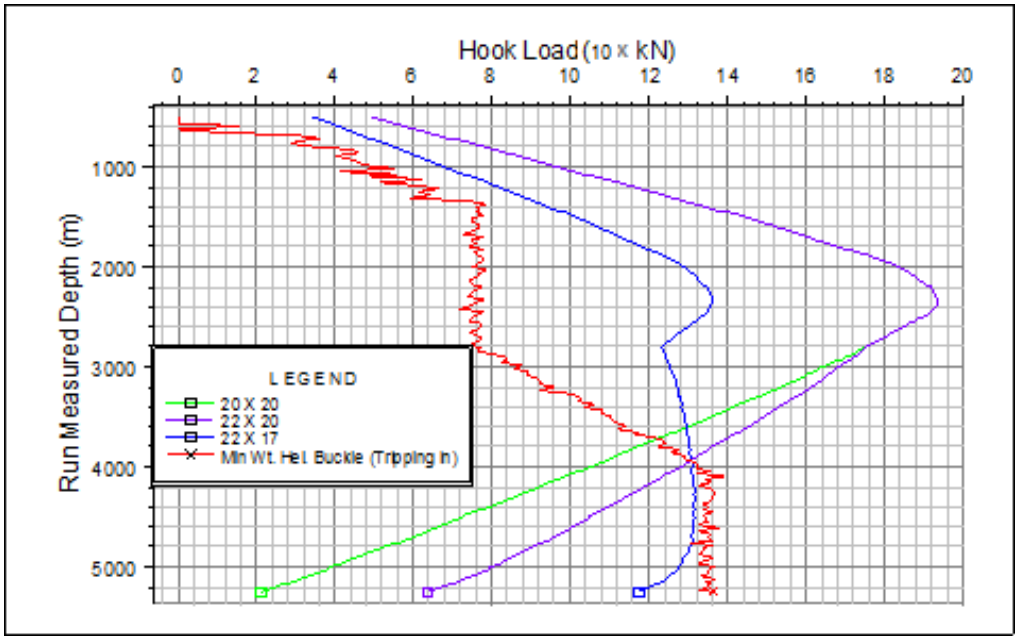

Figure 2.14. Torque and Drag modeling showing hookload predictions at different running depths for different casing weights.

2.4 Buckling

Buckling is an important phenomenon that occurs to pipe under certain axial conditions. It is an important concept for this project since the bending stresses resulting from casing buckling most likely cause permanent deformations[13]. Those trapped bending stresses must be included in the calculation of the Von Mises equivalent stress in order to determine how close the pipe is to yielding during the hydraulic fracturing pressure loading.

Buckling is defined as "a state of unstable equilibrium of thin-walled body when compressive loads are applied on its walls. The resultant deformation may be elastic or permanent. In some cases it may even lead to collapse of the structure"[14].

[13] Mitchell, Robert; Buckling of tubing inside casing, 2012.
[14] McGraw-Hill Dictionary of Aviation quoted by Menand.S, A new Buckling Severity Index to Quantify Failure and Lock-up risk in Highly Deviated Wells, 2012.

There are two different modes of buckling: Sinusoidal buckling, also known as snaking or 2D buckling, and Helical buckling which corresponds to a tube that snaps into a helical or spiral shape [15](Figure 2.15).

The determination of the loads required to cause both helical and snaking buckling is expressed through a single load parameter known as the effective force, *Fe*. The effective force is also known widely in the industry as the Lubinski[16] force. While the true force in a pipe is the one that could be measured using a strain gauge attached to the casing, the effective force at surface is the force that can be observed as hookload (on the rig weight sensor).

The effective force at any point along the axis of the tubular is defined as

$$Fe = Ftrue - (Pi \times Ai) + (Po \times Ao) \tag{2.11}$$

where:

Fe, effective force (newton)

Ftrue, buoyant load on the tubular (newton)

Pi, internal pressure in the tubular (pascal)

Po, external pressure on tubular (pascal)

Ai, cross-sectional area of ID ($meters^2$)

Ao, cross-sectional area of OD ($meters^2$)

[15] Menand, S; Buckling of Tubulars in Simulated Field Conditons, 2009.
[16] Lubinsky, A, Althouse W.S, Logan J.L; Helical Buckling of Tubing Sealed in Packers, 1961.

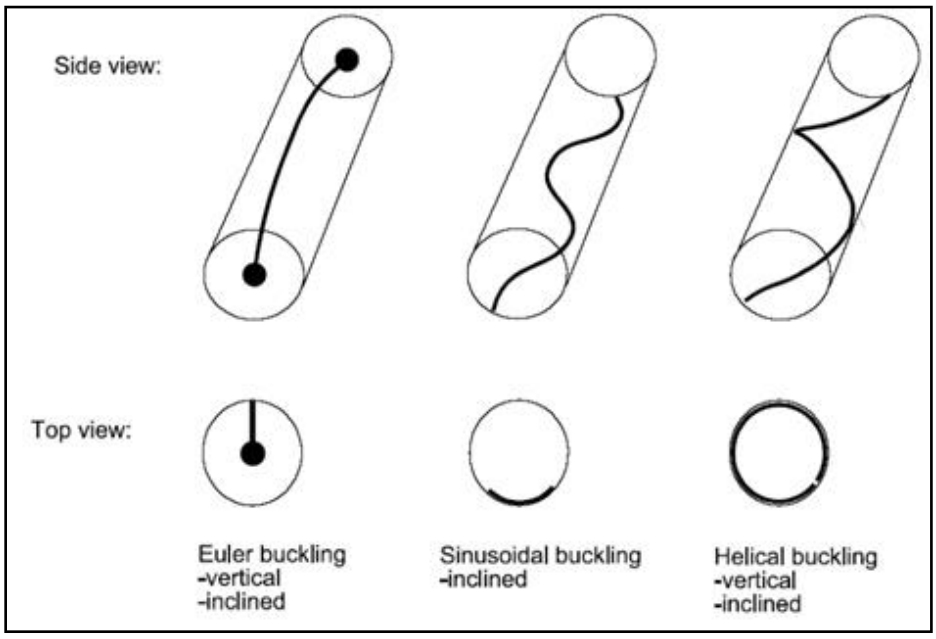

Figure 2.15. Forms of buckling in a constraint tubular (Shell Casing Design WLP).

Tubular resistance to buckling is also determined by the well bore angle. In a perfectly vertical hole, where a tubular is installed inside a confining casing or open hole, helical buckling will start to occur when *Fe* drops below zero. For an inclined well, the string will buckle when the effective force exceeds a critical value. The type and severity of the buckling mode depends on a number of factors including:

- Geometry of the string and the surrounding wellbore
- Degree of compression in the string
- Inclination of the well.

The sinusoidal buckling model was developed by Dawson and Paslay[17], and the most commonly used formula to calculate the lowest force needed to initiate helical buckling is the Chen and Cheatham model[18]. These models result in the following equation:

$$F_s = \lambda \sqrt{\frac{EIw}{r} sin\theta} \tag{2.12}$$

Where *Fs* (newton) represent the force required to initiate helical buckling, $\boldsymbol{\lambda}$ varies from 2.83 to 5.65 depending on the author and based on lab results and numerical analysis. 2.83 factor predicts the onset of the first helix and 5.65 predicts the full helical deformation in a perfect wellbore with no rotation. *E* is the Young's modulus (pascal), *I* is the second moment of inertia (meter^4), *w* is the weight of the pipe (newton per meter), θ is angular displacement (radians) and ***r*** is the radial clearance (meter). Buckling can be assessed by calculating the effective force (*Fe, newton)* acting on the pipe and comparing it to the inequalities defined in Table 2.1.

$Fe < 2 * \sqrt{\frac{EIw}{r} sin\theta}$	no buckling
$2 * \sqrt{\frac{EIw}{r} sin\theta} < Fe < 3.75 * \sqrt{\frac{EIw}{r} sin\theta}$	sinusoidal buckling initiated
$3.75 * \sqrt{\frac{EIw}{r} sin\theta} < Fe < 2\sqrt{2}\sqrt{\frac{EIw}{r} sin\theta}$	helical buckling initiated
$Fe > 2\sqrt{2}\sqrt{\frac{EIw}{r} sin\theta}$	helical buckling

Table 2.1. Buckling initiation threshold[19].

[17] Dawson, R. and Paslay, P.R; Drill Pipe Buckling in Inclined Holes, 1982.
[18] Cheatham, J. and Chen Y; New Design Considerations for Tubing and Casing Buckling in Inclined Wells; 1988.
[19] Kuru, E; Martinez, A; Miska, S; The Buckling Behaviour of Pipes and its Influence on the Axial Force transfer in Directional Wells, 1999.

One of the main consequences of casing buckling in the wellbore is the increase in contact forces between pipe and wellbore; this, consequently, increases drag and compressive stresses. The most common analytical expression to calculate the contact force (Wc) for helical pipe buckling is[20]:

$$w_c = -\frac{r * Fe^2}{4 * E * I} \qquad (2.13)$$

where:

Wc, contact force (newton/meter)

Fe, effective force (newton)

r, radial clearance between hole and tubular (meter)

I, polar moment of inertia for tubular (meter^4)

E, Young's Modulus (pascal)

Martinez et al (2000) proved with laboratory tests that the Equation (2.12) is only valid for some limited range of compressive forces[21]. This calculated force is included in most of the conventional Torque and Drag simulators. However, the equation only gives a rough indication of the extra contact force (drag) due to buckling. According to Menand et al (2009), buckling and drag calculations need to be done iteratively, since drag increases pipe compression which causes buckling that consequently causes more contact forces hence more drag.

The software used to calculate the stresses and forces acting on the casing (Wellscan®) runs a mathematical model that takes into account the contact forces generated by bending (pipe deformation) caused by buckling.

---

[20] Mitchell, R.F; Simple Frictional Analysis of Helical Buckling of Tubing, 1986.
[21] Marinez, A; Miska, s; Kuru, Experimental Evaluation of the lateral contact force in horizontal wells; 2000.

2.5 Wellscan® Simulator

Wellscan® is a computational tool created by the company Drillscan®, that models Torque and Drag (TAD) and Buckling for casing and drilling strings during various field operations. The algorithm embedded in the software is as accurate and robust as Finite Element Analysis application but it uses a high-quality scientific code (ABIS) developed at Mines ParisTech that makes it much faster.

Some the simulator features are[22]:

- 3D stiff-string & soft-string models
- Powerful casing string-hole interaction contact calculation algorithm
- Simultaneous torque/drag/buckling calculations
- Full casing string mechanical analysis: Axial Tension, Bending Moments, Contact Forces
- Hole size and clearance effects
- Micro and macro tortuosity effects
- Hydraulics effects on casing string mechanics
- Casing String 3D deflection in borehole

The ABIS model takes into account every element to the casing string such as: casing collars, packers and fracking sleeves which have different geometry properties than the casing pipe. The casing string is divided in small beam elements where any external forces (i.e mechanical and hydraulic) act on. The ABIS model works by utilizing integral equations which mimic FEA analysis. The model uses an iterative algorithm that first assumes no contact between the string

[22] Adapted from Wellscan® software platform presentation from Drillscan® documentation

and the wellbore, then points are calculated after introducing a series of points, one after the other starting from the heel of the well.

The model then splits up each section of casing pipe into multiple zones and performs an iterative process to calculate stresses at each step. In order to analyze the important parts of the casing the string is broken into multiple components, the connections, transition zones, and the pipe body (Figure 2.16).

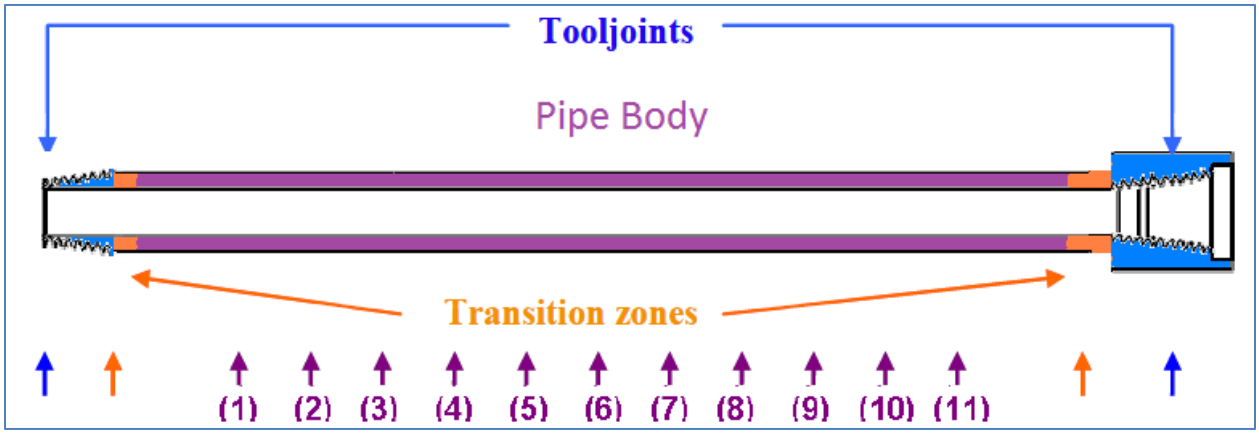

Figure 2.16. Casing pipe stress distribution by ABIS model (Adapted from SPE 116029).

The process gathers necessary data such as pipe weight, rotary speed, running speed, mud weight, and directional surveys and calculates the bending stress, and mean stress at each step. Once this iterative process is complete the model provides the bending stress throughout the string as well as the accumulated stress distribution of stresses throughout the pipe.

The iterative process follows the workflow shown in Figure 2.17.

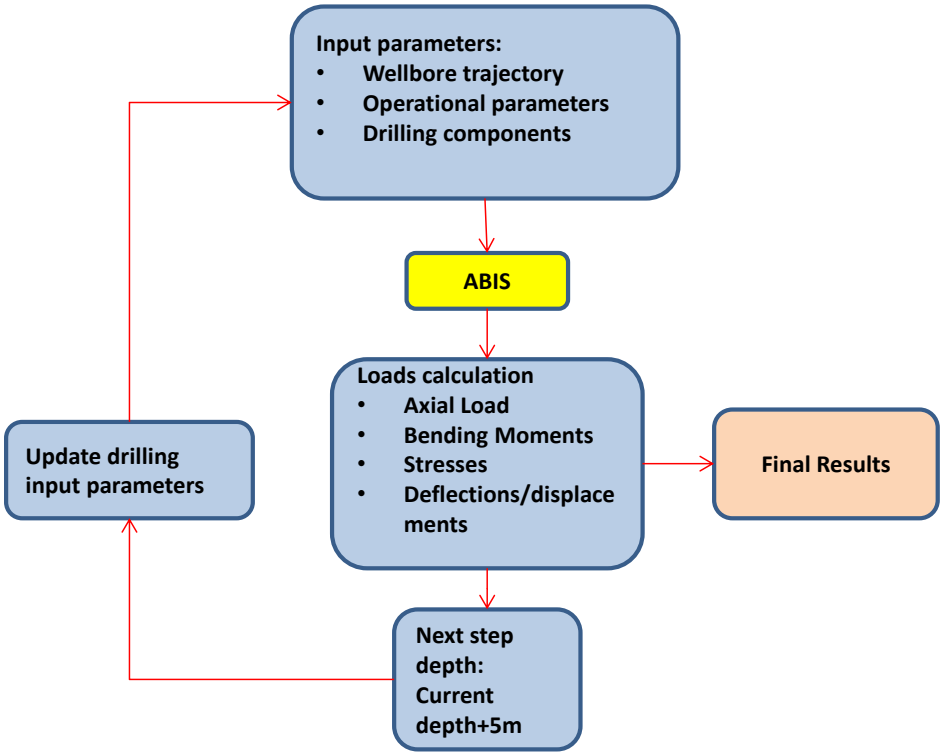

Figure 2.17 Iterative process of ABIS model (SPE 116029).

Figure 2.18 shows an example of the output of the ABIS model for a simulated buckled pipe in a horizontal wellbore. The model highlights the contact points and direction of the forces acting on the pipe.

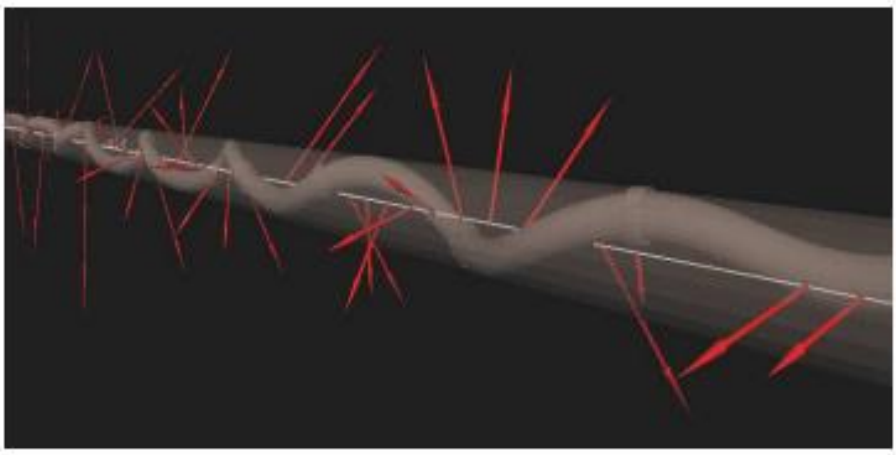

Figure 2.18. ABIS simulation results example, 3D contact of helically buckled pipe in a horizontal well (SPE 102850).

Chapter Three: **Production Casing Mechanical Modeling for Combined Pipe Installation and Hydraulic Fracturing Loading**

This chapter will show the process to determine, first, the forces involved during the installation of casing and, secondly, the loads experience by the casing at the moment in which a well is hydraulically fractured. The combination of all of those loads will provide the model for evaluating casing integrity before the well starts producing hydrocarbons.

The zone of interest in the casing string is the vertical section. It is here where most likely the pipe experiences buckling due to high compressive loads during the casing installation of the long horizontal wells. Since casing is landed using mandrel hangers (no reciprocation after landing), some of the compression is kept as residual stresses trapped after the casing is cemented in place. Afterwards, during the stimulation process (hydraulic fracturing); the burst load due to high pressures combined with high compressive stresses could cause the casing pipe or connections to fail.

3.1 Modeling Methodology

The modeling for evaluating the casing integrity problem during installation and hydraulic fracturing phases will be approached from two fronts: Global Casing String Analysis (GCSA) and Local String Component Analysis (LSCA).

In order to determine the several critical load cases, stresses and deformations along the entire string of casing during the installation process (axial forces, bending forces, pipe deflection, buckling), and specifically due to tubular buckling, a GCSA model will be used.

The GCSA is based on numerical torque and drag analysis for Stiff-string model. In this thesis, the Stiff model will be used. Stiff string model is a more accurate mathematical approach that predicts Buckling onset and estimates the contact side Forces properly on pipe. Stiff-string model is highly recommended to properly estimate casing loads.

The LSCA is the next level more detailed modeling. It consists in applying the critical loading case studied in the GCSA to the typical casing assembly for evaluating the condition and impact of the installation loads to the casing performance and for predicting any physical or geometric damage to the pipe section.

3.2 Global Casing String Analysis (GCSA)

As it was mentioned previously, the GCSA will evaluate the loads the casing is experienced during the installation phase (running-in loads). To model different scenarios and variables during the installation phase, a commercial engineering tool will be used: Wellscan®.

Wellscan® uses a stiff-string model that takes into account the stiffness of the casing and enables the accurate calculation of forces and stresses acting on the casing.

Wellscan® works similar to any other engineering application; it has pre-processing, processing and post-processing modules. In the pre-processing module all the variables of the problem are defined, the processing module is where all the intensive computation is developed, and the post-processing module is where all the results are visualized (2D and 3D graphs).

3.2.1 GCSA Variables Definition

Accurate and complete definition of the well configuration is the key step to obtain the mechanical forces and stresses that the casing experiences. Figure 3.1 shows the variables that define the well entity.

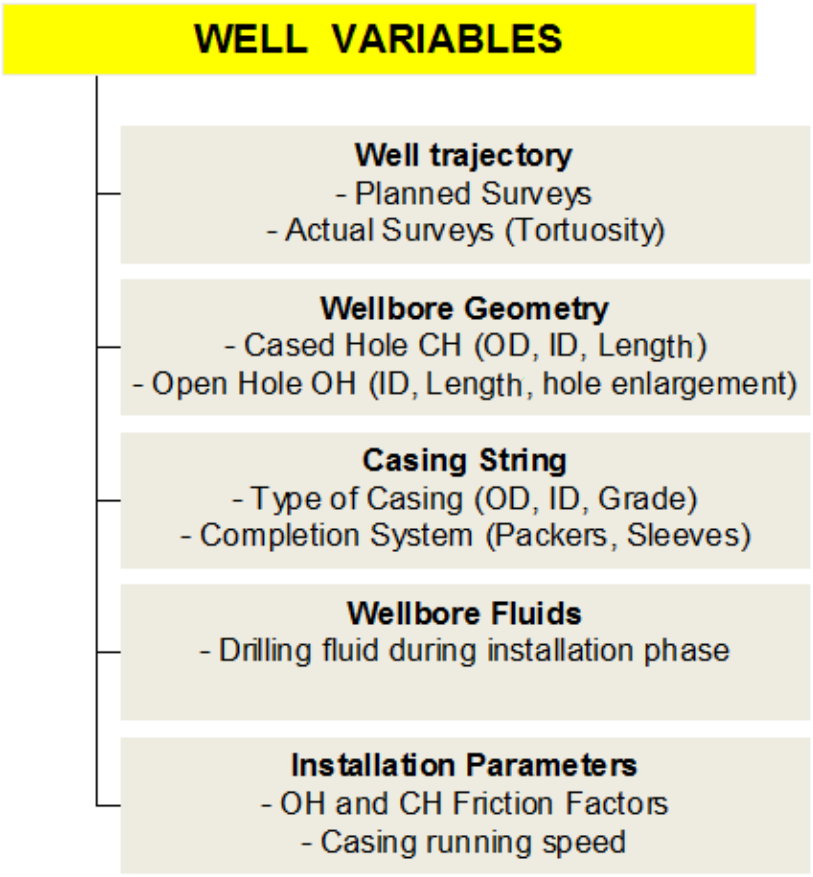

Figure 3.1. Modeling input parameters.

3.2.1.1 Well Trajectory

The first variable and perhaps the most important is the Well Trajectory. Well trajectory defines the points of contact between the casing string and the borehole wall. Since the initial position of the casing is straight, the mathematical model of the string finite element analysis accounts for

bending moments that are applied to the casing to keep the wellbore centerline configuration. The final state of the casing includes the stresses resulting from tension after applied friction forces, and side forces that develop at the contact points due to bending moments. The more realistic is the representation of the well trajectory, the more accurate the casing stresses can be computed.

The well trajectory can be defined in the original well plan, which has the main points (survey points) in the well such as point of deflection from the vertical (kick-off point), landing point and final depth of the well. In order to generate a complete trajectory, the minimum radius of curvature method is used to calculate the position of the well between survey points assuming a constant radius of curvature between survey points (Figure 3.2); therefore the entire well is well defined as a smooth curve in the space.

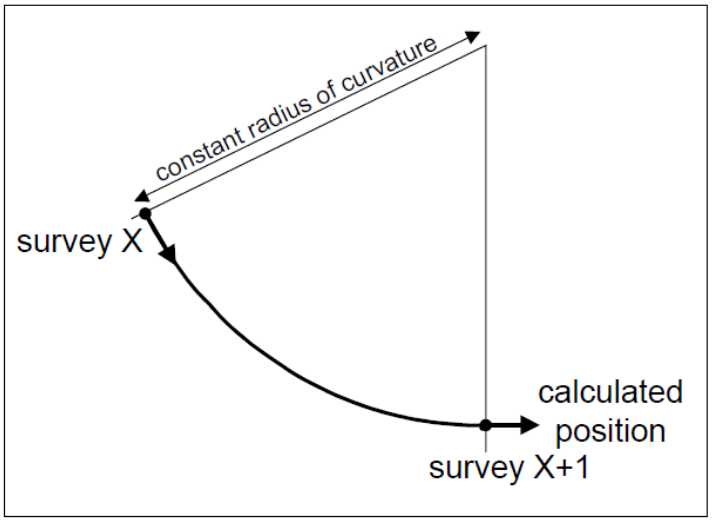

Figure 3.2. Minimum radius of curvature to calculate position between survey points (Source: E.J. Stockhausen, SPE/IADC 79917, 2003).

However, an actual well path is very irregular due to the effects of rotary and slide drilling and the effects of formation anisotropy in well direction. Therefore, a more realistic representation of the well trajectory is the actual surveys taken during the drilling process. However, surveys are taken during drilling every 10 meters in the curve section that brings the well from vertical to horizontal; and every 30 meters in the vertical, tangent and horizontal section The true curve shape between surveys is not completely known except in some cases when a continuous inclination tool is run which can give a better representation of the trajectory as frequent as every meter. In Figure 3.3, one can see that although the path between two survey points is calculated to be a constant curve (blue line), in reality there are so-called "microdoglegs" or "tortuosity" due to changes in well azimuth and inclination in short distances (red line) that will affect the determination of the forces acting on the casing and subsequently the deflections and stresses of the casing.

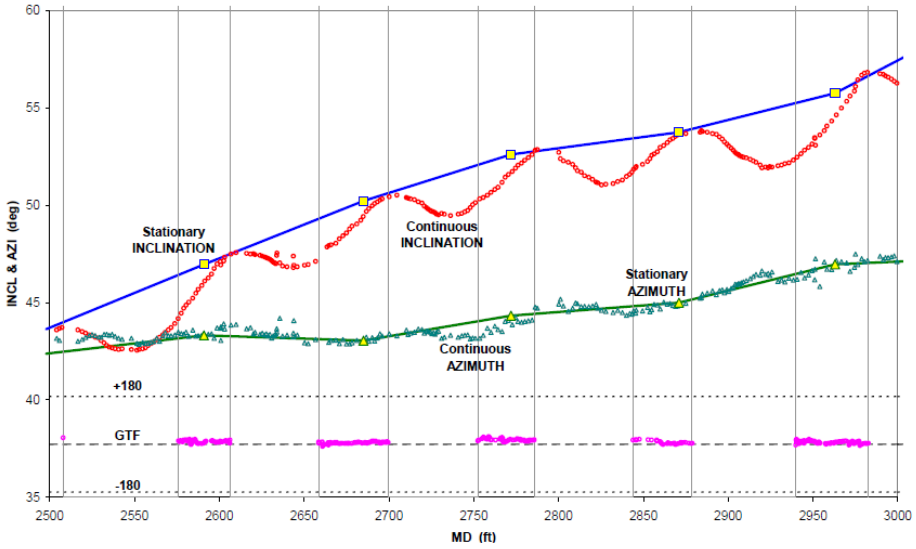

Figure 3.3. Continuous direction and inclination measurements versus "standard" stationary survey measurements during a build section using "pattern"slide/rotary drilling practices with a bend motor system. (Source: E.J. Stockhausen, SPE/IADC 79917, 2003).

In order to input a more accurate well trajectory into the GCSA, actual well surveys will be used and tortuosity will be induced using the Sine Wave Method.

According to G. Robello, SPE /IAD 92565 2005, The Sine Wave method modifies the inclination and azimuth of the well path based on the concept of a sine wave shaped ripple running along the wellbore using the magnitude (amplitude) and period (wave length of the ripple), the angle change $\Delta\alpha$ (degrees) is obtained using the following relationship:

$$\Delta\alpha = \sin\left(\frac{D}{P} * 2\pi\right) * M \qquad (3.1)$$

Where:

$\Delta\alpha$, inclination angle induced variation (degrees)

D, distance between points that the wellpath is divided (meter)

P, Angle change period (meter)

M, maximum variation of angle that will be applied to the inclination and azimuth of the native wellpath (degrees).

The new angle (degrees) is given as follows:

$\alpha_n = \alpha + \Delta\alpha$

Since the Groundbirch asset field development plan is based in drilling pads of up to 13 wells, two different well trajectories from a pad will be used in this project: The well with zero horizontal displacement[23] at the heel and the well with the maximum horizontal displacement at the heel (600 m). Figure 3.4 shows the 3D representation of the 2 wells that are used in the

[23] Horizontal Displacement or Step-out is the distance from the well slot at surface and the projection of the horizontal section to the horizontal plane.

project. Blue well is 650 m offset from the well center, and red line is virtually 0 m offset from the well center. It is important to use both referenced trajectories to evaluate the impact of trajectory in the loads calculation.

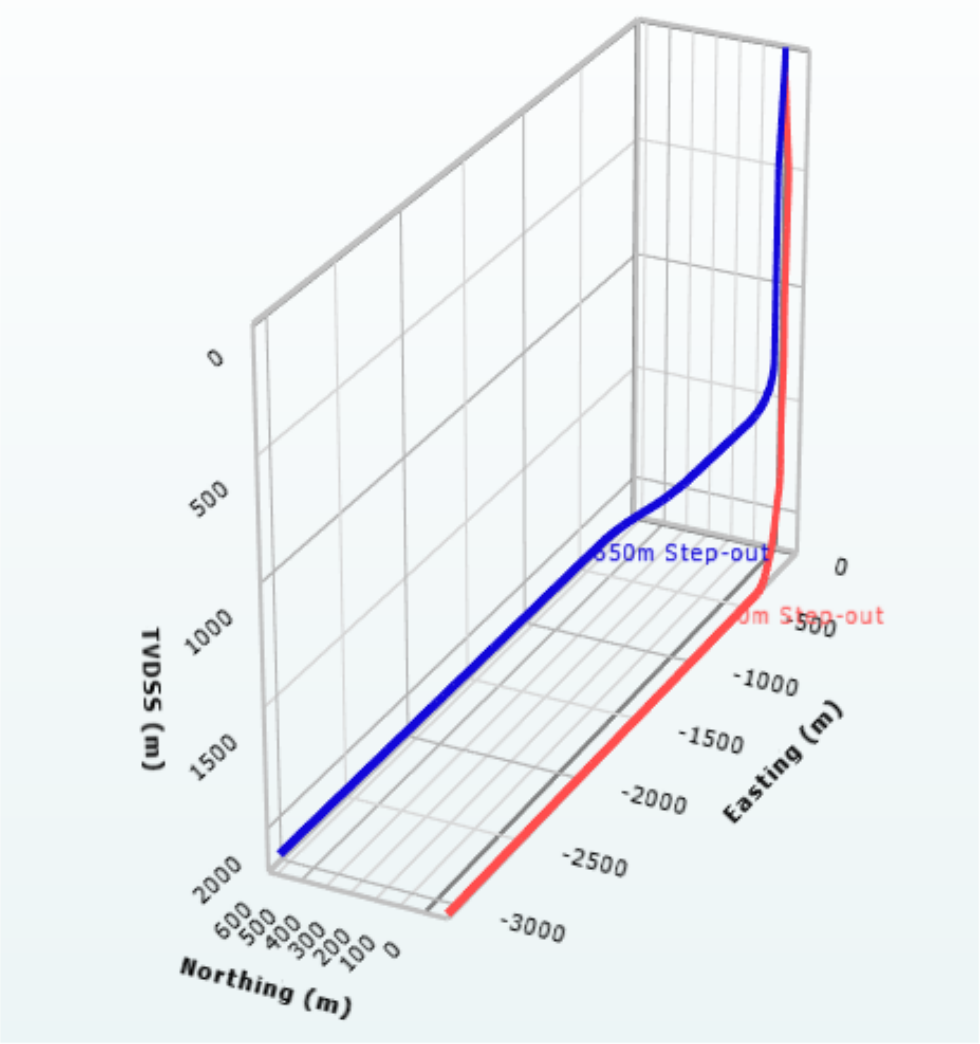

Figure 3.4. Visualization of 0 m and 650 m step-out wells.

The next step is to apply Sine wave tortuosity to the two well trajectories. Sine wave tortuosity method is applied using the following parameters:

D= 100 meters

P= 30 meters

M= 1 degree for both inclination and azimuth

Figure 3.5 and Figure 3.6 respectively show a comparison between planned, actual and tortuosity applied surveys for the 0 meters and 650 meters step-out well. Since during drilling the well, surveys were taken every 10 meters in the build section, and the vertical section is normally smoothly drilled, the tortuosity has been only induced in the lateral section.

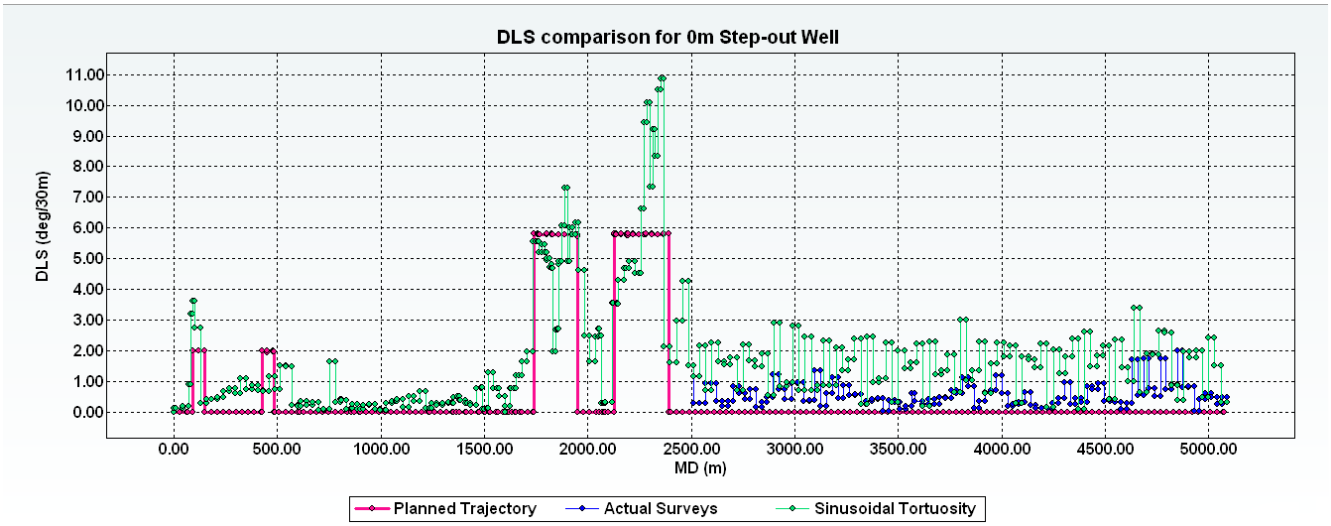

Figure 3.5. Dogleg severity comparison for the 0 meters step-out well.

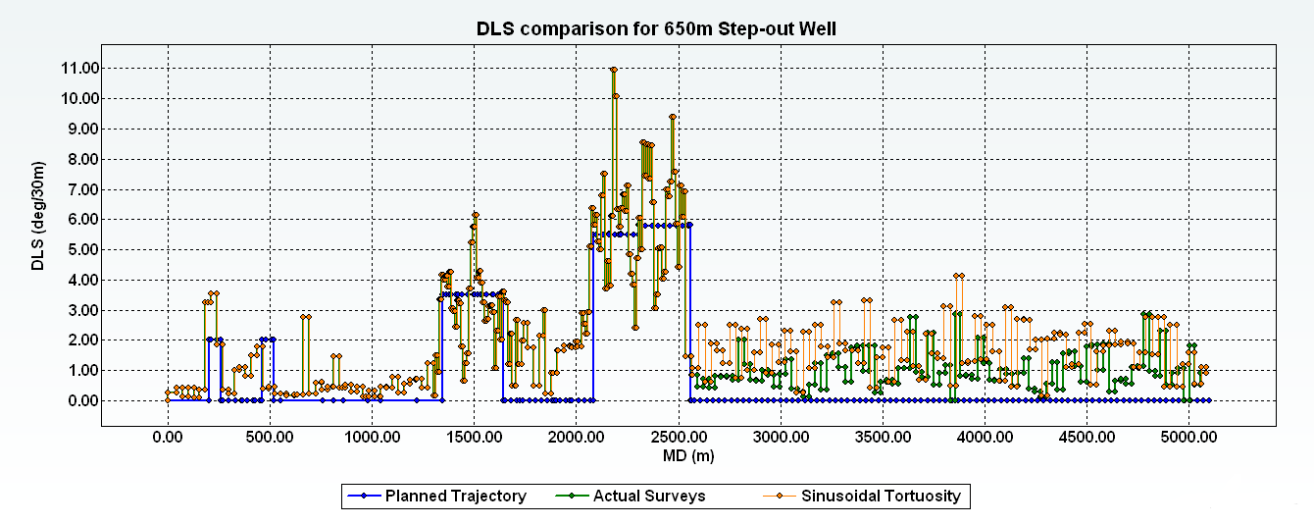

Figure 3.6. Dogleg severity comparison for the 650 meters step-out well.

The well paths with the induced sinusoidal tortuosity are used in the GCSA model.

3.2.1.2 Wellbore Geometry

The next Well Variable to be defined for the model is the Wellbore Geometry. The focus in this project is the monobore type well, this means a well that have only one section as the main production section. As described in Chapter one, a 177.8 mm casing is set in a 222 mm hole at ~620 m depth to protect aquifers. Next, the production hole is drilled to total depth. A single hole diameter for the production hole is considered in this thesis: 159 mm. Based in the field experience and caliper logs the average hole enlargement (washout) is approximately 20%, this percentage is used in the mode.

3.2.1.3 Casing String

The Casing strings used in the GCSA model is 114.3 mm (4.5 inch) 20.09 kg/m P110 LTC. The completion string deployed with the casing in the horizontal section of the well is conformed for a series of elements such as packers and fracturing sleeves, these elements are the key contributors to the drag forces that cause the compressive forces leading ultimately to buckling of casing located in the well above the build (curve) section.

Figure 3.7 shows a detailed diagram of the type of casing (completions) string analyzed in the model.

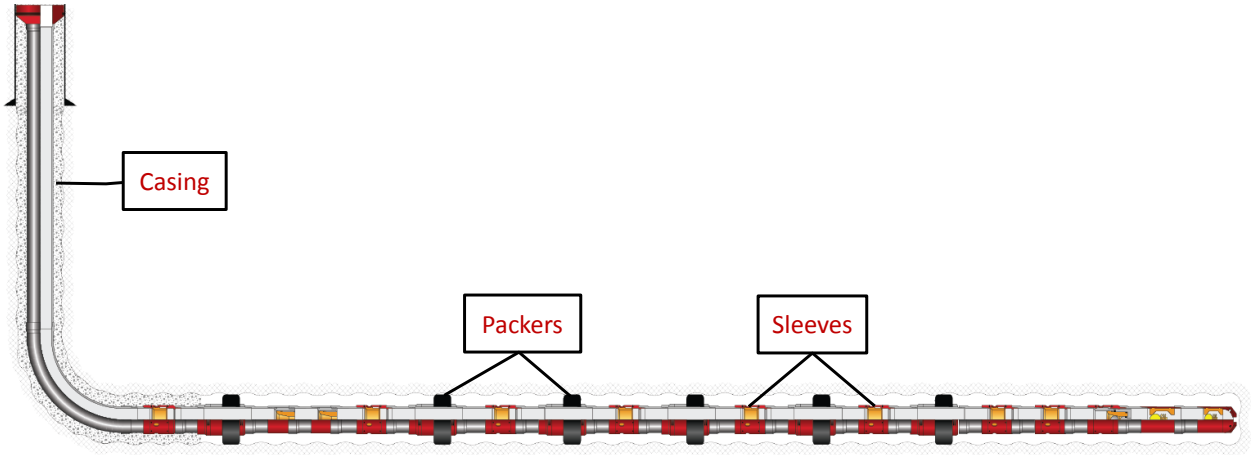

Figure 3.7. Open hole completion system diagram.

3.2.1.3 Wellbore Fluids and Installation Parameters

One more Force acting on the casing is the buoyancy force due to the fluids present in the wellbore at the moment the casing is installed. This force is the effective force. Effective force is a function of the fluid density present inside and outside the casing during the casing running operation. In Groundbirch, once the drilling phase is finalized, the entire wellbore is displaced to

a heavy invert drilling fluid with a density of 1.450 SG[24]. The main purpose of displacing to heavy invert fluid is to control the downhole pressure of the well at the reservoir level during pulling of drilling pipe out of the hole. The same heavy invert fluid is left in the well while the casing string is run into the wellbore. For modeling purposes 1.45 SG is used.

As for the casing installation parameters, there are two main inputs that are considered for the modeling: Friction factor and casing running speeds.

As mentioned in Chapter Two, friction factors used in torque and drag modeling is a dimensionless parameter that represents not only mechanical friction but other factors such as mechanical obstructions due to wellbore instability, and variations or loss in lubricity (Mason and Chen, SPE/IAD 104609, 2007). In order to determine a proper friction factor to be used in the GCSA modeling, a friction factor calibration has been performed for different wells that Groundbirch has drilled and cased.

The friction factor calibration consists in correlating actual casing running loads with modeled casing running loads. Figure 3.8 shows in blue the actual numbers captured by the rig instrumentation system with a frequency of 10 seconds, and the model numbers in red. The friction factor is computed for two well sections, the cased hole section going from surface to 620 meters, and the open hole section that goes from 620 meters to the final depth of the well. The average computed friction factors are: 0.1 for cased hole and 0.32 for the entire open hole section.

[24] SG is the specific gravity of the fluid referenced to the water density. Water density is 1.0 SG.

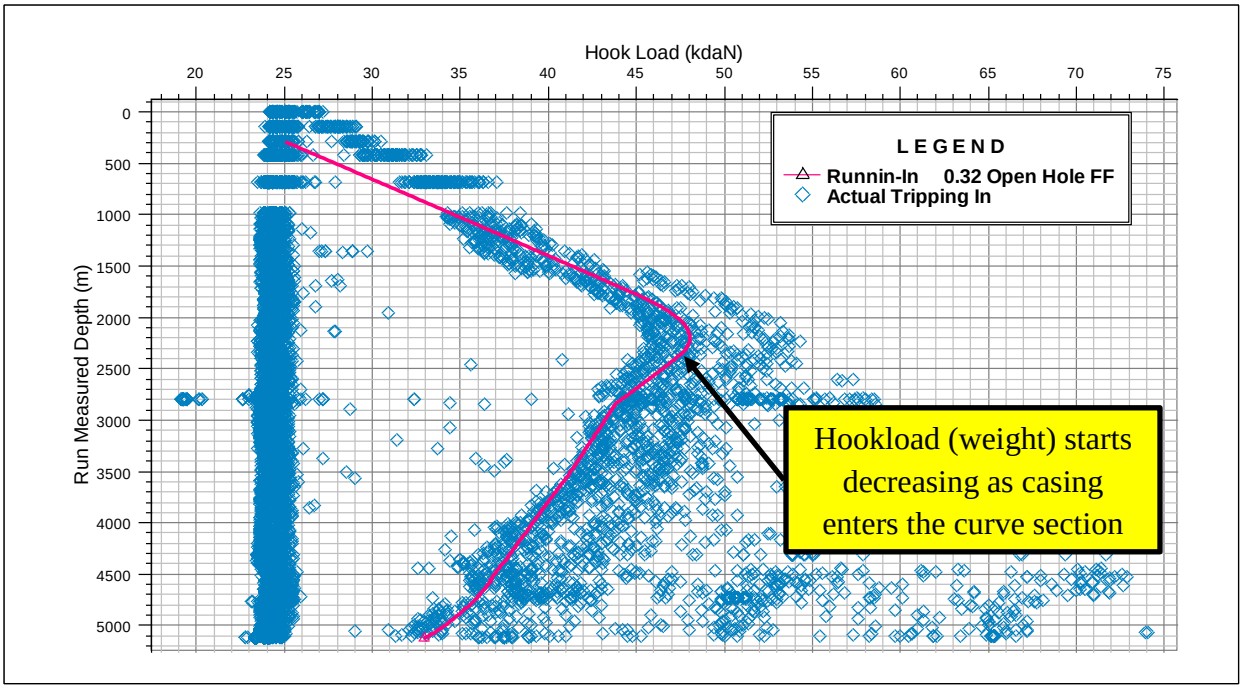

Figure 3.8. Friction factor calibration for casing installation (0.1 CH, 0.32 OH).

3.2.2 Completions System Installation Modeling

Once all the parameters have been defined, the next step is to model the different scenarios for the completions string installation operation. For the 114.3 mm 20.09 kg/m P110 casing and each step-out distance (0 meters and 650 meters), the simulation is done at different depths: 3000, 3500, 4000, 4500, and 5000 meters. Modeling prior to these depths is not required since the drag force is not high enough to cause pipe buckling that can affect the integrity of the casing string, Figure 3.9 shows how the running load (axial compression) never goes below the onset critical force for both sinusoidal and helical buckling.

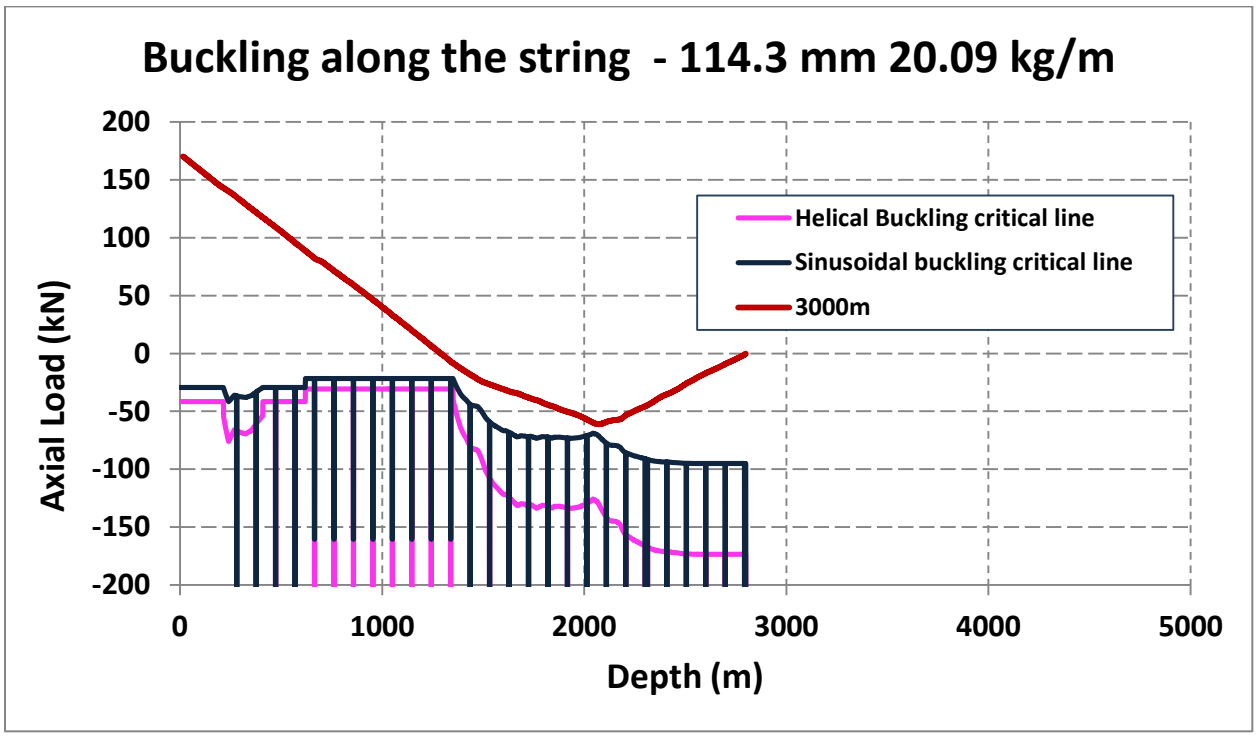

Figure 3.9. Running loads and buckling critical force lines prior to 3000 meters depth.

Before running the model at different depths, a minimum hookload that the rig crew could see when running casing has to be defined; this is to simulate the installation loads to that minimum hookload. A minimum hookload between 30 and 50 kilo newton is considered the minimum acceptable load. This is because the rig still needs a minimum weight available to continue pushing the string downwards, if a minimum load of 0 newton was assumed the rig would not be able to continue pushing casing since there is no weight to push available. In order to achieve the minimum hookload, different friction factors are increased progressively.

3.2.3 Global String Modeling Results

The following are the results for modeling done with the 114.3 mm, 20.09 kg/m P110 completions system at different depths and for two different step-out: 0 meters an 650 meters step-out.

Running in hole the completions system (casing, packers, fracturing sleeves) is generally the scenario for which the casing string undergoes the maximal compression load due to the high contact forces between the pipe and wellbore. The higher the contact side force is, the higher the compression in the casing. Figure 3.10 shows the decrease in axial load as casing is run at different depths; a maximum compression is experienced at around 2000 m along the string.

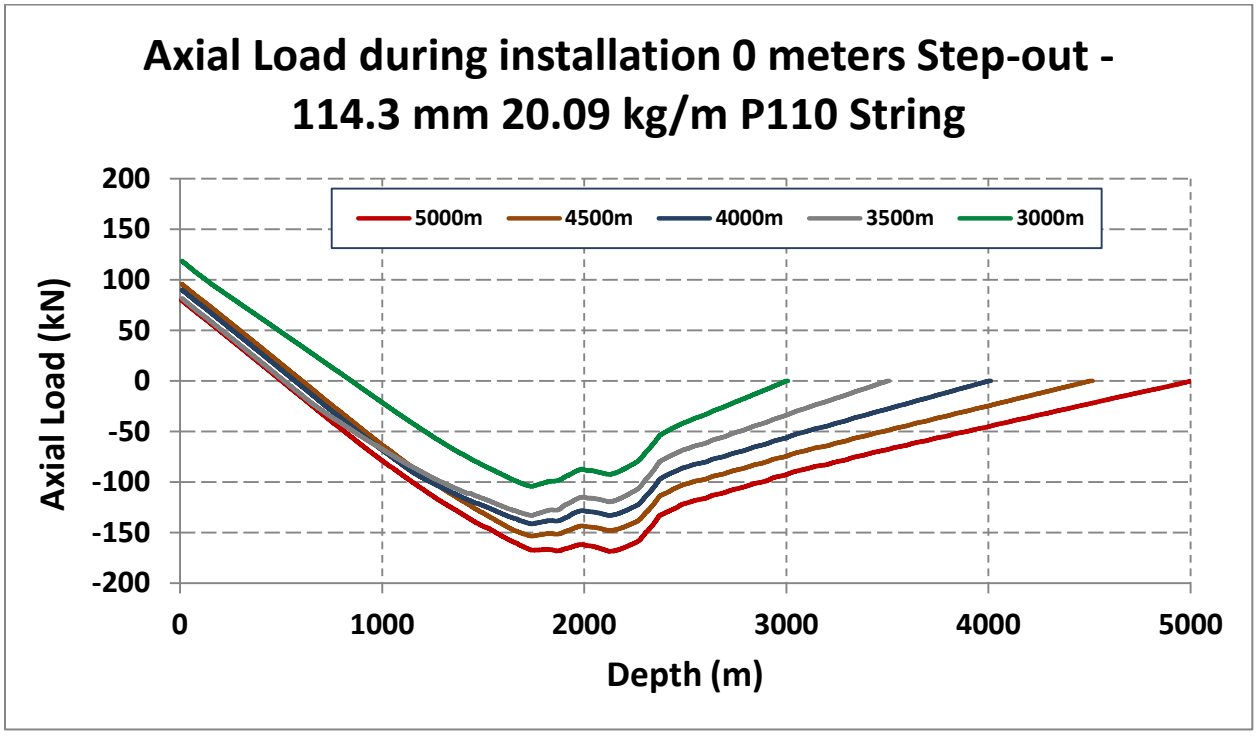

Figure 3.10. Axial load showing high compression while running casing in hole at different depths for a 0 m step-out well.

As the casing string is run into the wellbore, the compressive force increases to the point that it exceeds the critical force for helical and sinusoidal buckling onset (Figure 3.11). Generally, the helical buckling load is assumed as the limit upon which the pipe might be fully buckled with the risk of getting stuck or with the risk of large bending stresses that can lead to mechanical failure of pipe. It is also recognized that sinusoidal buckling is a safe condition since additional bending stress is low. On the other hand, helical buckling is generally perceived as a relatively dangerous situation. As for helical buckling, an additional contact side force is generated between the casing and the wellbore, since there is a shape change of the pipe. This new contact force will contribute to the total drag (friction) acting on the pipe, increasing consequently the compressive load along the casing string.

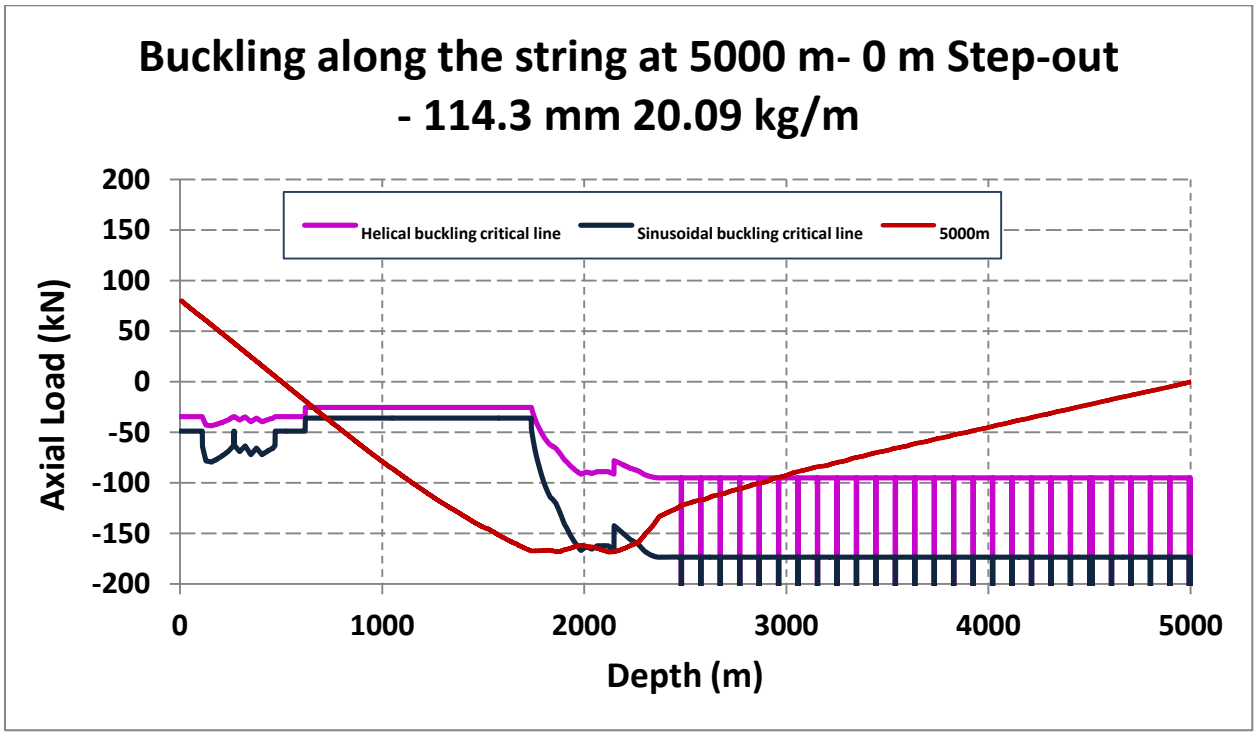

Figure 3.11. Helical and sinusoidal buckling prediction for running casing string as it is landed at total depth of 5000 m for a 0 m step-out well.

Figure 3.12 illustrates the calculated bending stresses for the pipe fiber at the internal diameter of the casing. As expected, the highest bending stresses are located in the curve section of the well where the high dogleg severity is present; however, the bending moments are not only generated by the doglegs but also by the buckling effect although to a lesser extent. By assuming the helical shape of the pipe, the software numerical model can calculate the bending moments and therefore the stresses. Generally speaking, bending stresses created by doglegs are much higher that stresses created by helical buckling deformation.

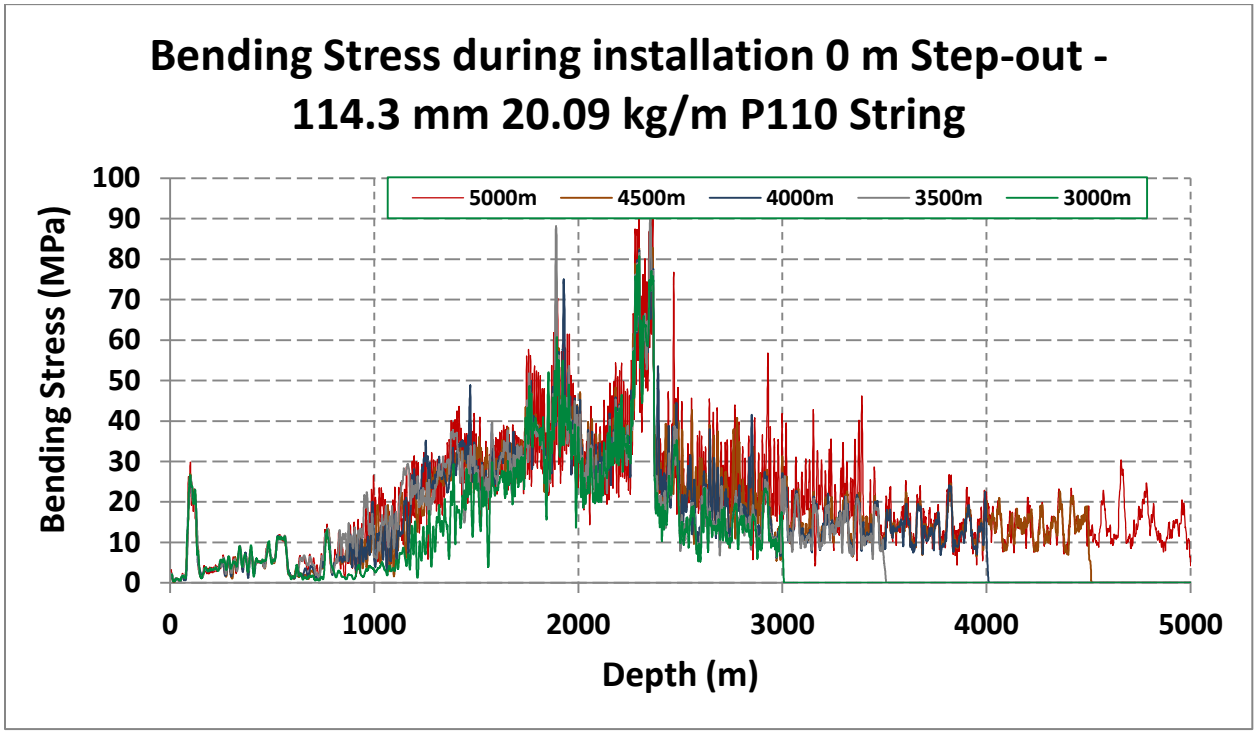

Figure 3.12. Bending stress along the casing string as the casing is run in hole at different depths for a 0 m step-out well.

The combination of all the stresses (axial, tangential and radial) in the form of a triaxial stress is the Von Mises Stress shown in Figure 3.13. It is important to maintain the Von Mises stress below the yield strength of the casing material with the proper design factor.

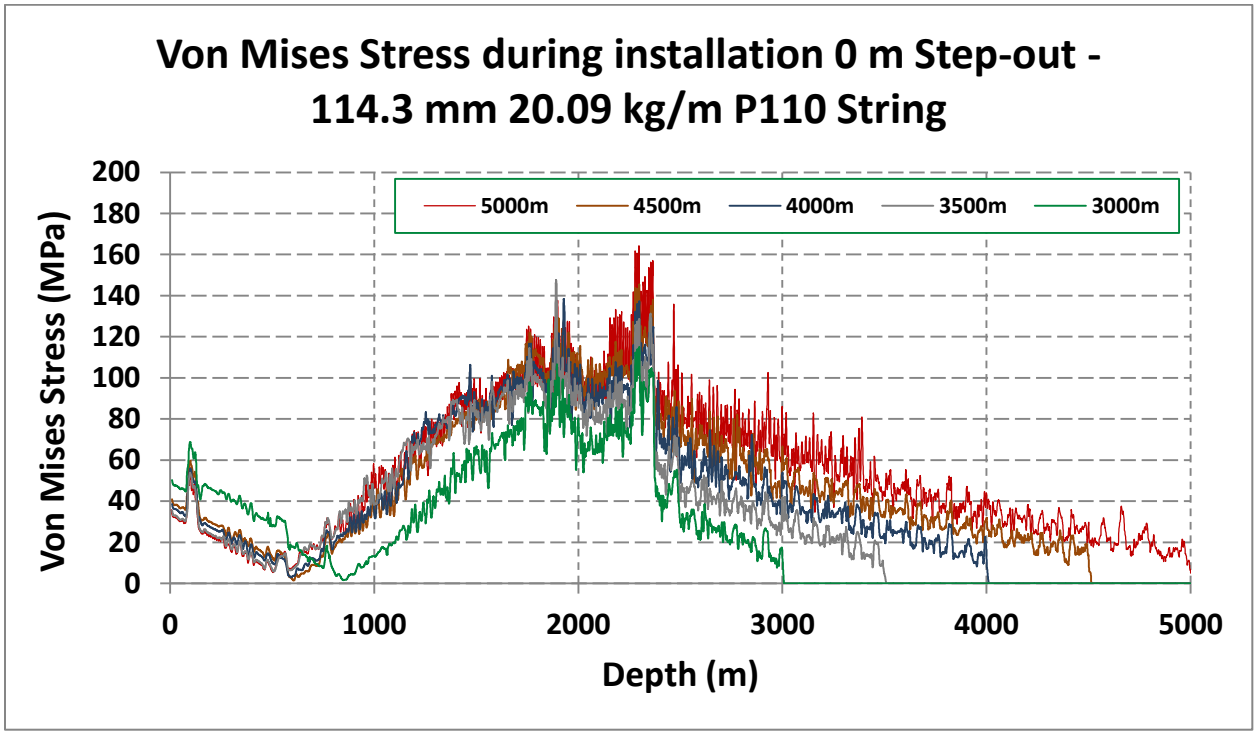

Figure 3.13. Von Mises stress along the casing string as the casing is run in hole at different depths for a 0 m step-out well.

A good indication of the shape adopted by the casing pipe once it goes into buckling state is provided by the calculation of the deflection of the center of the pipe inside the wellbore. Figure 3.14 depicts the concept of lateral, normal and radial deflection. By analysing the radial deflection of the pipe, it is possible to identify the areas with high buckling deformation. Figure 3.15 shows radial displacement experienced by casing once it is landed at 5000 m in a well with no step-out.

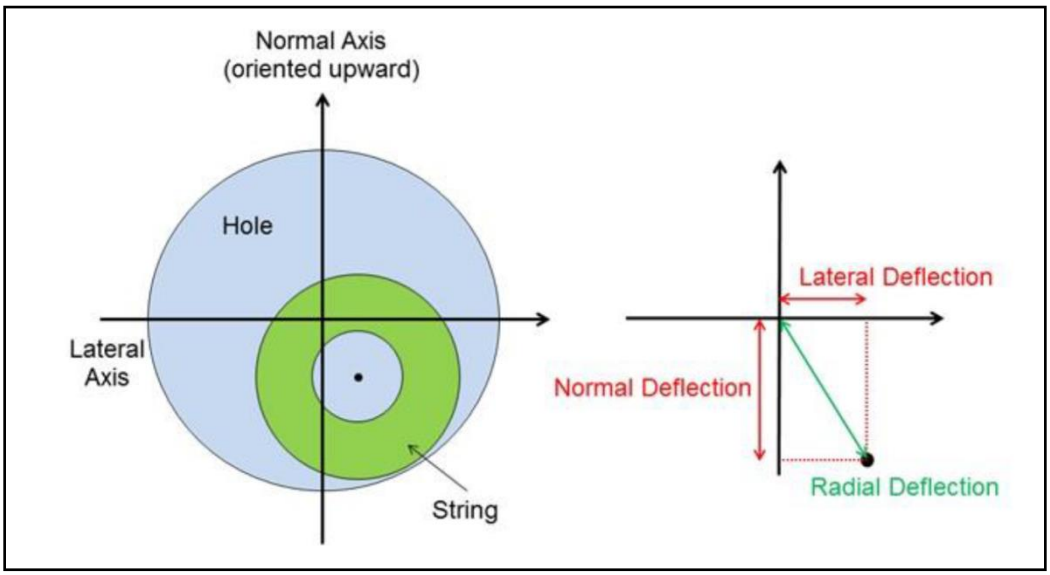

Figure 3.14. Concept of radial, lateral and normal displacement of casing string (Wellscan documentation, Drillscan March 2014).

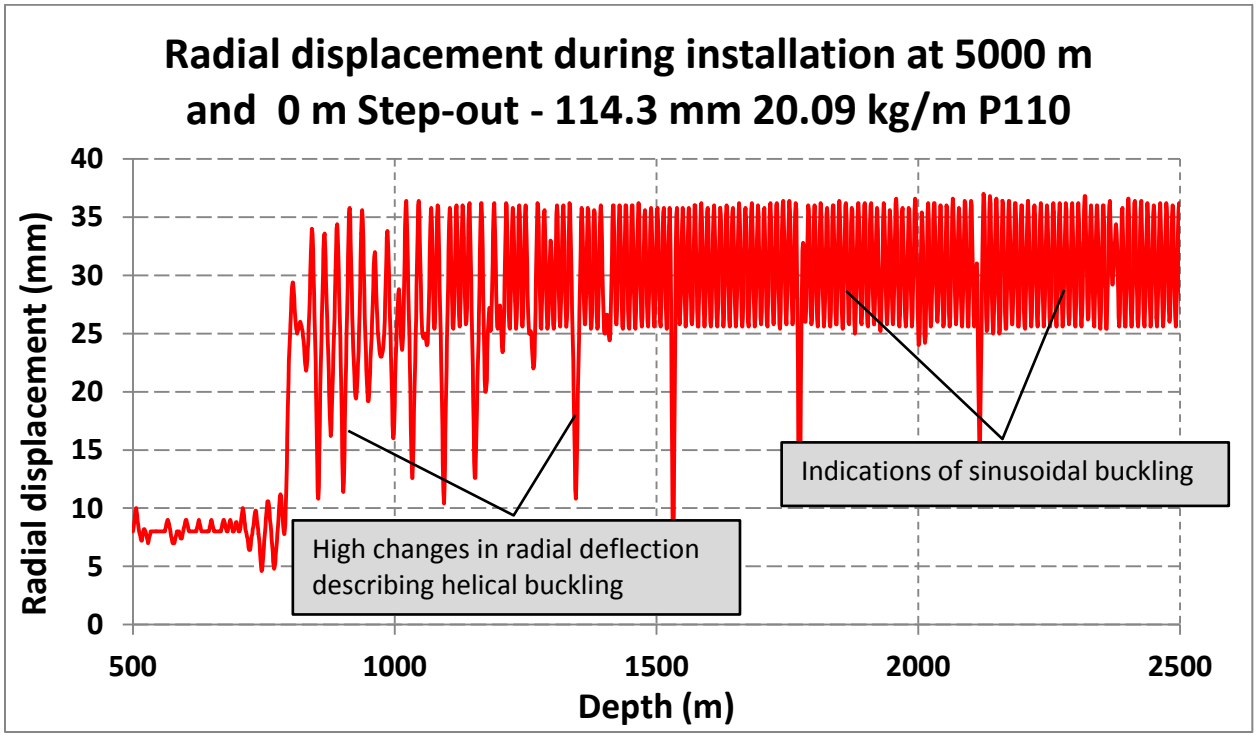

Figure 3.15. Radial displacement along the casing string from 500 m to 2500 m when the casing is landed at 5000 m for a 0 m step-out well.

Figure 3.16 and Figure 3.17 show the locations of high bending, side forces and compressive force along the drill string. The side forces indicate the contact points between casing and the wellbore where the friction is generated due to buckling and high doglegs.

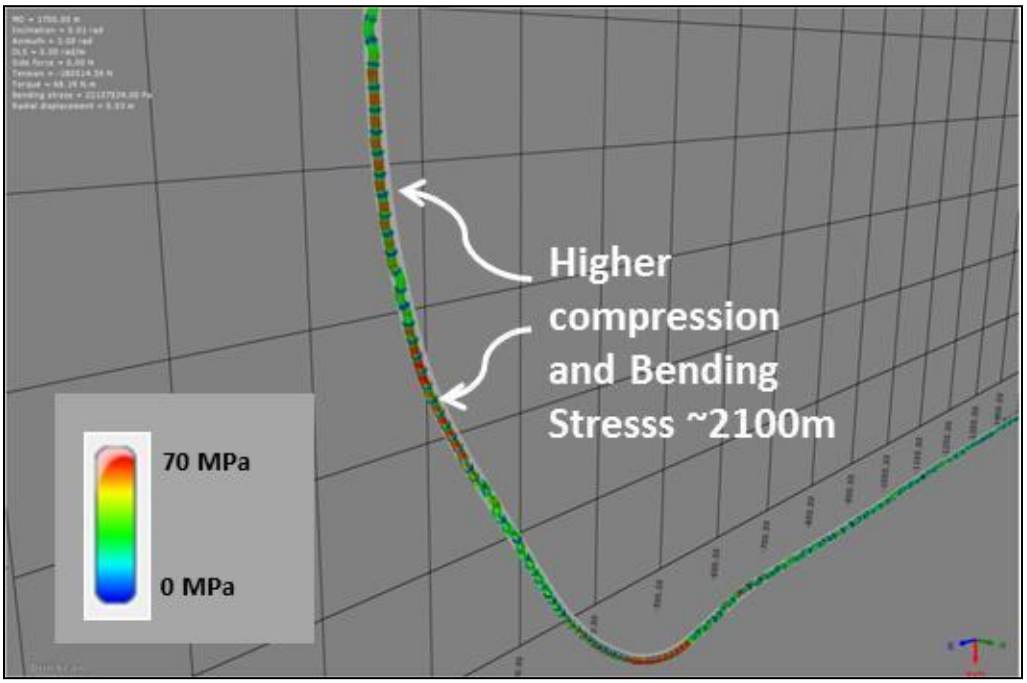

Figure 3.16. Numerical simulation of the 114.3 mm casing string showing high compression and bending stress when the casing is as-landed at 5000 m for a 0 m step-out well.

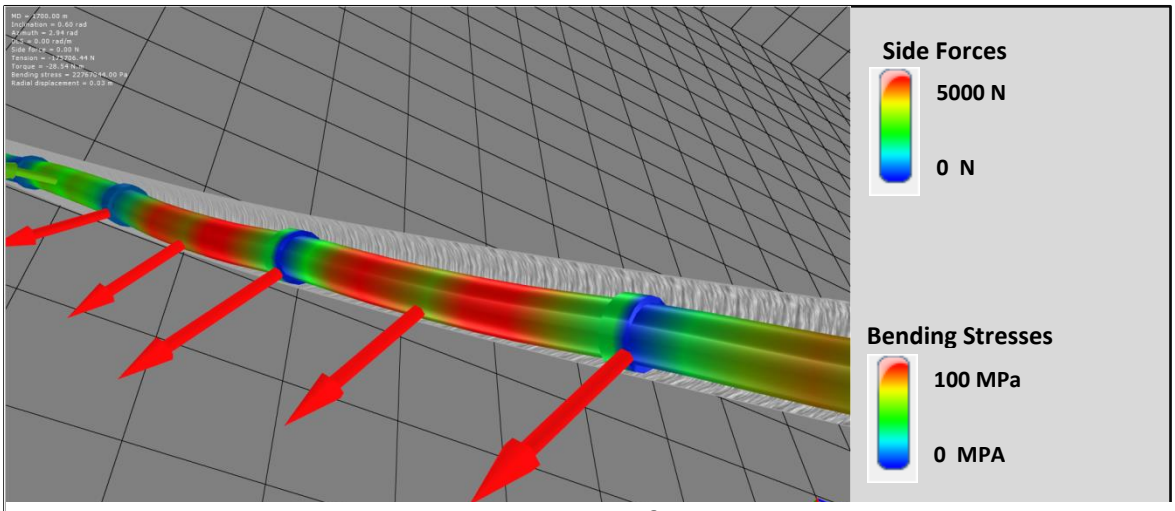

Figure 3.17. Numerical buckling simulation of the 114.3 mm casing string showing high side forces, compression and bending stress while buckling pipe.

3.2.3.1 Step-out at 650 Meters

The following are results for similar modeling done as in 3.2.3.1 but this time with a well trajectory that corresponds to a well with 650m step-out. As in the previous case, axial load, bending and Von Mises stress and radial displacement were simulated for the 650m step-out well as shown in Figure 3.18 to Figure 3.23.

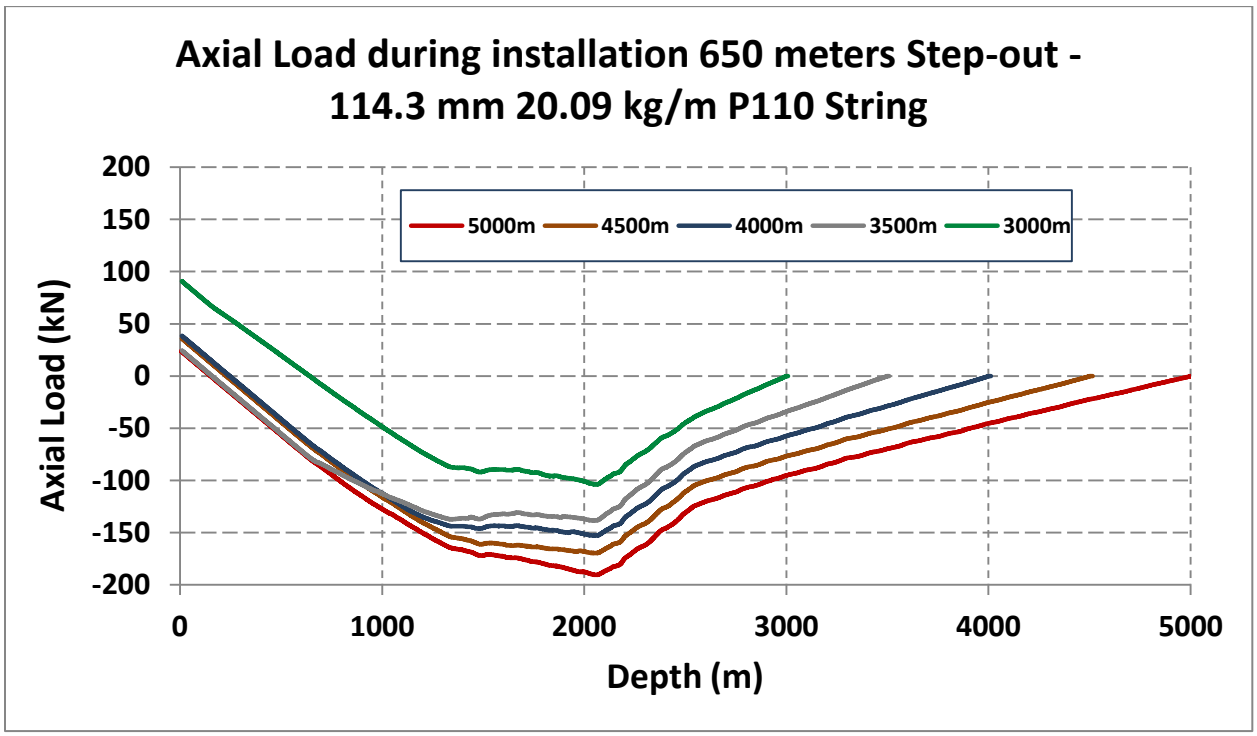

Figure 3.18. Axial load showing high compression while running casing in hole at different depths for a 650 meters step-out well.

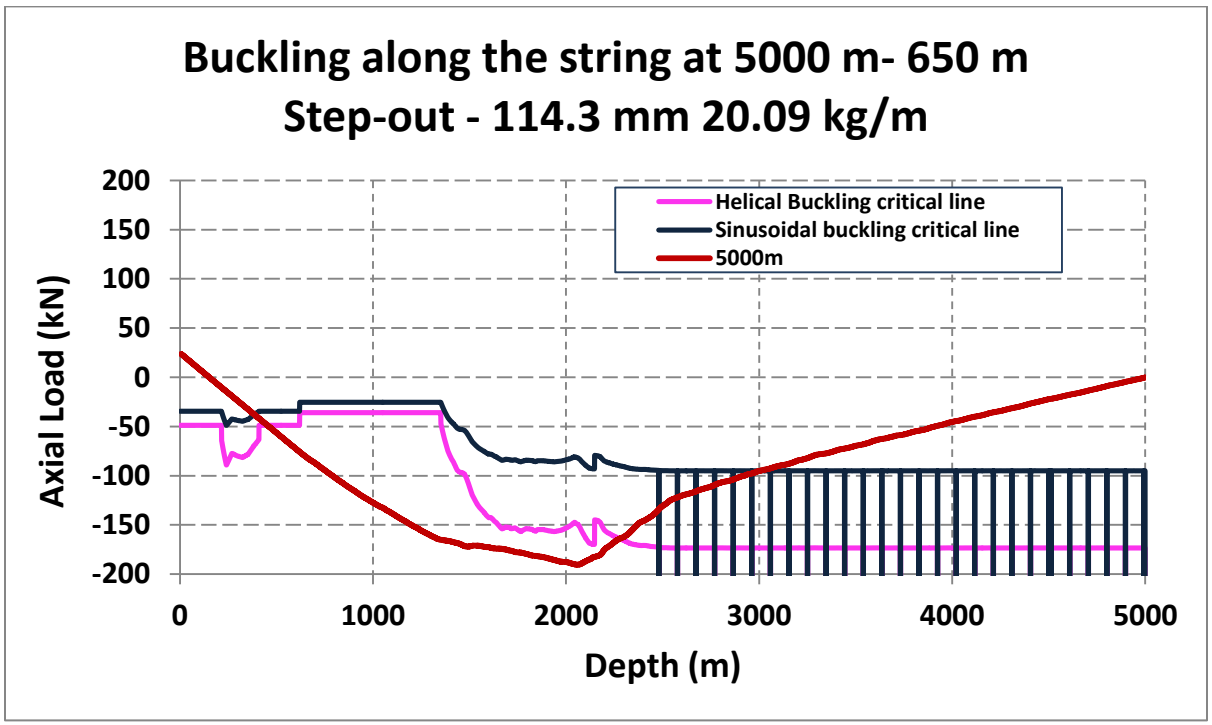

Figure 3.19. Helical and sinusoidal buckling prediction for running casing string as it is landed at total depth of 5000 m for a 650 m step-out well.

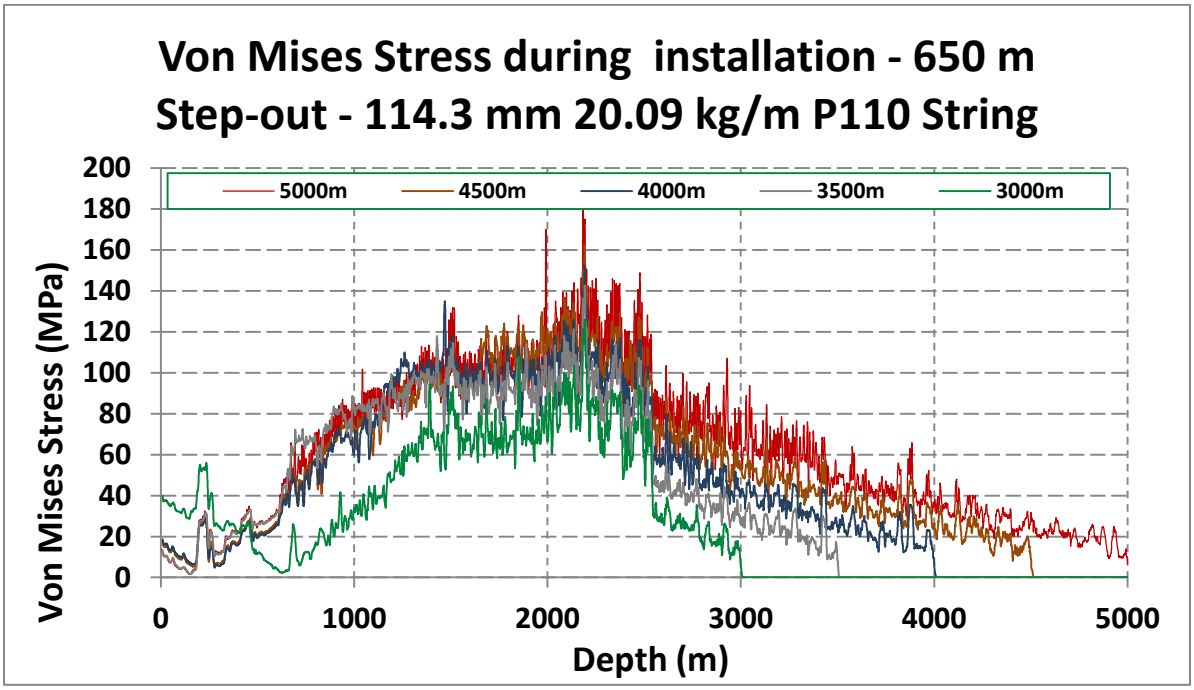

Figure 3.20. Von Mises stress along the casing string as the casing is run in hole at different depths for a 650 m step-out well.

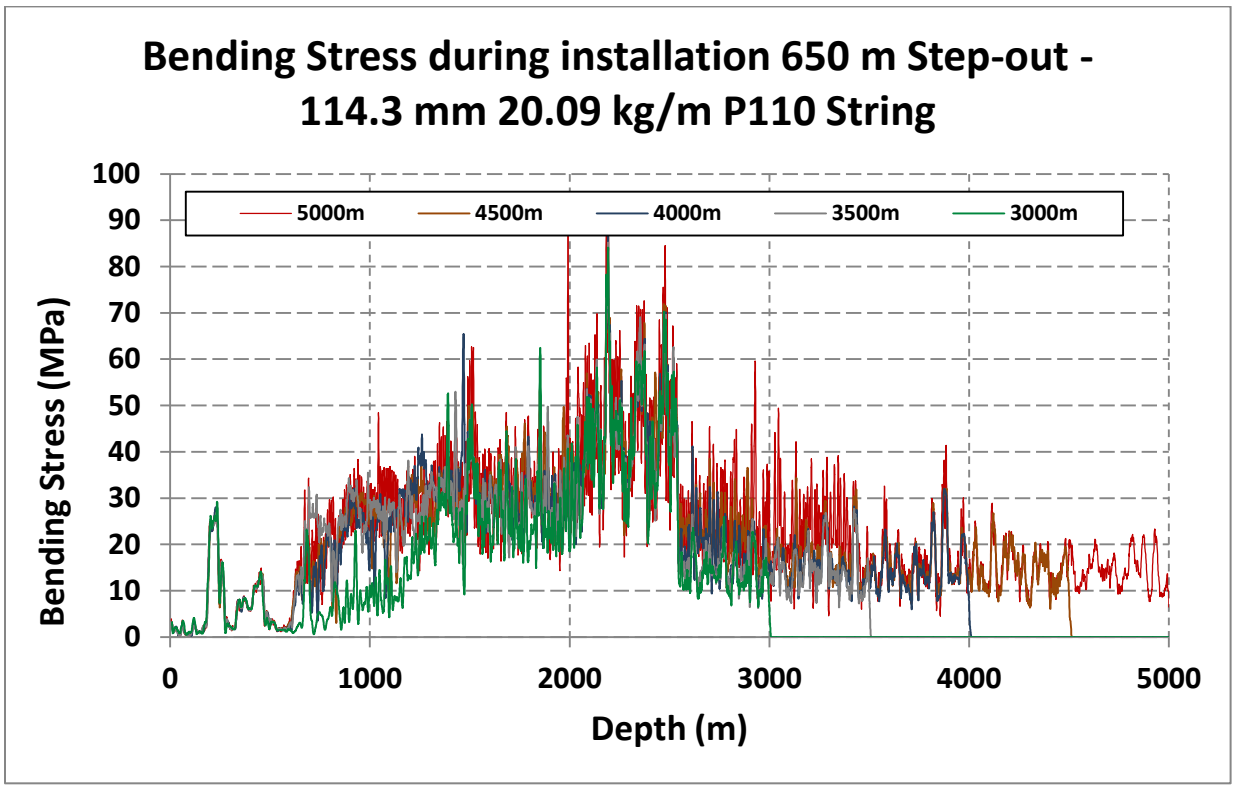

Figure 3.21. Bending stress along the casing string as the casing is run in hole at different depths for a 650 m step-out well.

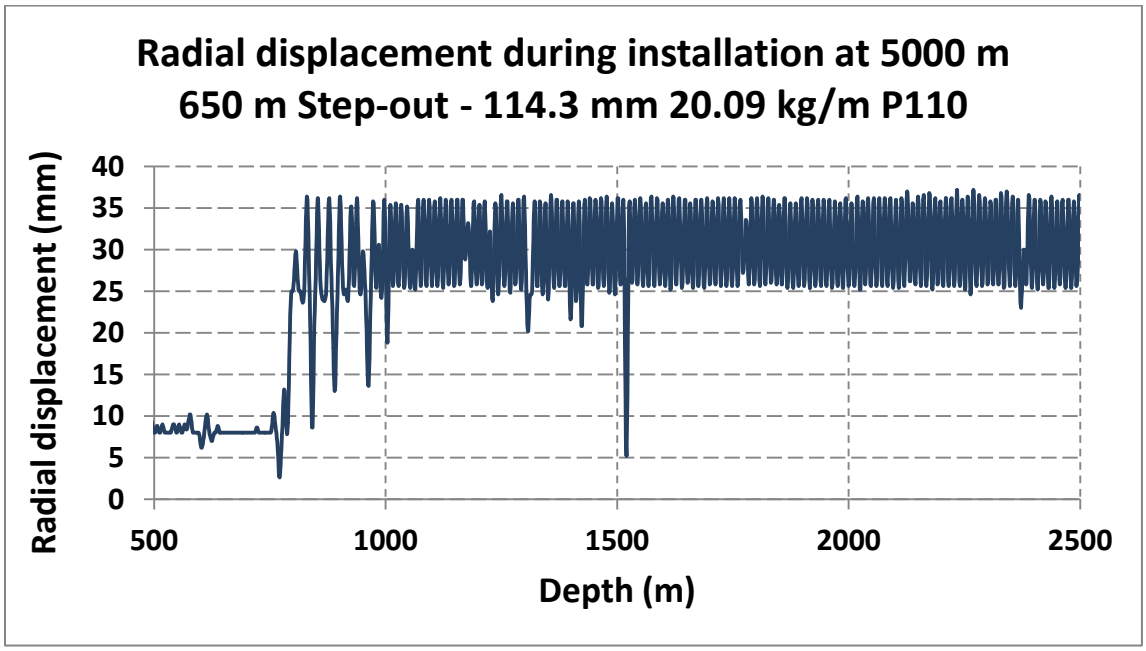

Figure 3.22. Radial displacement along casing string from 500 m to 2500 m when the casing is landed at 5000 m for a 650 meters step-out well.

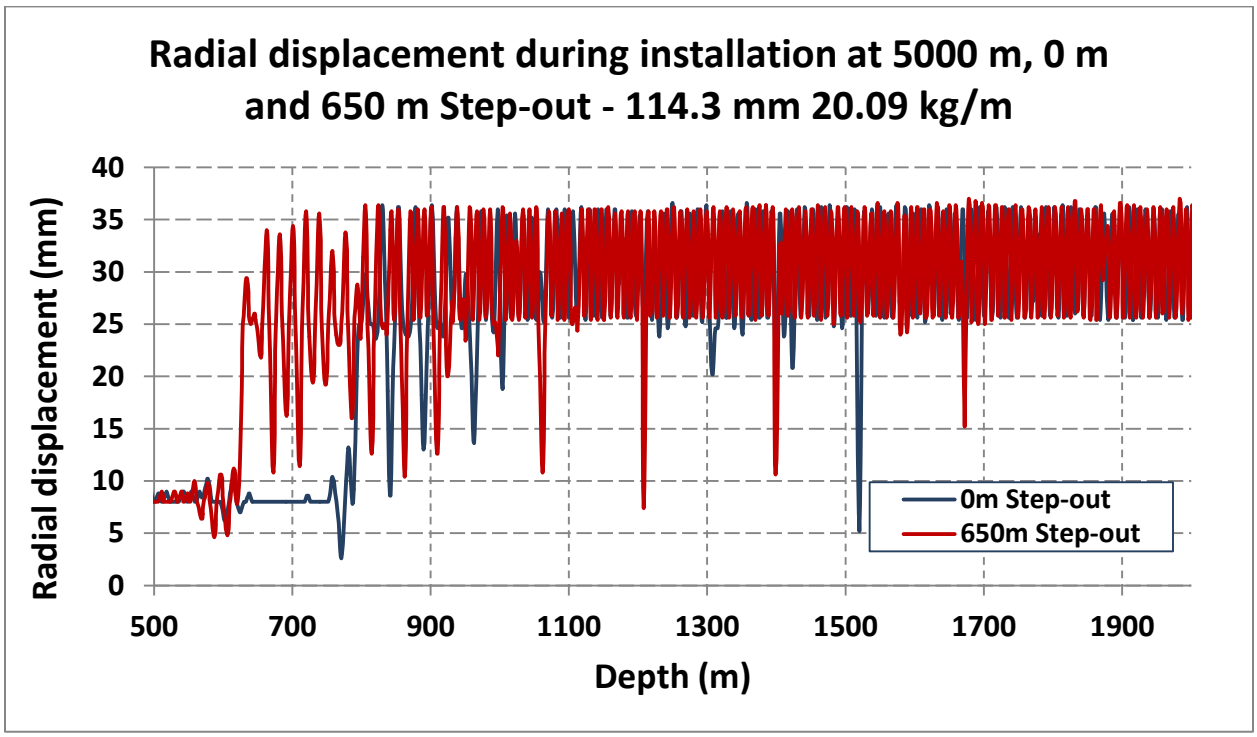

Figure 3.23. Comparison of radial displacement along the casing string from 500 m to 2500 m when the casing is landed at 5000 m for a zero and 650 m step-out well.

3.3 Local String Component Analysis (LSCA)

The main objective of the LSCA is to verify the casing pipe integrity by evaluating the mechanical stresses experienced by casing at a specific point along the string but with the addition of burst loads acting during the hydraulic fracturing stimulation. Then the effective loads are compared with the yield strength of the pipe material applying the operator's standard design factors. The method to evaluate the mechanical stress state of the pipe is the triaxial analysis explained in detail in Chapter Two. Once again, the first step is to define the variables involved in the analysis.

3.3.1 LSCA Variables Definition

The key inputs to perform the LSCA are: Pressure profiles along the casing string (internal and external pressure) at initial conditions and hydraulic fracturing conditions, and the mechanical stresses at initial conditions (casing landed at total depth).

3.3.1.1 Pressure Profiles

Fluids pressure inside the casing and outside the casing need to be considered at prevailing conditions right before the hydraulic fracturing, casing filled with fracturing fluid at ~1300 kg/m^3, and at the fracturing stage when pressure is applied at the wellhead on top of the hydrostatic column of the fracturing fluid (63 MPa for cold fracking and 69 MPa for screen-out scenario) as shown in Figure 3.24. For both cases, pre-fracturing and at-fracturing, the external pressure has a hydrostatic gradient to approximately 2300 m and pore pressure gradient from there to final depth (Figure 3.25).

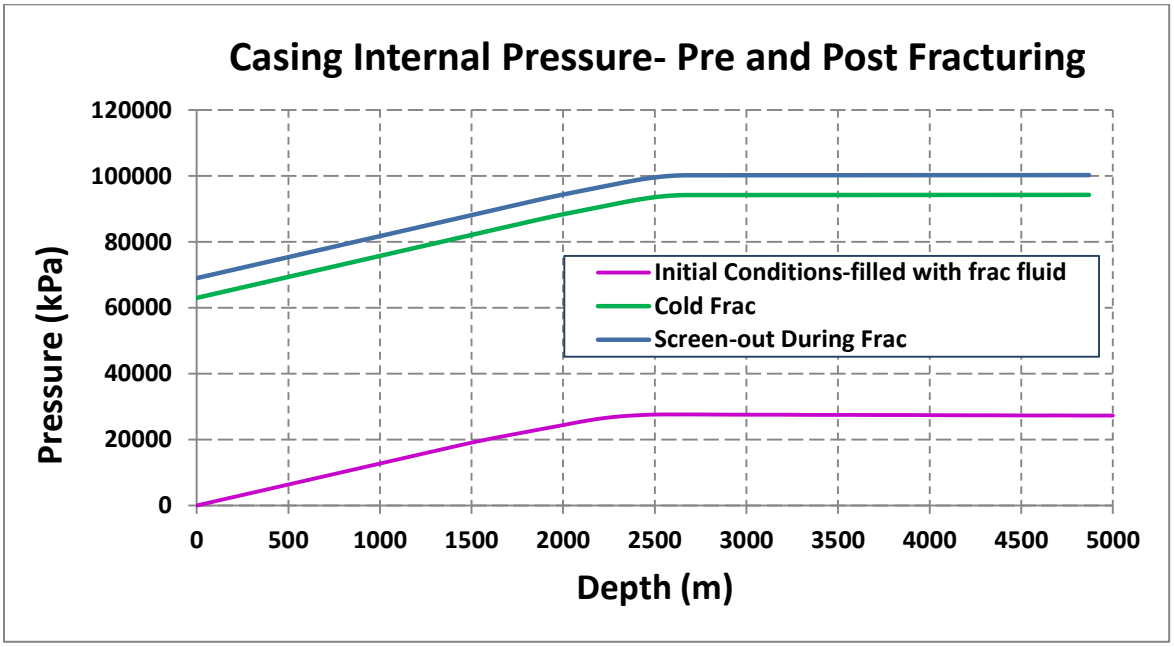

Figure 3.24. Casing internal pressure profile before and during hydraulic stimulation operations.

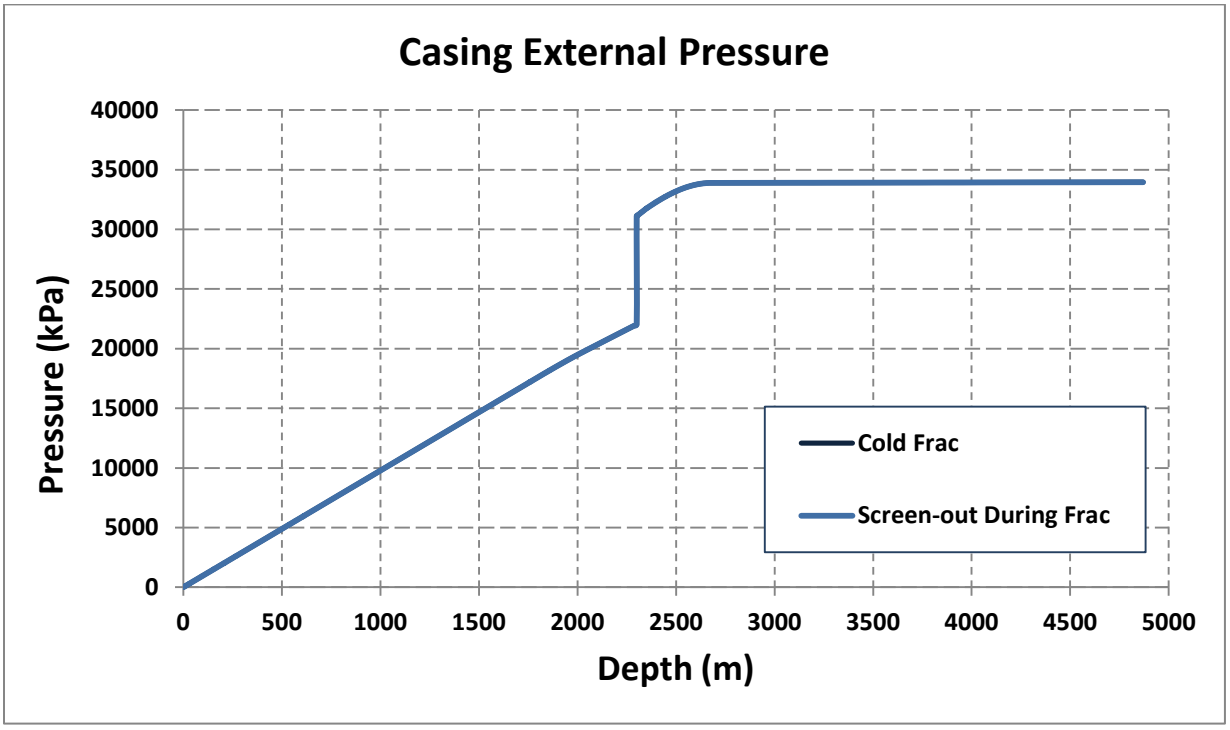

Figure 3.25. Casing external pressure profile (annular) before and during hydraulic stimulation operations (pressure is the same for both scenarios).

3.3.1.2 Casing Mechanical Stresses

The mechanical stresses acting on the casing are: Tangential (hoop), radial, axial and bending. By combining all these stresses, one can calculate the Von Mises stress as shown in Chapter Two. These stresses were calculated in the GCSA section for wells at 0m and 650 m step-out. Figure 3.26 shows all the stresses for the zero meters step-out well and Figure 3.27 shows the stresses for the 650 m step-out well.

The maximum compression load experienced by the pipe while casing is being run in the hole will also be used in the local component analysis. Figure 3.28 shows a summary of the maximum compressive loads acting on the casing at different depths during the installation.

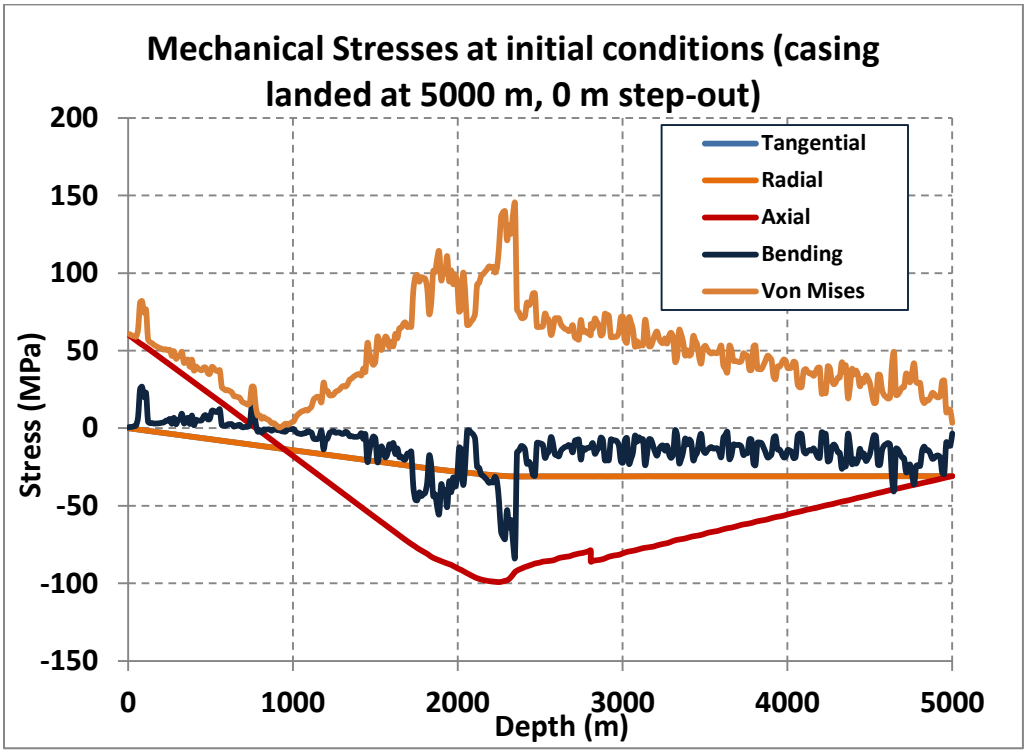

Figure 3.26. Mechanical stresses along the casing string for a 0 m step-out well.

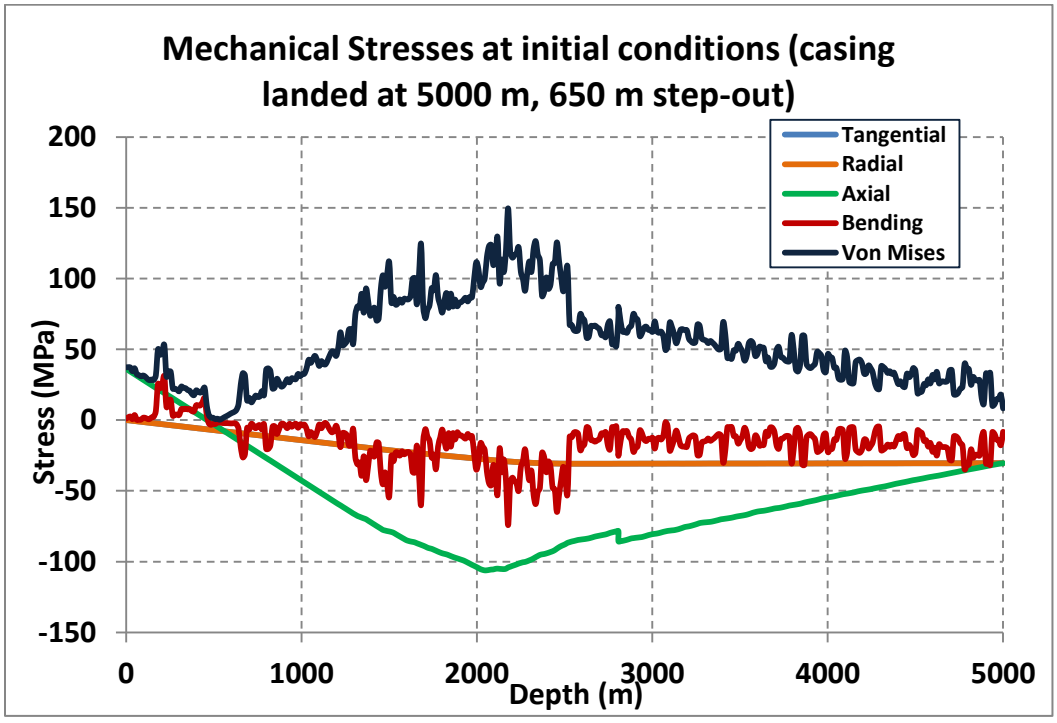

Figure 3.27. Mechanical stresses along the casing string for a 650 m step-out well.

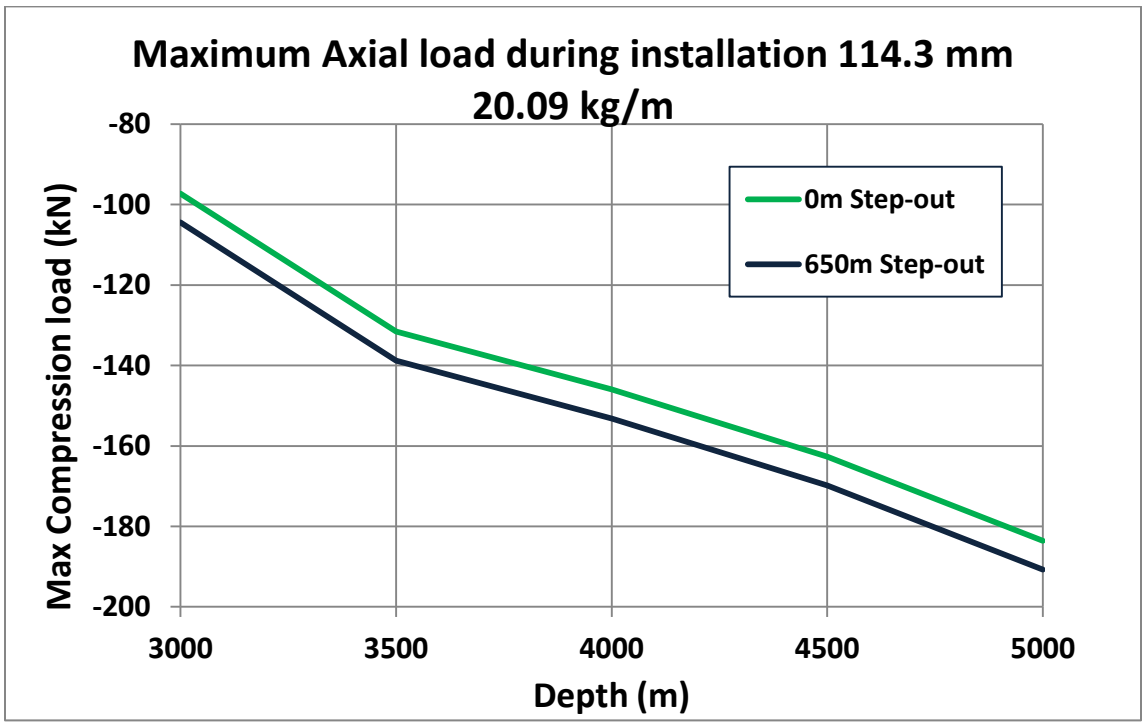

Figure 3.28. Maximum compressive load along the casing string at different running depths.

3.3.2 Casing Integrity Evaluation

3.3.2.1 Design Limit Envelope

In order to evaluate the integrity of the casing, a failure criteria mechanism has to be used to compare actual casing mechanical loads against the strength properties of the casing material. The failure criteria method to be implemented is the triaxial yield analysis using the triaxial yield ellipse method. In Chapter two, there is a detailed description on the triaxial analysis concepts.

The first step is to develop the triaxial ellipse (envelope). The envelope was generated based on the guidelines developed in API 5C3 where:

$$\sigma_e = \sqrt{[\sigma_r^2 + \sigma_t^2 + \sigma_a^2 - \sigma_r\sigma_t - \sigma_r\sigma_a - \sigma_t\sigma_a]} \quad (3.2)$$

$$\sigma_r = \frac{(P_i D_i^2 - P_o D_o^2) - (P_i - P_o)\frac{D_i^2 D_o^2}{4r^2}}{D_o^2 - D_i^2} \quad (3.3)$$

$$\sigma_h = \frac{(P_i D_i^2 - P_o D_o^2) + (P_i - P_o)\frac{D_i^2 D_o^2}{4r^2}}{D_o^2 - D_i^2} \quad (3.4)$$

Pi, Casing internal pressure (pascal)

Po, Casing external pressure (pascal)

Di, pipe inside diameter (meter), calculated based 87.5% of pipe wall thickness API tolerance for burst

Do, pipe outside diameter (meter)

r, radial coordinate (meter), assumed at the internal wall of the pipe

Combining equations (3.3) and (3.4) with equation (3.2) and simplifying results in the basic governing equation for developing the triaxial ellipse envelope:

$$f_y^2 = \left[\sigma_a - \frac{P_i D_i^2 - P_o D_o^2}{D_o^2 - D_i^2}\right]^2 + 3\left[\frac{(P_i - P_o) D_o^2}{D_o^2 - D_i^2}\right]^2 \quad (3.5)$$

Where f_y is the yield strength (MPa) of the species the envelope is being developed for (P110 casing grade). Equation (3.5) is then rearranged into quadratic form and a set of internal pressure (*Pi, MPa*) values are generated for a given external pressure. The equivalent axial stress required to meet the yield criteria is then calculated to form the ellipse. The quadratic form of the equation can be written as:

$$0 = \sigma_a^2 - 2\sigma_a\left(\frac{P_i D_i^2 - P_o D_o^2}{D_o^2 - D_i^2}\right) + \left(\frac{P_i D_i^2 - P_o D_o^2}{D_o^2 - D_i^2}\right)^2 + 3\left[\frac{(P_i - P_o)D_o^2}{D_o^2 - D_i^2}\right]^2 - f_y^2 \quad (3.6)$$

Where in terms of the quadratic equation $y = \sigma_a$ and the a, b and c terms are equal to

$$a = \sigma_a^2 \quad (3.7)$$

$$b = -2\left(\frac{P_i D_i^2 - P_o D_o^2}{D_o^2 - D_i^2}\right) \quad (3.8)$$

$$c = \left(\frac{P_i D_i^2 - P_o D_o^2}{D_o^2 - D_i^2}\right)^2 + 3\left[\frac{(P_i - P_o)D_o^2}{D_o^2 - D_i^2}\right]^2 - f_y^2 \quad (3.9)$$

For Equations 3.5 to 3.9, units are: f_y , σ_a, *Pi* and *Po* are in pascal; *Di* and *Do* are in meter.

The solution to the quadratic equation is equal to the two solutions to the equation. This formula generates two axial loads at which the failure criterion is satisfied for any set of fixed external pressures with a varying internal pressure. The limits of the equation are found by extending the internal pressure until the equation no longer has a solution.

Once the design envelope is built, the critical loads are calculated and plotted on the triaxial ellipse. Two loads are required to define the casing mechanical state right before and during hydraulic fracturing: Maximum compression load and casing inside pressures before and after fracturing.

The pressures were discussed in Section 3.3.1.1, and they are shown in Figure 3.24 and Figure 3.25. The loads to plot on the design envelope are the differential pressures (P external minus P internal).

As for the compressive loads, the numbers shown in Figure 3.28 are used. However, a further calculation should be done to add the ballooning effect on the axial load due to the high internal pressure applied to the casing during fracturing.

Ballooning can be explained with the use of Poisson's ratio (taken from Tubular Design Technology Training, Viking Engineering, L.C). Poisson's ratio (ν) is the relationship between lateral expansion or contraction of the tubular and its change in length. When a tubular is pressurized on the inside, its diameter slightly expands or "balloons". This causes the length to decrease (negative).

$$\Delta L = -2\frac{\nu L}{EA_p}(P_i A_i - P_o A_o) \tag{3.10}$$

L is in meter, Pi and Po are in pascal, E is in pascal, Ai, Ao and Ap (cross-section area) are in square meter, and ν is dimensionless.

However, if the top and bottom of the tubular are constrained, an increase in internal pressure or a decrease in external pressure results in added tension (positive) in the tubular due to this effect. To calculate the added tension, equation (3.11) is used.

$$\Delta F = -2\nu(P_i A_i - P_o A_o) \tag{3.11}$$

The ΔF (in newton) is added to the maximum compression load. This will reduce the compressive load on the casing pipe. Table 3.1 shows a summary of the axial loads including ballooning and pressures to be plotted on the design envelope for different running depths starting from 3000 m to 5000 m for both 0 meters and 650 m step-out wells.

	Effective loads during hydraulic fracturing			
	0m Step-out		650m Step-out	
Depth	**Axial (kN)**	**Pressure (kPa)**	**Axial (kN)**	**Pressure (kPa)**
3000m	221.2	78828.2	214.0	78828.2
3500m	186.9	78841.4	179.7	78841.4
4000m	172.5	78881.1	165.3	78881.1
4500m	155.8	72167.6	148.6	75543.7
5000m	134.9	72167.6	127.7	75747.5

	Effective loads before hydraulic fracturing			
	0m Step-out		650m Step-out	
Depth	**Axial (kN)**	**Pressure (kPa)**	**Axial (kN)**	**Pressure (kPa)**
3000m	-97.2	9828.2	-104.4	9828.2
3500m	-131.6	9841.4	-138.8	9841.4
4000m	-146.0	9881.1	-153.2	9881.1
4500m	-162.7	3167.6	-169.8	6543.7
5000m	-183.5	3167.6	-190.7	6747.5

Table 3.1 Casing effective loads for design plot analysis.

The final step is to plot axial load against differential pressure on the triaxial ellipse envelope. Figure 3.29 shows the design limit envelope for the 20.09 kg/m P110 casing for different depths and the load cases for the two types of wells considered in this thesis, zero meters and 650 meter step-out.

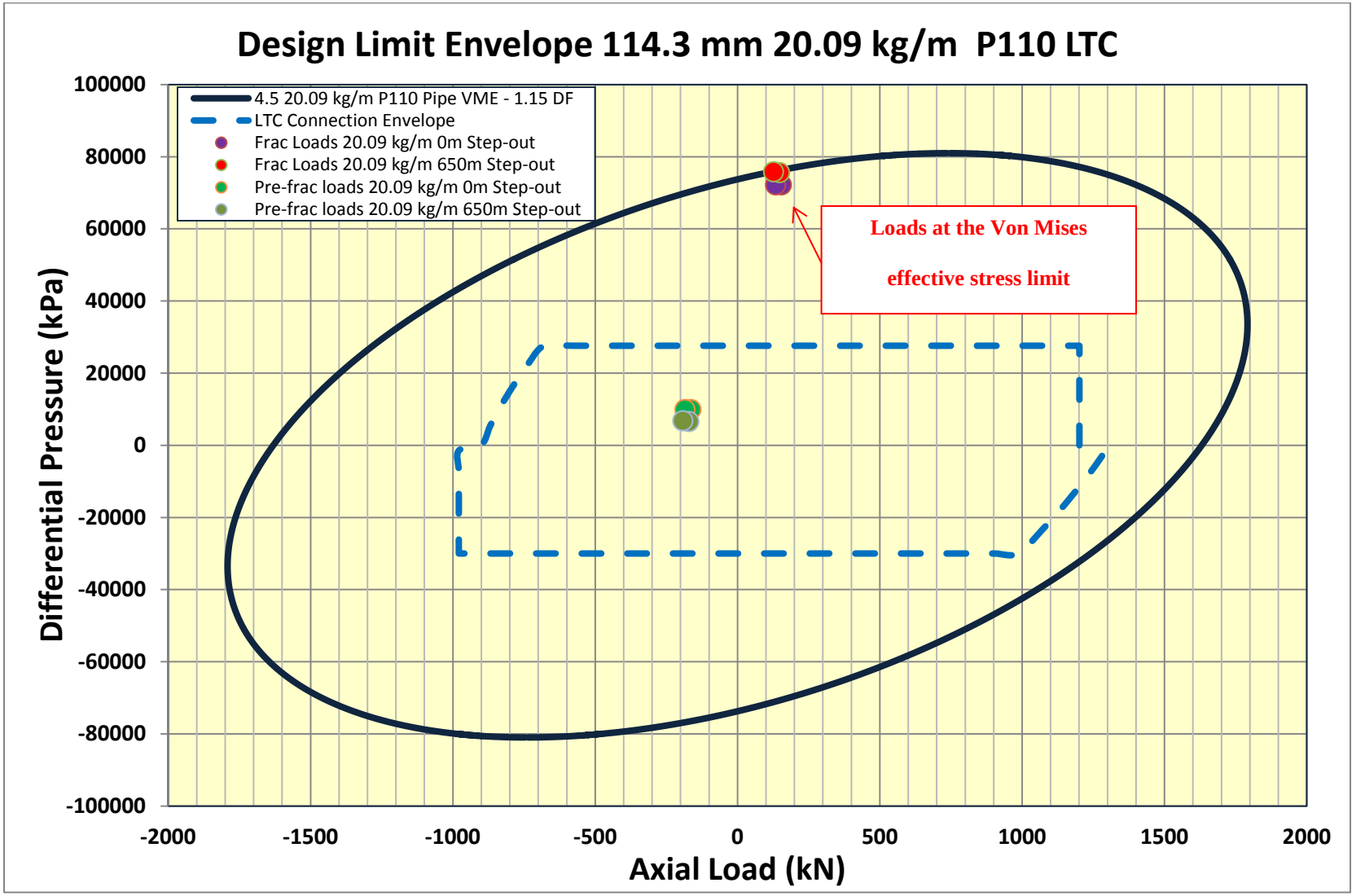

Figure 3.29. Design limit envelope for 20.09 kg/m P110 LTC casing under hydraulic fracturing stimulation operations.

3.3.2.2 Mechanical Stresses Approach

The final integrity analysis for casing is the stresses evaluation approach. In this analyis, two stresses along the pipe are evaluated against the yield strength of the casing derated with a proper design factor (see Appendix A for standard safety factors).

The first stress to be analyzed is the Tangential stress or hoop stress. This stress would cause the pipe to burst if the yield strength of the pipe material is exceeded. Figure 3.30 shows the tangential stress along the pipe for the highest stress values of the 650 m step-out well (650 m step-out is the critial case according to the design limit envelope).

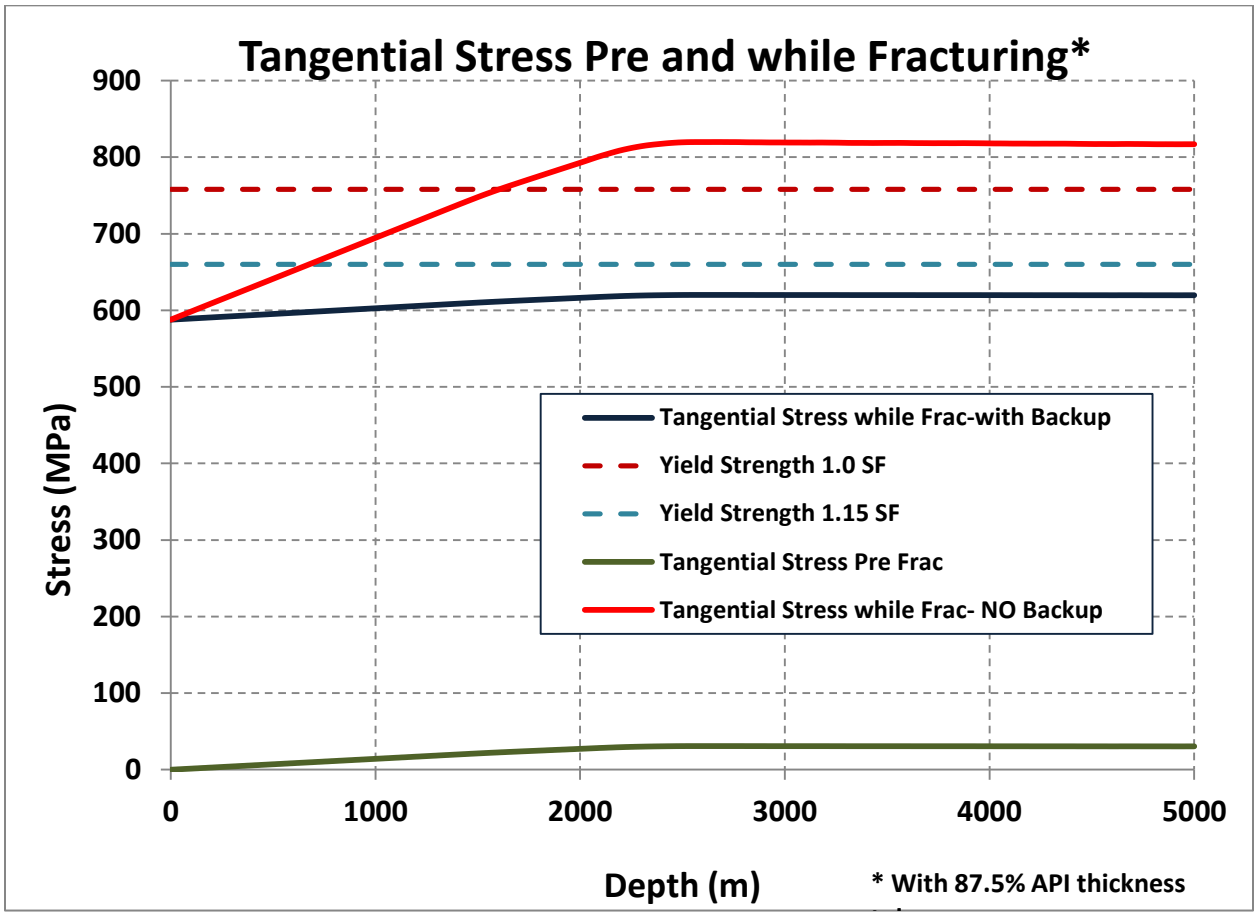

Figure 3.30. Tangential (Hoop) stress for 20.09 kg/m P110 LTC casing at initial conditions and under hydraulic fracturing loads.

Since the tangential stress is not dependant on the axial load (compression due to bending and buckling), the second stress to be analyzed is the Von Mises stress, which gives the indication of how the axial stress contributes to the total stress state of the pipe. The Von Mises stress must be below the yield strength of the pipe to guarantee the mechanical integrity of casing. Figure 3.31, shows the Von Mises stress along the pipe for the highest stress values of the 650m step-out well (as indicated above 650 m step-out is the critial case according to the design limit envelope).

In both Figure 3.30 and Figure 3.31, the stress is also calculated assuming no casing external back-up in the annular; this means zero external pressure. This is done to evaluate the effect of having no fluids or pore pressure at the back of the casing string.

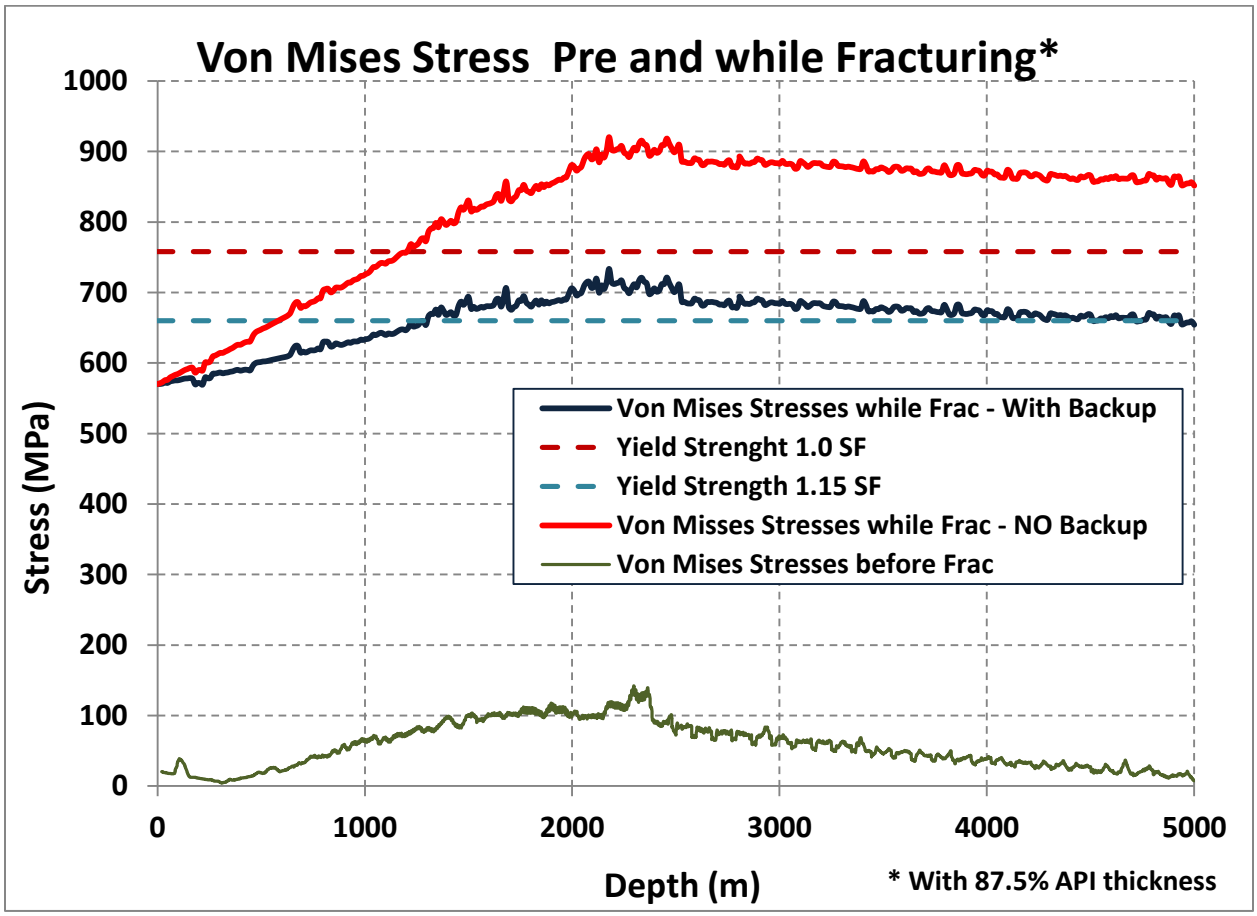

Figure 3.31. Von Mises stress for 20.09 kg/m P110 LTC casing at initial conditions and under hydraulic fracturing stimulation loads.

3.4 Summary of Modeling Results

Each one of the modeling processes, Global Casing String Analysis (GCSA) and the Local String Component Analysis (GCSA), provide a good understanding of mechanical conditions the production casing string experiences while being run in the well and during the hydraulic fracturing operations.

As the casing is run in hole, the load measured with the drilling rig surface sensor indicates the total weight of the pipe that is being installed in the well (this is the hookload). As pipe is added to the casing string, and lowered into the well, the hookload increases. However, the contact forces between casing and wellbore as the well deviates from vertical cause friction. Therefore at some point during the running operation, the hookload starts decreasing until all the weight of the string is transformed into friction, and there is no more weight available to continue pushing casing into the horizontal well. During this process, the string experiences compressive forces, and when the compressive forces exceed the critical buckling limits, the pipe enters into an instability state and it buckles.

From the modeling results shown in Figure 3.8, one can see that as the casing goes into the well the weight increases until approximately 2000 m. After this point the weight decreases progressively until the casing is deployed to the planned total depth. The inflection point at which the casing starts losing hook weight coincides with the kick-off point of the well or the start of the build section where the well is deviated from vertical (or lower inclination) to 90 degrees (horizontal). As the casing continues losing weight through the build and the horizontal section, the effective compressive force increases to the point that casing enters into sinusoidal buckling first and then into helical buckling. It can be seen in Figure 3.9 that pipe buckling is not initiated until casing reaches a depth of approximately 2800 m. For this reason, it is generally

considered that up to this depth the casing is in a "safe" state and there are no concerns that excessive slack-off can cause any casing integrity problems when hydraulic fracturing is performed. For rig personnel, the meaning of this conclusion is that they can apply all the weight available to run casing until about 3000 m depth as long as the casing is not pushed with rig equipment (block and top drive), which means that the hookload would be negative. For safety reasons and to have a margin to keep pushing casing into the well, a minimum hookload of 30-50 kN is recommended.

The axial load calculations show that the maximum compressive force acting on the casing occurs when casing reaches the final depth of 5000 m. Compressive load is as high as 190 kN and 183 kN for the 650 m and 0 m step-out wells, respectively (Figures 3.10 and 3.18). The maximum compression is located at approximately 2100 m along the casing string for both wells step-outs. This point is considered the critical point of stresses where Von Mises equivalent stress and the buckling bending stress are at their maximum value. This critical point is where that combined axial load and burst from hydraulic fracturing has to be studied.

It is also seen from the buckling charts (Figures 3.11 and 3.17) that once casing is landed at the final depth of 5000 m, the pipe axial force exceeds the sinusoidal and helical limits. For the 650 m step-out well the pipe starts buckling 300 m earlier than for the 0 m step-out well at 500 m depth. This is explained by the higher tortuosity of the well with higher step-out.

It is also noticed that casing stays in helical buckling mode until around 2250 m depth and then in sinusoidal buckling mode until 3000 m depth. From the latter and to the final depth the casing is not buckled. Since the model shows that the casing is into helical mode buckling at the depth of 2100 m when the compressive force is at its highest value, a possible pipe wrinkling or plastic deformation in combination with hydraulic fracturing pressures could affect integrity of the pipe.

Although casing goes into buckling along a major part of the well, this does not mean that there is a risk of failure or string lock-up (pipe unable to move up or down the well). As a matter of fact, when the Local String Component Analysis (LSCA) is done, one can appreciate that effective stresses before hydraulic fracturing are significantly lower than the casing yield strength (Figure 3.31). From the stress results, it is also clear that the bending stress which eventually affects the total axial stress is the most important contributor to the high installation stresses. Added to stresses coming from high fracturing pressures will exceed the casing yield strength. Bending stress comes mostly from well doglegs and pipe shape deformations due to buckling.

Once all the mechanical stresses that act on the casing as a result of the combination of high bending/compressive stress and hydraulic fracturing pressures are obtained, the design limit plot is used to evaluate casing integrity due to combined loads. Both the design limit envelope method and the mechanical stresses approach show that for the 650 m step-out well, the effective loading state falls beyond the casing material yield strength. This means that the integrity of the 114.3 mm 20.09 kg/m P110 casing is compromised if the casing running loads (slack-off) are not well controlled to keep the compressive stresses within safe limits. As for the 0 meters step-out well, the stress state is approaching the design limit envelope. Consequently pipe yielding risk is also considerable.

Knowing the implications of compromising casing integrity because of mechanical factors, it is recommended to find an alternative to prevent casing failure during the hydraulic fracturing operation phase.

Chapter Four: **A New Production Casing Design Approach**

In the findings of the Global Casing String Analysis (GCSA) and the Local String Component Analysis (LSCA), it is evident that the casing is subjected to loads that may exceed material strength and design criteria.

The total equivalent stress experienced by the casing increases considerably as a function of two main factors as follows:

- Hydraulic fracturing treatment high pressures
- Amplified bending stresses

The fracturing pressures cannot be reduced or changed since they are dictated by the stress and pressure regime of the reservoir, therefore they are a fixed factor in the casing design process and the reservoir stimulation operations.

Bending stress are mainly attributed to high Dogleg severity particularly in the curve section of the well and pipe buckling caused by high contact forces (friction) between casing and wellbore. It is worth mentioning once more that the contact forces increase when the well tortuosity (doglegs and microdoglegs) is higher, or as the length of the well further extends.

The mechanical stresses analysis demonstrated that, with the current well design conditions and limiting the wells to a total length of 5000 m (2700 m approximately of horizontal length), the risk of having loads conditions that may exceed the casing limits is high, especially for wells with the larger step-out.

The main concern for the operator is that the field development plan for the asset requires increasing complexity of the well trajectories with even higher than 650 m step-out and longer wells to optimize the reservoir drainage (3000 m approximately of horizontal length).

Evidently, bending stresses are governed by both well construction and installation or running procedures. This introduces the Wells Engineer with an opportunity to optimize the well design and to recommend field practices for running casing into the wellbore, with the main goal of reducing bending stresses.

4.1 Well Design Optimization

Two main aspects are discussed as opportunities for design optimization: Well trajectory and casing selection.

4.1.1 Well Trajectory

As previously discussed the bending stresses are produced by the well dogleg severity and the deformation caused by the buckled pipe.

From the well trajectory factors, the best way to control the bending stresses is by reducing the dogleg severity in the build and the horizontal section of the well. This can be achieved by reducing the planned doglegs to achieve geological targets (well heel) or by controlling the actual build rates achieved by the directional tools. Efforts have already been done to reduce the required planned and the actual doglegs in the build section, therefore no further optimization on this aspect is considered on this thesis.

Currently, even though the horizontal section of the well is planned with relatively low dogleg severity (practically zero), the actual doglegs can be so high that they increase the drag that

eventually translates into additional pipe buckling in the top section of the well and more bending stresses. Sometimes the combination of buckling and drag prevents the casing from being deployed to its final planned depth.

The first simple but important recommendation to reduce drag in the horizontal section is to limit the dogleg severity by running rotary steerable tools or controlling the amount of sliding done in the lateral so that no unexpected aggressive changes in inclination or azimuth are introduced.

Figure 4.1 shows how a more controlled horizontal section helps to reduce drag and bending stress.

4.1.2 Casing Design

The current well design is using only one type of casing: 114.3 mm P110 20.09 kg/m. This has been identified as the proper type casing because it meets both the completions specifications requirements and the casing design standards (analysis for several loads during the well life cycle). However, after analysing the results from the modeling section in this thesis, the author of this thesis recommends evaluating the option of an alternative casing type.

Mechanical stresses are also determined by the geometry of the casing (external and internal diameters). There is no flexibility to change the external diameter of casing (114.3 mm) since this has already been optimized for the drilling and production phases. As per Equations 2.2, 2.3, 2.4 and 2.7 mechanical stresses are a function of the pipe diameters; the lower the internal diameter (thicker pipe wall) the less the magnitude of the stresses is. Likewise, one to the terms in Equation 2.12 is the second moment of inertia[25] (***I***). The larger ***I*** is, the higher the buckling

[25] Second moment of inertia for a cylinder is $I = \pi (do^4 - di^4) / 64$

critical force is; therefore more effective force is required to buckle. In summary, thicker wall casing is more difficult to buckle than a lesser thick wall casing; also the mechanical resistance to installation and fracturing loading is higher for a thicker wall pipe.

The solution would be obvious: an increase in casing wall thickness could solve the integrity issues. However, a thicker wall casing translates into a heavier pipe. From Equations 2.8 and 2.9 and 2.10, the normal forces (contact forces) that cause drag are heavily determined by the pipe weight. An increase in drag will diminish the capability to deploy casing to current total depths, and consequently to more extended wells.

The majority of drag experienced by casing pipe during the installation process is caused by pipe being pushed into the lateral section of the well. All the weight of the pipe is laid down on the low side of the wellbore.

The ideal solution would be to have a heavy pipe in the top portion of the well that can withstand the high combined stresses, and a lighter casing in the horizontal segment that can reduce the normal forces and consequently minimize drag.

Additionally, there are two external factors that can affect the casing selection: Compatibility with the hydraulic fracturing completions system and casing market availability.

In the current completion system, balls are pumped downhole to activate packers and open fracturing sleeves. The maximum ball diameter is 84 millimetres, therefore this dimension should be the minimum optimum casing internal diameter.

After checking the market availability and prices of heavier and lighter casing, it has been determined that casing that will be readily available is 114.3 mm P110 22.47 kg/m for the heavier option and 114.3 mm P110 17.2 kg/m for the lighter casing to be placed in the

horizontal section. The 22.4 kg/m casing has an internal diameter of 95 mm. This meets sufficiently the completions requirement.

The next step is to understand the effect of the new tapered casing string while being run into the wellbore, and the load behaviour in the proposed casing string under combined installation and hydraulic fracturing conditions.

4.1.2.1 Maximum Well Length

In order to check if the proposed casing can reach the planned final depth, a simulation in Wellscan® is done to predict how far (maximum depth) the casing string could be run in the wellbore. Figure 4.1 shows modeling results for key possible scenarios.

Some very interesting points can be made here; one can see that basically all casing strings except for the 22.4 kg/m can make it to the current total depth (~5000 m). This is understandable since the 22.4 kg/m has more weight available to keep pushing pipe along the wellbore as it is demonstrated with the highest inflection point (~325 kN) of all the options.

However, the benefit of the heavy weight becomes a downside for this string since that entire load has to be dragged along the horizontal section of the well. It can be noticed that this string loses weight quickly in the lateral section to eventually prevent the casing from getting to the 5000 m planned depth. If the minimum hookload to keep moving pipe into the wellbore is zero, the 22.4 kg/m can only be run to approximately 4600 m of total well depth. The high drag of the 22.4 kg/m-only string comes mostly from contact forces (friction) and only a small percentage is due to pipe buckling. These arguments clearly eliminate the 22.4 kg/m-only casing to be a viable recommendation for this project.

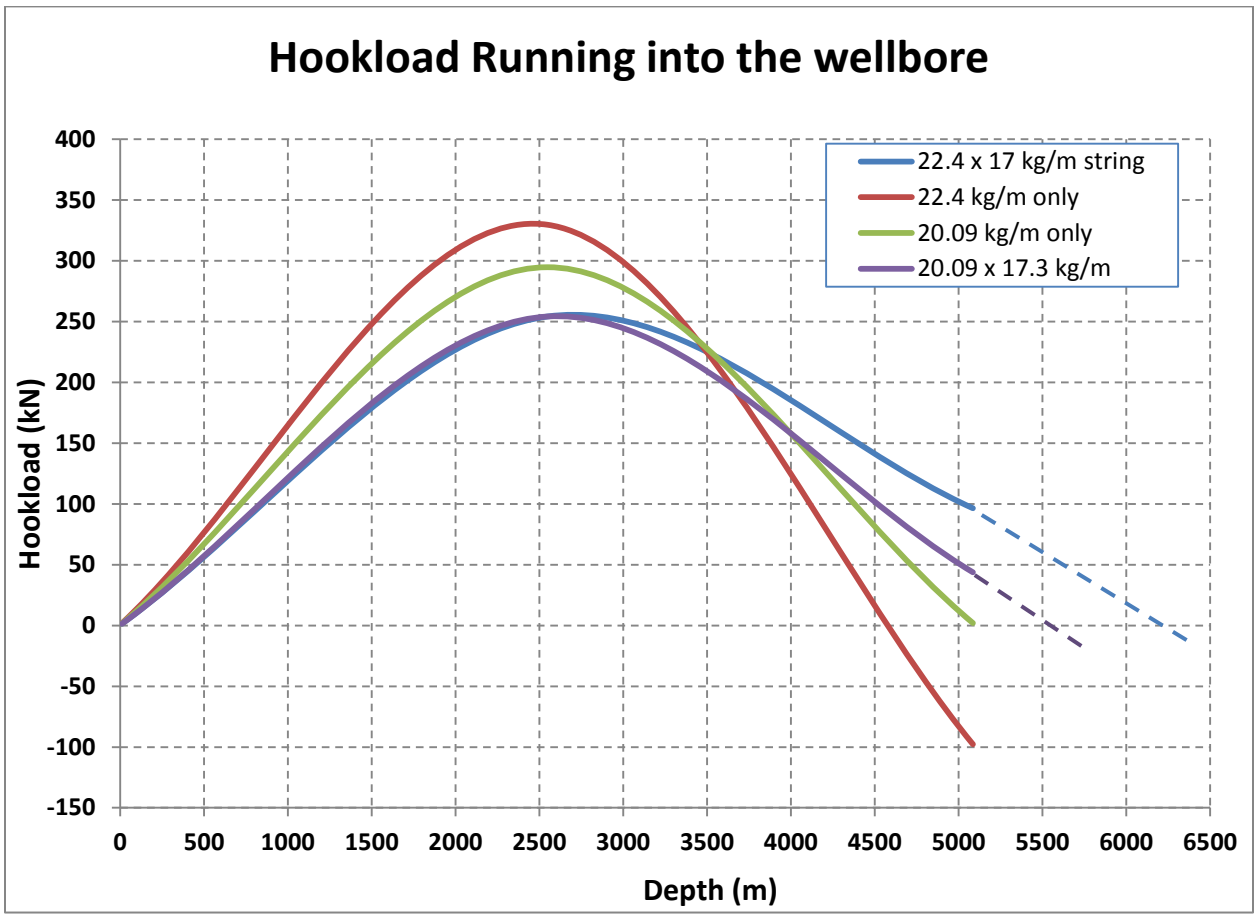

Figure 4.1 Hookload chart for different casing string options.

On the other hand, the 20.09 kg/m-only option (currently being used by the operator's asset) can be deployed to the current planned depth of 5000 m. However, it is not a recommended option for two reasons: Firstly, the total maximum length that the casing can be installed is already maxing out at 5000 m; therefore, there is not much potential for increasing further the length of the wells as the operator is planning to do. Secondly, the 20.09 kg/m-only casing has had integrity problems in the past and it has been proven that is already at the mechanical limit under combined loading.

The next option would be the tapered string 20.09 x 17.3 kg/m. The modeling indicates that this string is a good alternative to extend the maximum length of the well to a final depth of approximately 5500 meters (3000 meters horizontal section). This capability would satisfy the operator's field development plan of drilling longer wells.

However, from the mechanical stresses and combined loading perspective the previous string does not have a better strength than the 20.09 kg/m-only option. The 20.09 kg/m casing still goes under considerable helical buckling and the stresses approach the yield strength of the material. Nevertheless, there is an option to use this casing string by controlling the hookload during the installation process. The latter alternative will be analyzed in more detail later in this document.

The final tubular system option is the tapered 22.4 x 17.3 kg/m. It is clearly shown that the casing can be run up to 6200 meters total depth (3700 meters horizontal section). The heavy weight pipe can push the lighter casing which, at the same time, presents reduced contact forces in the lateral section of the well. Therefore, this would be the best choice for implementing extended reach wells. Next is the verification that the 22.4 x 17.3 kg/m casing string meets the casing design requirements by modeling the pipe under loading.

4.1.2.2 Tapered String under Combined Loading

This section presents the mechanical loading modeling carried out for the tapered string 22.4 x 17.3 kg/m. As done in Chapter 3, the first parameter to model is the axial force acting on the string. Since the most severe installation loading occurs when the casing is being landed at the final planned depth, the modeling is done only at 5000 meters depth and for the most critical well profile which is the 650 meters step-out well. Figure 4.2 shows how the compressive force is

reduced in the top section of the tapered string up to 20%. Also, note that the tapered casing goes into buckling 150 meters later than in the 20.09 kg/m casing. This means 150m of pipe that is buckled. All these factors would reduce considerably the total stresses acting on the casing.

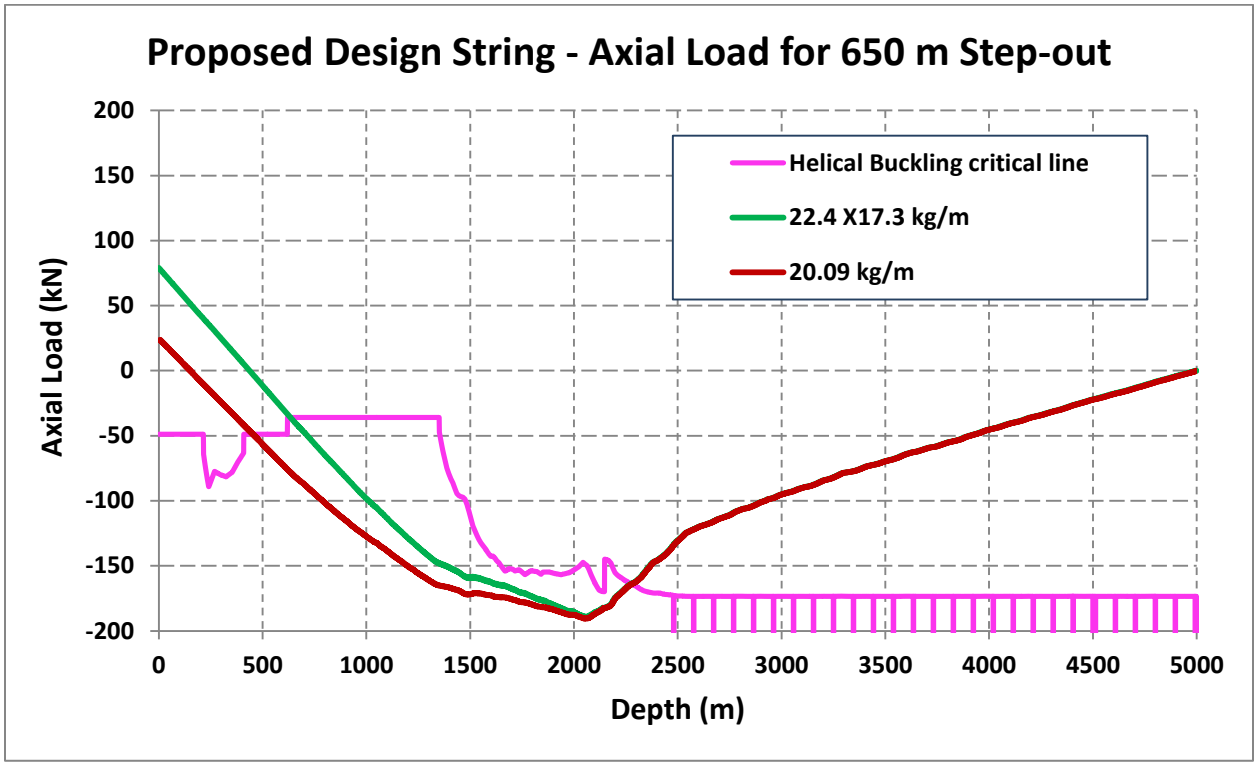

Figure 4.2. Axial load in the proposed casing string.

Figure 4.3 shows the bending stress analysis. The tapered string shows significant lower bending stress than the 20.09 kg/m-only string. It is also noticed that the bending stress line for the 20.09 kg/m is more erratic. This is most likely due to the higher pipe deformation caused for more severe buckling in both the top and the horizontal section of the well. The tapered string does not present aggressive bending peaks (~80 MPa) like the one seen at 2100 m for the 20.09 kg/m casing.

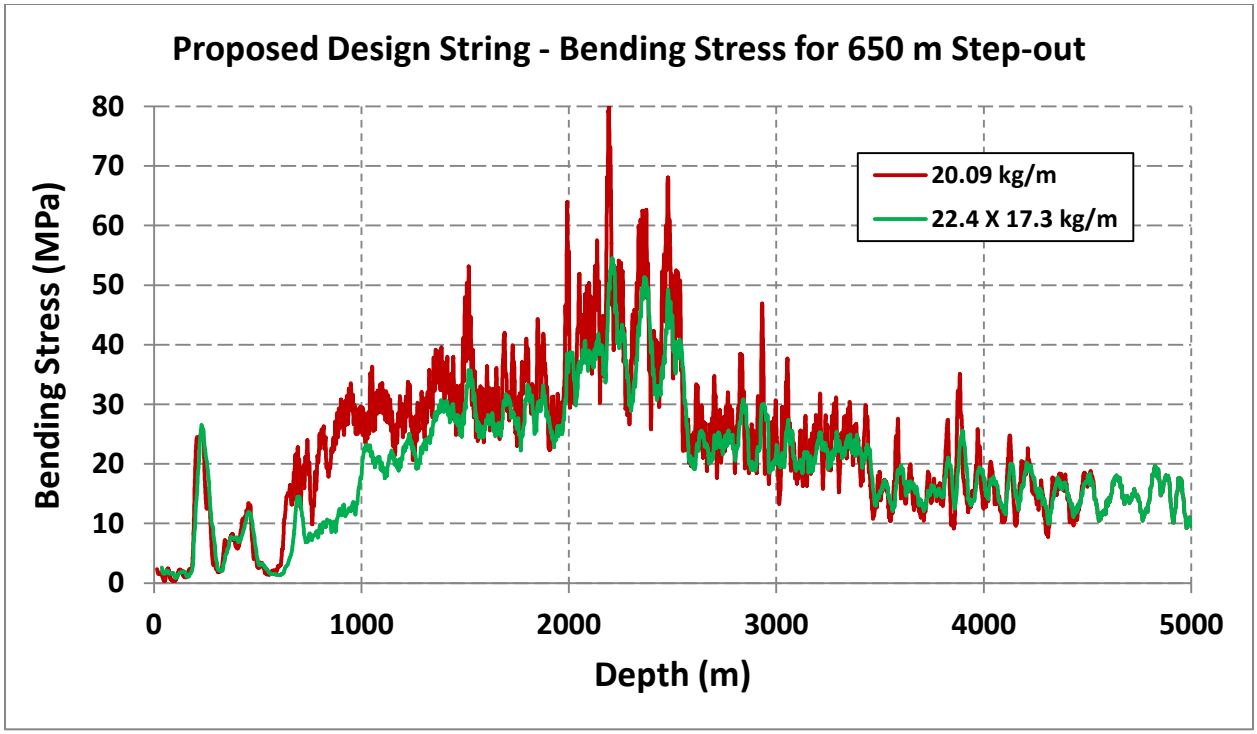

Figure 4.3. Bending stress for proposed casing string.

Similarly, the Von Mises stress is lower in the tapered 22.4 x 17.3 kg/m string than in the 20.09 kg/m casing (Figure 4.4).

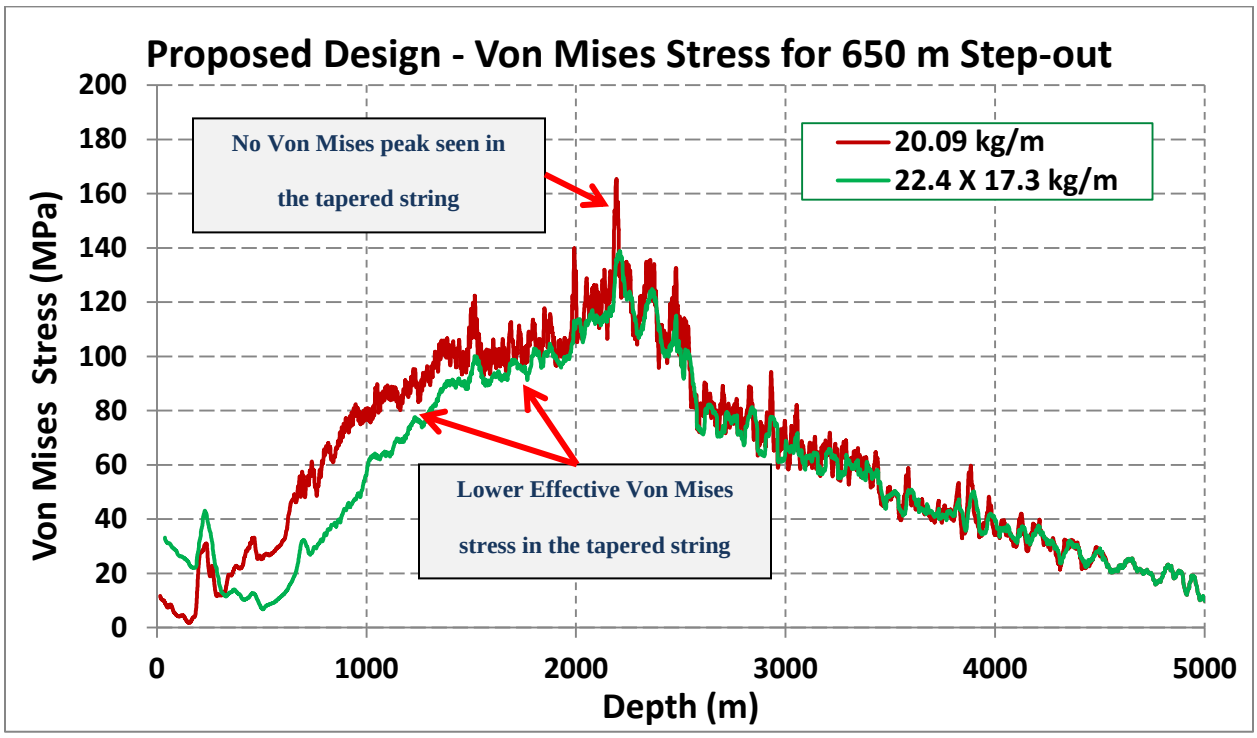

Figure 4.4. Von Mises stress for proposed casing string.

The stress analysis has also been done for the other type of well, the 0 meters step-out well. The results are not included in this document but they will be used later in the failure criteria.

Having defined all the forces and stresses acting in the casing, the next step is to develop the Von Mises ellipse and plot in it the combined loading acting on the pipe. This would be the final failure criteria to determine if the new proposed casing string meets the design conditions.

The triaxial ellipse envelope for the proposed casing string was develop following the process described in Section 3.3.2.1 section and according to API 5C3. Figure 4.5 shows the design envelope, which indicates that the proposed tapered string is adequate to withstand the combined loading of installation and hydraulic fracturing loads

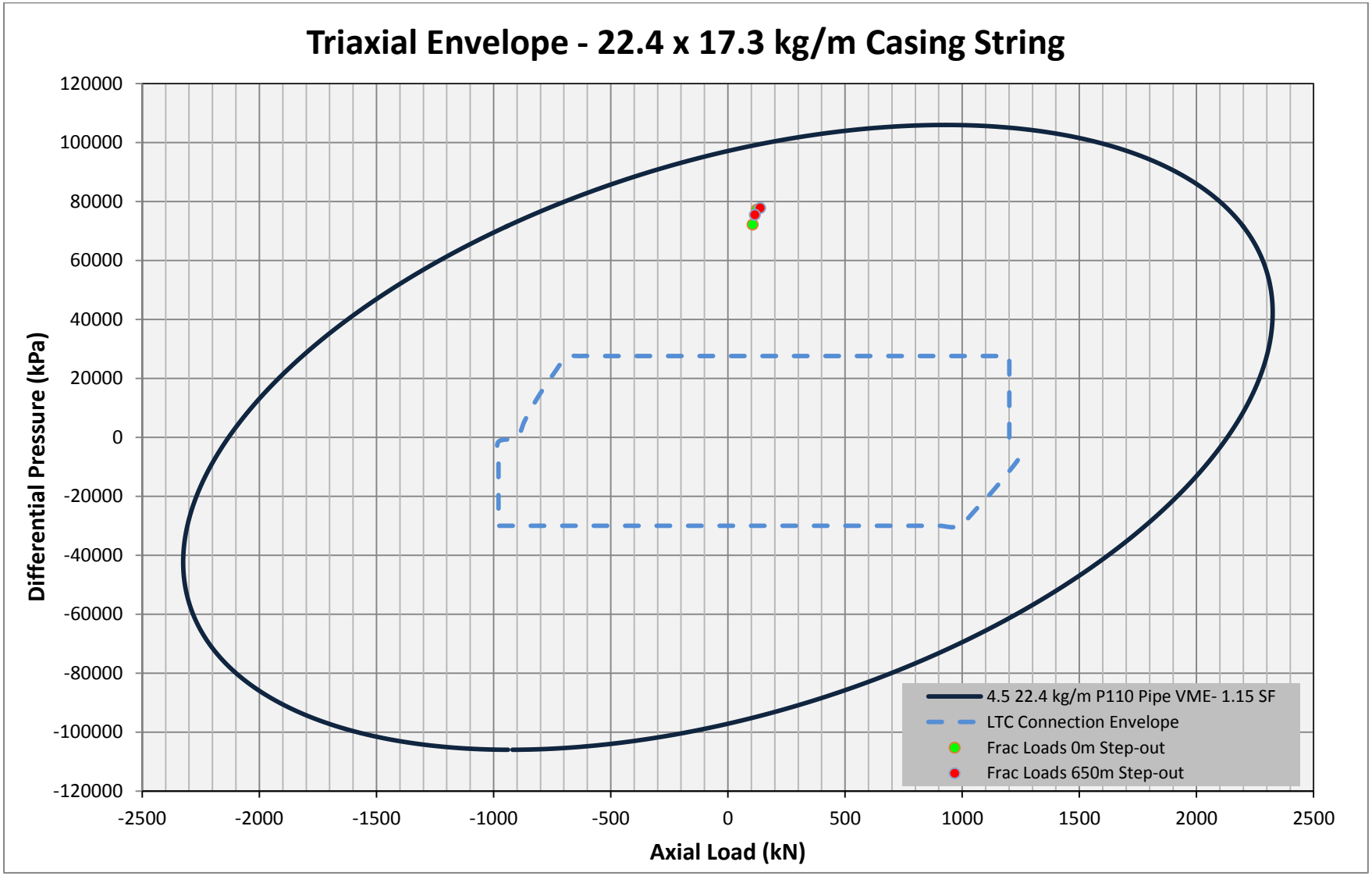

Figure 4.5. Design limit envelope for 22.4 x 17.3 kg/m under hydraulic stimulation operations.

4.1.2.3 Cost Impact of Implementing New Design

Table 4.1 shows costs for different casing strings options including the current one and the design proposed in this thesis (22.4 x 17.3 kg/m).

Casing	Unit Cost (CAD$/meter)
17.33 kg/m	42.24
20.09 kg/m	49.13
22.4 kg/m	56.80

	20.09 only	20.09 x 17.3	22.4 x 17.3
Top (2300 meters)	$ 112,999.00	$ 112,999.00	$ 130,640.00
Bottom (2700m)	$ 132,651.00	$ 114,048.00	$ 114,048.00
TOTAL COST (CAD$)	$ 245,650.00	$ 227,047.00	$ 244,688.00

Table 4.1. Cost of casing options.

The proposed design cost is equivalent to the current casing design cost (~$244k vs $245k). This makes the proposed casing string an attractive option, not only from a mechanical perspective, but also from the cost point of view.

4.2 Operations Recommendation: Controlling Running Loads

If the total well length is limited to 5000 meters and it is beneficial to run the lighter 20.09 x 17.4 kg/m tapered string because of completions requirement (internal diameters restriction) or

economic advantages, it is possible to maintain the integrity of the casing by controlling the amount of "slack-off" weight during the casing installation process.

As the casing is being run in the wellbore, the hookload weight starts decreasing as the friction increases. The more casing weight is lost in the running process, the higher is the compression force acting on the pipe.

By providing the rig personnel with a defined number on how low the weight in the hookload sensor (Martin-Decker) can be, one is limiting the amount of compression in the pipe. Since this compression is applied at different running depths (from 3000 m onwards); a limiting number must be given for each depth.

As explained previously, the tapered 20.09 x 17.3 kg/m string could be potentially run to 5500 meters depth. However, that maximum length would be decreased by controlling the "slack-of" weight.

Figure 4.6, shows the model of hookload measurements at surface (0 meters depth) when running casing into the wellbore and still keeping the casing within the strength limits. By applying these limits its maximum length would be 5000 m, i.e., the casing run would be short of the desired 5500 meters. This means the tapered string with lighter 20.09 kg/m casing on top, will not meet the expectations of having longer wells (up to 3200 meters horizontal length), however it would be a good solution for shorter wells (2700 meters horizontal length).

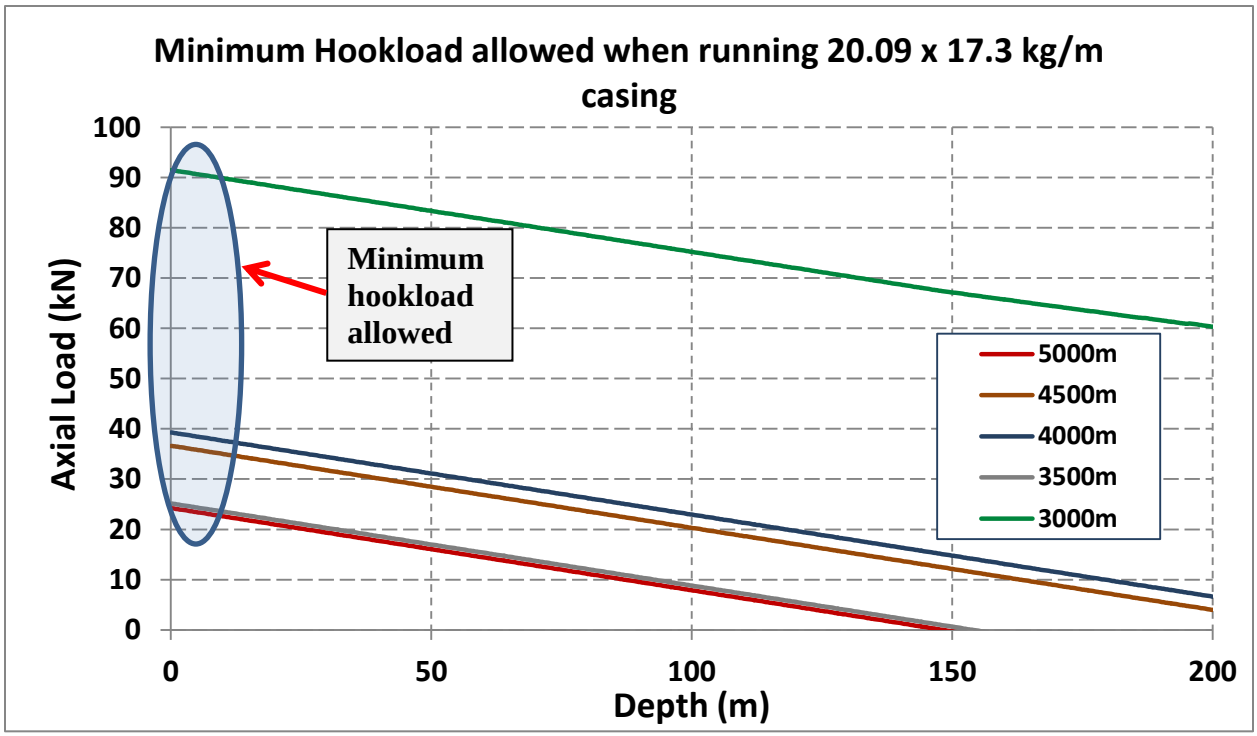

Figure 4.6. Minimum hookload allowed while running casing.

To implement this recommendation, a table with the minimum allowed hookload has to be provided to the field. It is also recommended that once the 3000 meters depths is reached, the running casing speed be reduced 20% to guarantee that minimum hookload requirements are met and that no load peaks are induced due to fast running speed.

Depth range (m)	kN
3000-3500	90
3500-4000	40
4000-4500	36
4500-5000	24

Table 4.2. Minimum hookload allowed when running-in casing.

4.3 Limiting Dogleg Severity through the Entire Well

It has been noted that bending stresses are highly dependent on tortuosity of the well (dogleg severity). Although dogleg severity is mostly dictated by the spacing available to the well to achieve geological targets (kick-off point and target lateral displacement), there are few recommendations worth of mentioning that can help preventing high stress concentrations, therefore reducing the risk of having casing exceeding the strength limits.

As depicted in Figure 4.7, bending stresses increase as the well gets more tortuous; this means aggressive changes in azimuth or inclination generate more bending. Any effort to control high doglegs will surely contribute to reduce stress concentration in the casing.

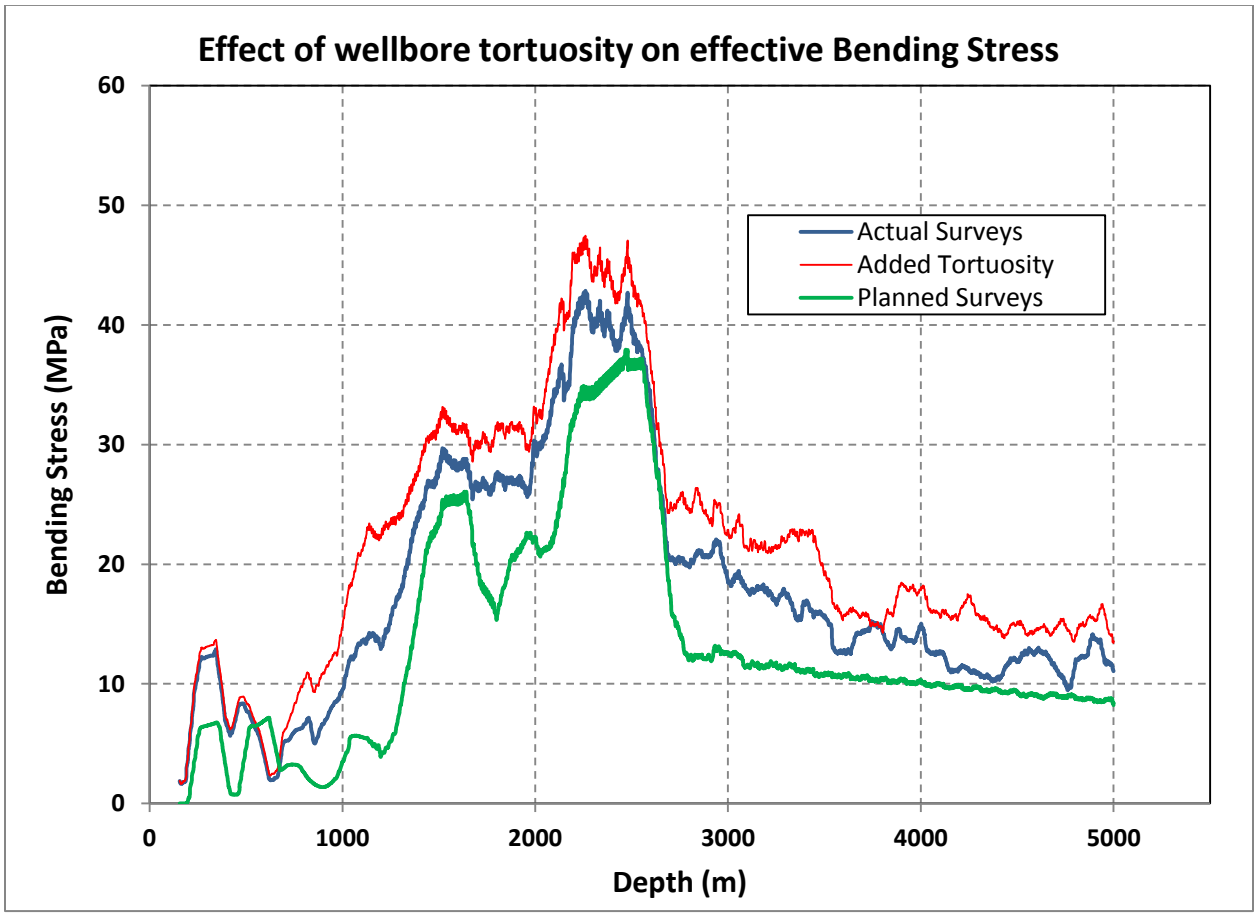

Figure 4.7. Effect of wellbore tortuosity on bending stresses.

The following practices are recommended to keep well tortuosity as low as possible:

- Set the kick-off point as deep as possible in the well. Normally, the kick-off point is dictated by the directional drilling requirements (tools capability and preference to do deviation work in competent formations).
- Design the well trajectory with inclination angle in the tangent section as low as possible. This has to be planned in accordance with the previous recommendation since the tangent angle is a function of the kick-off point depth. Usually, the kick-off set point rules over the inclination of the tangent.
- Plan the curve section with low dogleg severity, and control the aggressiveness of the build rates by using low directional motors bend settings (1.83 vs 2.12 degrees)
- Reduce percentage of sliding drilling in the horizontal section by increasing geological well path windows, and avoid use of aggressive directional motors
- Using Rotary Steerables Systems (RSS) will eliminate the sliding drilling totally, therefore the wellbore can have an excellent shape to run casing smoothly

Chapter Five: **Conclusions and Recommendations**

1. The method presented on this thesis can be introduced into the standard casing design process to prevent casing failures during hydraulic fracturing operations. The production casing string reliability has been evaluated under the combination of the burst fracturing loading and the high installation compressive forces. This new methodology assists the operator to optimize well production casing integrity in the Montney shale.

2. By implementing a new casing design approach with a tapered string, 22.4 x 17.3 kg/m casing, the operator will be able to run the production casing in long extended reach wells with more than 3000 meters horizontal sections. The more robust casing (22.4 kg/m) on top of the string allows for more force available to push the pipe into the wellbore. The lighter casing (17.3 kg/m) in the horizontal section reduces drastically the friction caused by contact forces. Therefore the design factors for the installation loads acting on the casing are reduced as well.

   The 22.4 kg/m casing is mechanically stronger than the casing currently being used; therefore it can withstand better the combined loads of installation and hydraulic fracturing with practically no risk of having pipe integrity problems.

3. There is practically no increase in cost by switching to the proposed tapered design. Therefore it is strongly recommended to start using the proposed tapered casing string.

4. If a lighter casing (20.09 kg/m) has to be used because of availability, technical or economic reasons, then the maximum well length must be limited to 2700 meters horizontal sections. In this case the running procedure must be controlled by limiting the minimum hookload the rig crew can go to while pushing casing into the wellbore. The drilling engineer must provide the rig personnel with the minimum allowed hookload for different depth ranges starting at 3000 meters depth. If the minimum hookload is exceeded, the risk of having a casing integrity problem while hydraulic fracturing the well will increase substantially.

5. All possible efforts must be made to reduce well tortuosity by controlling dogleg severity and the amount of sliding drilling. Running torque and drag models for optimizing the well trajectory (lowering kick-off points, designing lower tangents, and reducing build rates) can help reduce well tortuosity. It is not recommended to use aggressive directional tools, such as short-bit-to-bend motors that can give unexpected high build rates outputs and will require additional directional work later, resulting in increased wellbore tortuosity. Rotary steerable tools are highly recommended to drill the horizontal section of the well as experience has shown that those tools drill smoother and more consistent well trajectories.

6. All the previous recommendations will doubtlessly contribute to prevent excessive mechanical loading on the completions strings and will save capital in remedial work, loss in production and/or possible well abandonments.

Bibliography

ANSI/API, 2008. Technical report on Equations and Calculations for Casing, Tubing, and Line Pipe used as Casing or Tubing, and Performance Properties Tables for Casing and Tubing – 5C3. First Edition.

Craig, H; 1987. Mechanical Design Considerations for Fracture-Treating Down Casing Strings. SPE Terra Resources.

Christman, S; 1976. Casing Stresses Caused by Buckling of Concentric Pipes. SPE 6059

Cunha, J; 2003. Buckling of Tubulars Inside Wellbores: A Review on Recent Theoretical and Experimental Works. SPE, Petrobras.

Gorokhova, L; Parry, A; Flamant, N; 2007. Comparing Soft-String and Stiff-String Methods Used to Compute Casing Centralization. SPE 163424.

ISO 13679, 2002. Procedures for Testing Casing and Tubing Connections. First Edition.

Johancsik, C.A; Friesen, D.B; Dawson, R; 1984. Torque and Drag in Directional Wells – Prediction and Measurement. SPE.

Lubinski, A. et Al; 1962. Helical Buckling of Tubing Sealed in Packers. SPE.

McSpadden, A. et Al; 2011. Advanced Casing Design with Finite Element Model of Effective Dogleg Severity, Radial Displacements and Bending Loads. SPE 141458.

Menand, S. et Al; 2009. Buckling of Tubulars in Simulated Field Conditions. SPE 102850.

Menand, S. ; 2012. A New Buckling Severity Index to Quantify Failure and Lock-up Risks in Highly Deviated Wells. SPE 151279.

Menand, S. et Al; 2013. Safely Exceeding Buckling Loads in Long Horizontal Wells: Case Study in Shale Plays. SPE 163518.

Mitchell, R; 1996. Buckling Analysis in Deviated Wells: A Practical Method. SPE 36761.

Mitchell, R; 2005. The Pitch of Helically Buckled Pipe. SPE 92212.

Mitchell, R; Samuel, R; 2007. How Good is the Torque-Drag Model? SPE IADC 105068.

Paslay, P; 1991. Bending Stress Magnification in Constant Curvature Doglegs with Impact on Drillstring and Casing. SPE 22547.

Popov, E; Balan, T; 2000. Engineering Mechanics of Solids. Pearson Education, Second Edition.

Roylance, D; 2001. Yield and Plastic Flow. Masschusetts Institute of Technology.

Samuel, R; Kumar, A. 2012. Effective Force and True Fore: What are They? SPE 151407.

Shell International; 2012. Wells Learning Process (WLP), Well Engineering Round II.

Stockhausen, E. et Al; 2012. Directional Drilling Tests in Concrete Blocks Yield Precise Measurements of Borehole Position and Quality. SPE 151248.

Zhang, Y; 2006. Modeling of Casing Running in High Angle Wells. University of Tulsa, Drilling Research Projects.

APPENDICES

Apendix A. Minimum Design Safety Factors for Design Check Equations.

Description	Label	Pipe Body		Connection		
					Tested	Legacy
Running, tension						
	RT1	$^{P}DSF_{1t}$	1.40	$^{C}DSF_{1t}$	1.40	1.55
	RT2	$^{P}DSF_{1t}$	1.20	$^{C}DSF_{1t}$	1.20	1.35
Running, compression	RC	$^{P}DSF_{1c}$	1.10	$^{C}DSF_{1c}$	1.10	1.25
Collapse	C	$^{P}DSF_{2}$	1.00	$^{C}DSF_{2}$	1.00	1.15
Burst - Triaxial						
	B1	$^{P}DSF_{3}$	1.25	$^{C}DSF_{3}$	1.25	1.40
	B2	$^{P}DSF_{3}$	1.15	$^{C}DSF_{3}$	1.15	1.30
	B3	$^{P}DSF_{3}$	1.25	$^{C}DSF_{3}$	1.25	1.40
	B4	$^{P}DSF_{3}$	1.20	$^{C}DSF_{3}$	1.20	1.35
	B5	$^{P}DSF_{3}$	1.15	$^{C}DSF_{3}$	1.15	1.30
	B6	$^{P}DSF_{3}$	1.10	$^{C}DSF_{3}$	1.10	1.25

Triaxial Burst

Given a tubular string has been installed in place, the burst DSF min shall apply for those operation design load cases where internal pressure exceeds, or equals, external pressure (see Equations 12.8 and 12.9). A range of different burst DSF min values is defined, discriminating between situations with higher or lower risk. These situations are labeled as follows:

B1

For production tubing, production casing, injection tubing, injection casing, intermediate casing and surface casing in non-sour service where the alloy has not been ordered to comply with Supplementary Requirements (SR)16+75% shear toughness and SR2 of ISO 11960/API 5CT20 (75% shear toughness does not apply to Grades H40, J55, K55, L80 Type 9Cr and L80 Type 13Cr) or NDT and impact/flattening test requirements per ISO 13680/API 5CRA2.

B2

For production tubing, injection tubing, production casing, injection casing, intermediate casing and surface casing in non-sour service where the alloy has been ordered to comply with

SR16+75% shear toughness and SR2 of ISO 11960/API 5CT (75% shear toughness does not apply to Grades H40, J55, K55, L80 Type 9Cr and L80 Type 13Cr) or NDT and impact/flattening test requirements per ISO 13680/API 5CRA

B3

For production and injection tubing where the alloy has been ordered to the sour service material specification herein and where the tubing is at a temperature below 150 °F (65.5 °C)

B4

For production casing, injection casing, and intermediate casing where the alloy has been ordered to the sour service material specification herein and where the casing is at a temperature below 150 °F (65.5 °C)

B5

For production tubing, injection tubing, production casing, injection casing, intermediate casing, and surface casing where the alloy has been ordered to the sour service material specification herein and where the pipe is at a temperature of 150 °F (65.5 °C) or higher

B6

For tubing and casing; only for design load cases where a known maximum pressure is applied (including injection, reservoir fracture, pressure testing) where the alloy has been ordered to comply with SR16+75% shear toughness and SR2 of ISO 11960/API 5CT (75% shear toughness does not apply to Grades H40, J55, K55, L80 Type 9Cr and L80 Type 13Cr) or NDT and impact/flattening test requirements per ISO 13680/API 5CRA, or where the alloy has been ordered to the sour service material specification herein.

Apendix B. 114.3 mm P110 Casing Properties and Specifications

Weight (kg/m)	ID (mm)	Drift (mm)	Burst (kPa)	Collapse (kPa)	Axial (kgf)	Yield (kPa)	UTS (kPa)	Young's Modulus (kPa)	Poisson's Ratio	Thermal Expansion Coeff (E-06/°C)
16.37	102.26	99.09	69901.35	45268.66	158369.7	758423.3	861844.7	2.15E+08	0.28	12.42
17.263	101.6	98.42	73735.6	52237.56	166547.2	758423.3	861844.7	2.15E+08	0.28	12.42
18.751	100.53	97.36	79929.39	63495.01	179645.1	758423.3	861844.7	2.15E+08	0.28	12.42
18.974	100.53	97.36	79929.39	63495.01	179645.1	758423.3	861844.7	2.15E+08	0.28	12.42
20.09	99.57	96.39	85533.3	73680.33	191376.4	758423.3	861844.7	2.15E+08	0.28	12.42
22.471	97.18	95.25	99395.59	98875.58	219909.8	758423.3	861844.7	2.15E+08	0.28	12.42
23.067	97.18	94.01	99395.59	98875.58	219909.8	758423.3	861844.7	2.15E+08	0.28	12.42
27.977	92.46	89.28	126825.2	131093	274328.6	758423.3	861844.7	2.15E+08	0.28	12.42
28.573	92.46	89.28	126825.2	131093	274328.6	758423.3	861844.7	2.15E+08	0.28	12.42
32.144	88.9	85.72	147471.2	149812	313500.5	758423.3	861844.7	2.15E+08	0.28	12.42
36.609	85.85	82.68	165167.7	165272.6	345853.8	758423.3	861844.7	2.15E+08	0.28	12.42
39.436	82.3	79.12	185813.7	182628.3	382172.8	758423.3	861844.7	2.15E+08	0.28	12.42

Source: American Petroleum Institute API5CT - Casing Dimensions and Strengths

Apendix C. Casing Buckling Modeling Results from 3000 m to 4500 m Depth

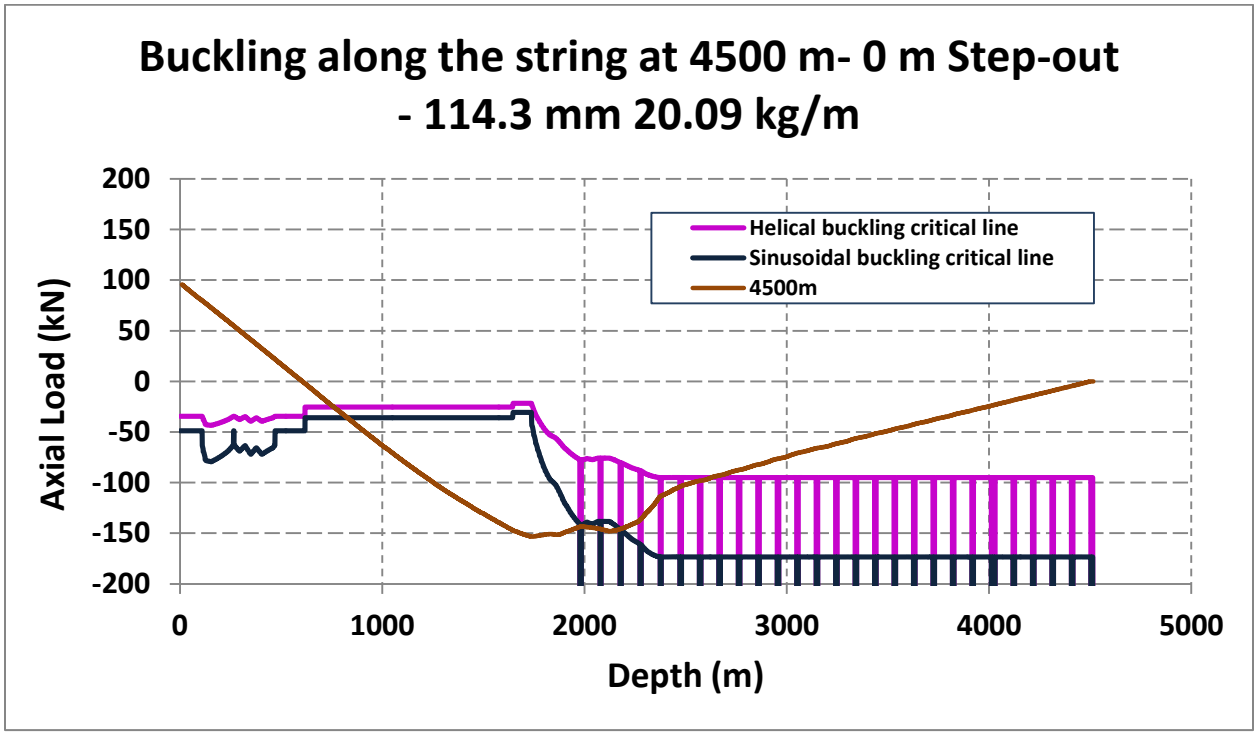

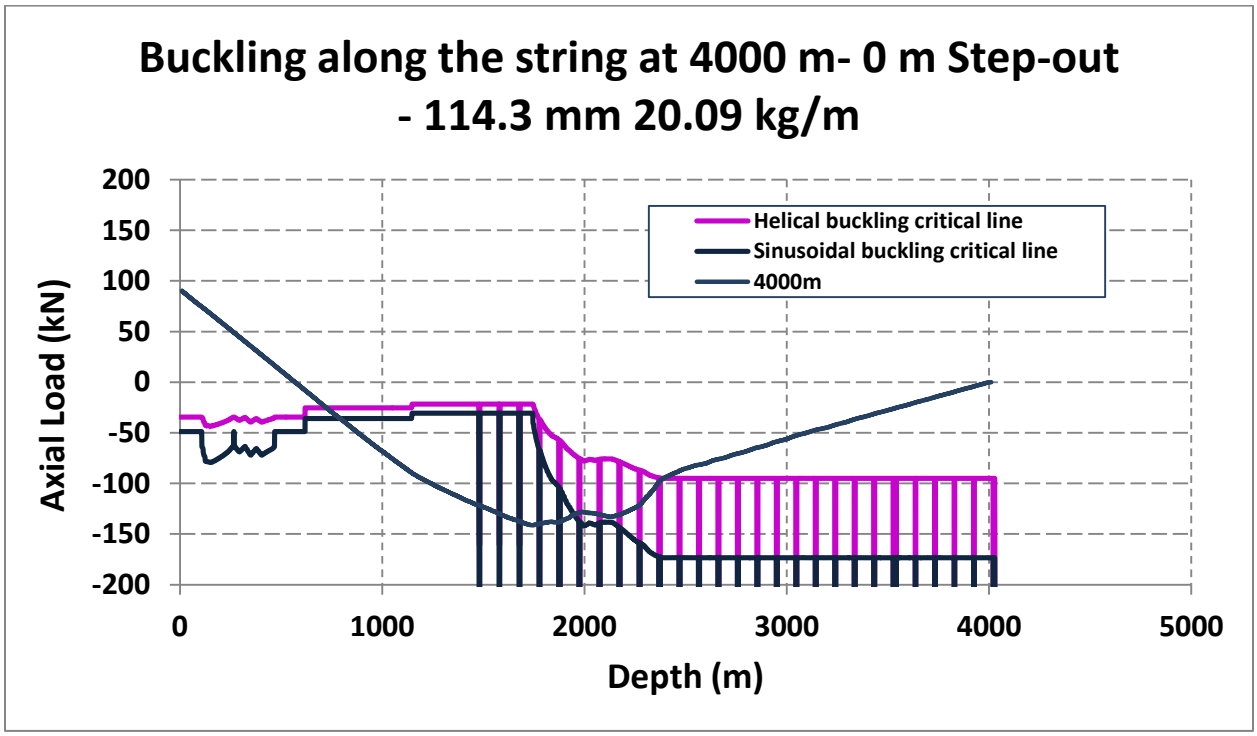

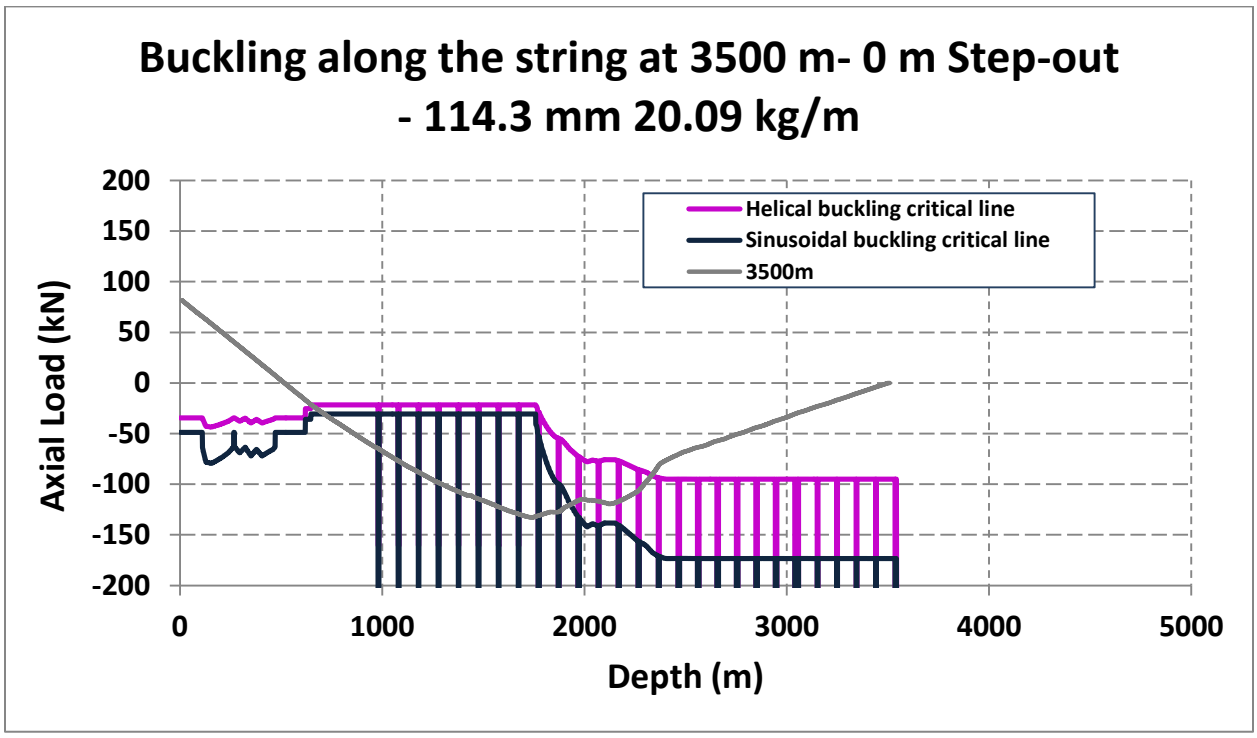
Buckling along the string at 3500 m- 0 m Step-out
- 114.3 mm 20.09 kg/m
Helical buckling critical line
Sinusoidal buckling critical line
3500m
Axial Load (kN)
200
150
100
50
0
-50
-100
-150
-200
0
1000
2000
3000
4000
5000
Depth (m)

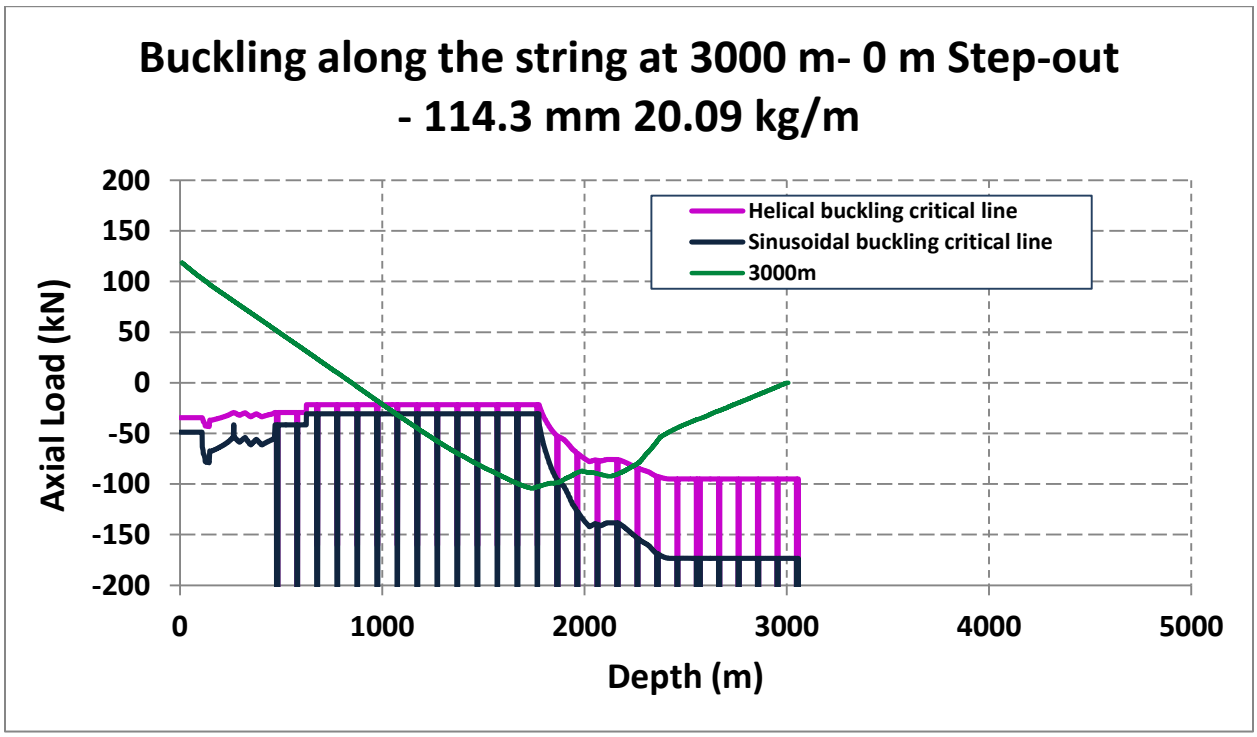
Buckling along the string at 3000 m- 0 m Step-out
- 114.3 mm 20.09 kg/m
Helical buckling critical line
Sinusoidal buckling critical line
3000m
Axial Load (kN)
200
150
100
50
0
-50
-100
-150
-200
0
1000
2000
3000
4000
5000
Depth (m)

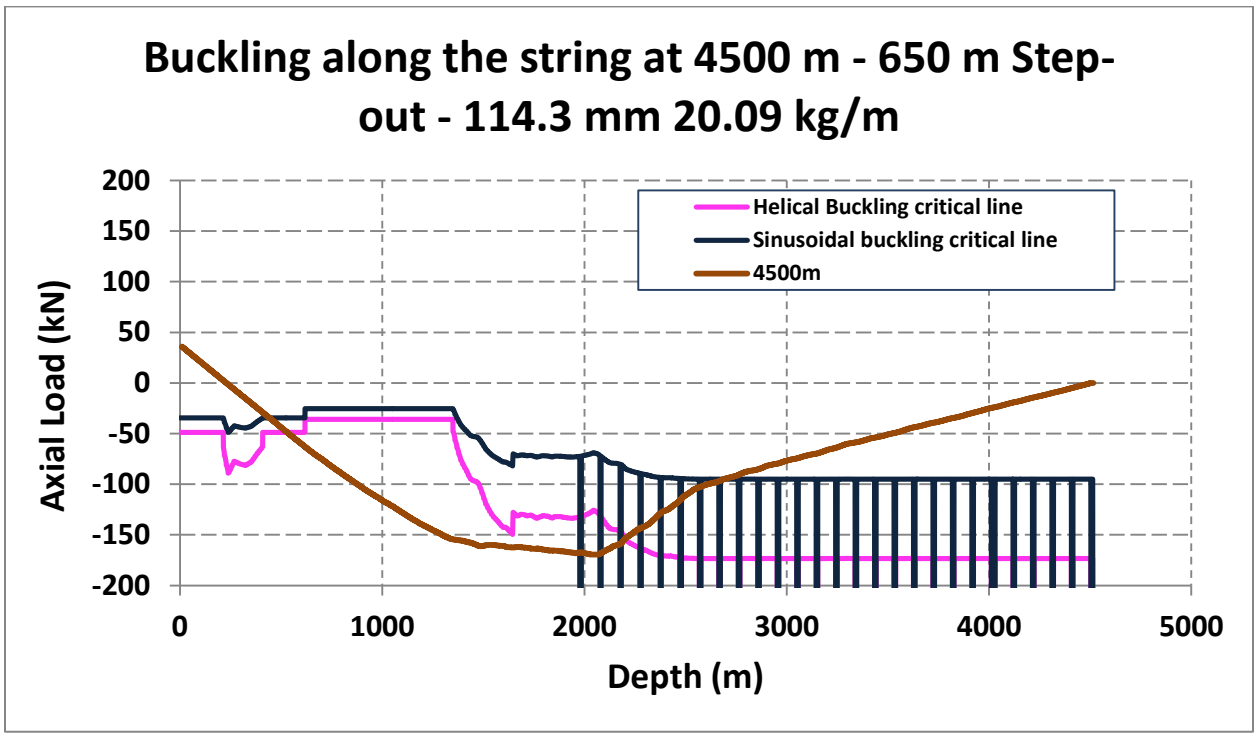
Buckling along the string at 4500 m - 650 m Step-out - 114.3 mm 20.09 kg/m
Axial Load (kN)
200
150
100
50
0
-50
-100
-150
-200
0
1000
2000
3000
4000
5000
Depth (m)
Helical Buckling critical line
Sinusoidal buckling critical line
4500m

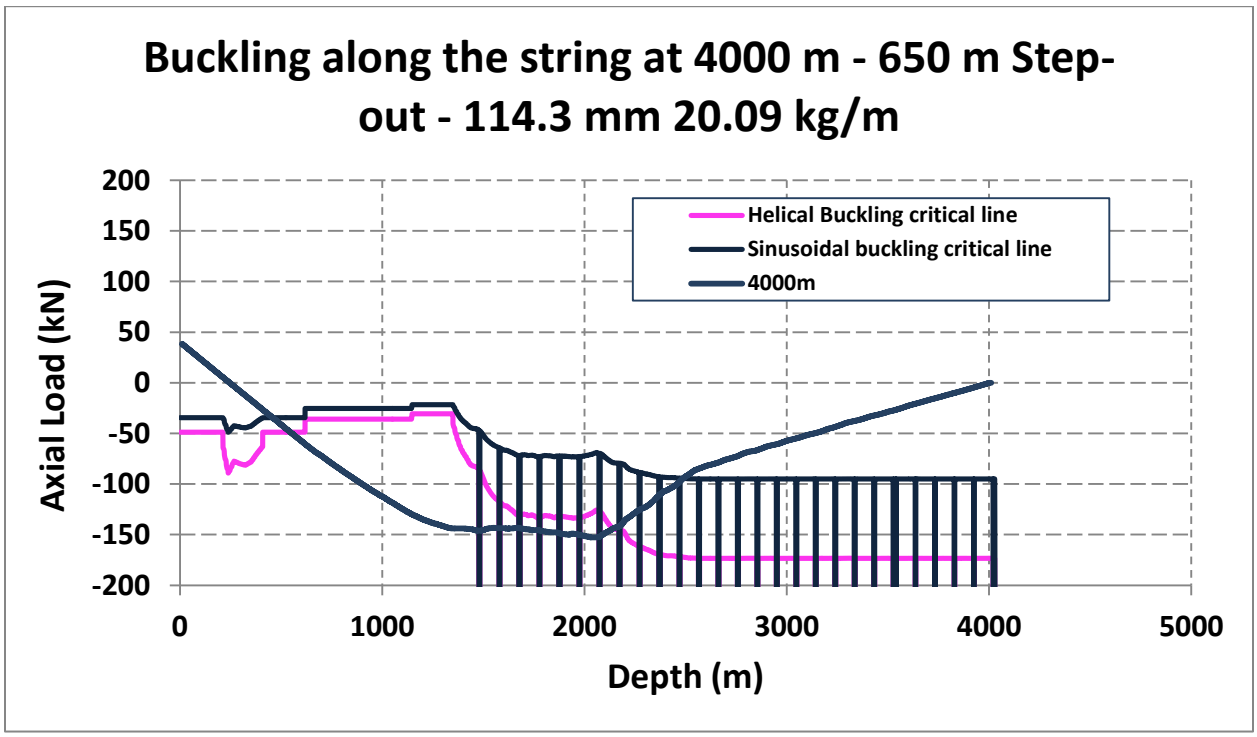
Buckling along the string at 4000 m - 650 m Step-out - 114.3 mm 20.09 kg/m
Axial Load (kN)
200
150
100
50
0
-50
-100
-150
-200
0
1000
2000
3000
4000
5000
Depth (m)
Helical Buckling critical line
Sinusoidal buckling critical line
4000m

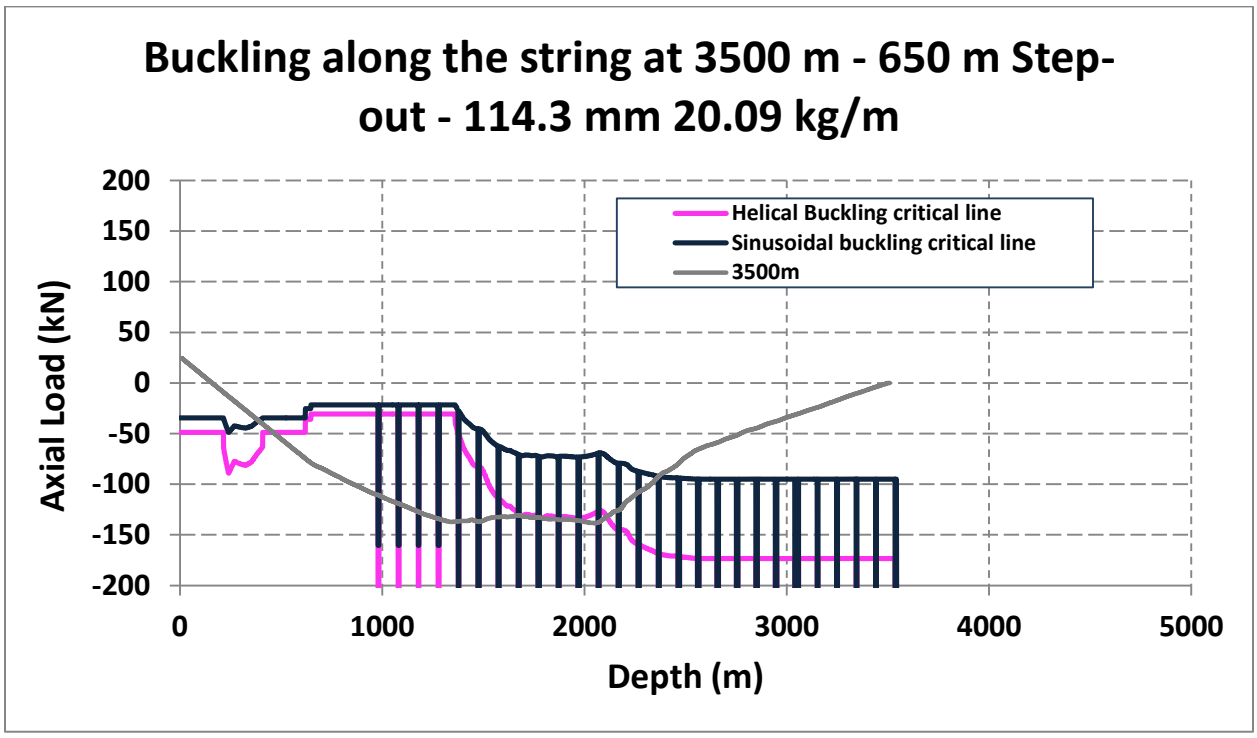
Buckling along the string at 3500 m - 650 m Step-out - 114.3 mm 20.09 kg/m
Axial Load (kN)
200
150
100
50
0
-50
-100
-150
-200
0
1000
2000
3000
4000
5000
Depth (m)
Helical Buckling critical line
Sinusoidal buckling critical line
3500m

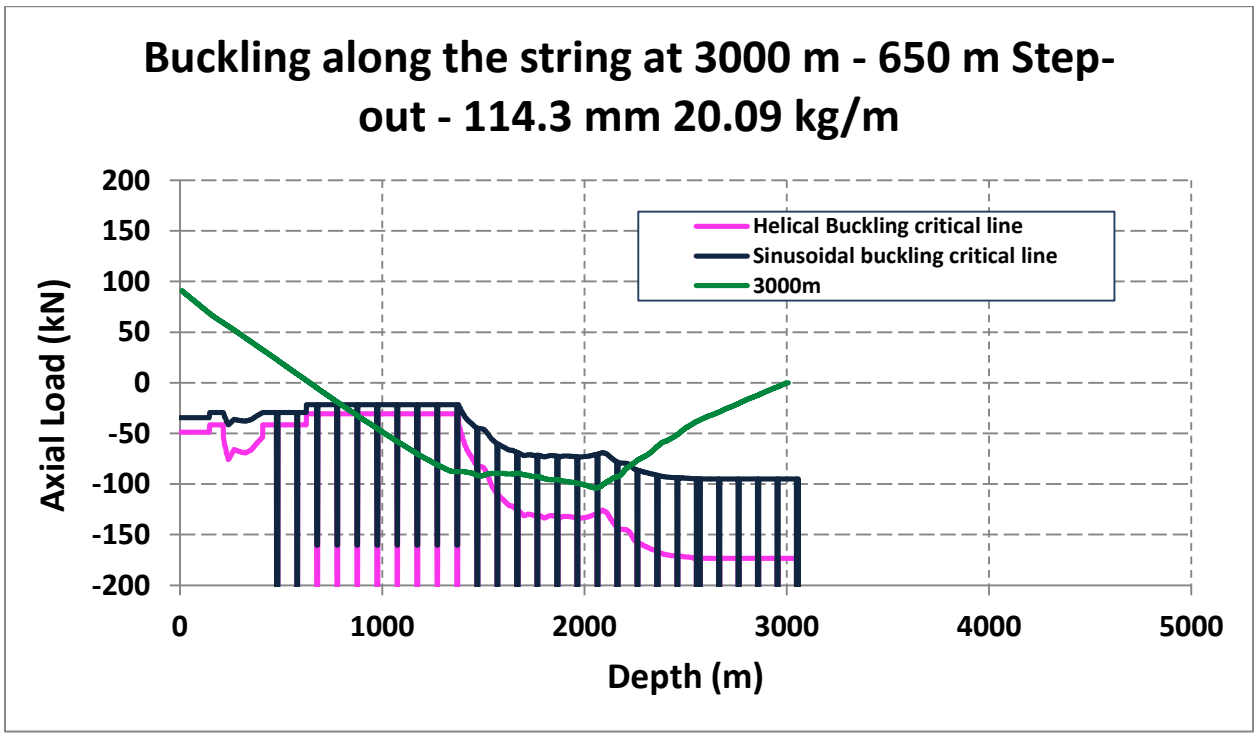
Buckling along the string at 3000 m - 650 m Step-out - 114.3 mm 20.09 kg/m
Axial Load (kN)
200
150
100
50
0
-50
-100
-150
-200
0
1000
2000
3000
4000
5000
Depth (m)
Helical Buckling critical line
Sinusoidal buckling critical line
3000m